DEFLUORIDATION OF POTABLE WATER IN CKDu PREVALENT AREAS OF SRI LANKA BY FUNCTIONALIZED MODIFIED-FLY ASH

Wanigasuriyage Dona Madhurangi Chathrapani Perera

(168883C)

Thesis submitted in partial fulfillment of the requirements for the Degree of Master of Environmental Management

Department of Civil Engineering

University of Moratuwa
Sri Lanka

March 2019

Declaration

"I declare that this is my own work and this thesis does not incorporate without acknowledgement any material previously submitted for a Degree or Diploma in any other University or institute of higher learning and to the best of my knowledge and belief, it does not contain any material previously published or written by another person except where the acknowledgement is made in the text.

Also, I hereby grant to the University of Moratuwa the non-exclusive right to reproduce and distribute my thesis, in whole or in part in print, electronic or other medium. I retain the right to use this content in whole or part in future works (such as articles or books)."

Signature: Date:

The above candidate has carried out research for the Master's thesis under my supervision.

Name of the supervisor: Prof. M. W. Jayaweera

Signature of the supervisor: Date:

The above candidate has carried out research for the Master's thesis under my supervision.

Name of the co-supervisor: Dr. (Ms.) W. B. Gunawardana

Signature of the supervisor: Date:

Abstract

The last two decades marked a progressive increase in an epidemic of Chronic Kidney Disease of unknown ('u') origin (CKDu) among the farming communities in Sri Lanka. In the presence of the combination of fluoride, with other potential nephrotoxic ions or constituents can lead to the development of CKDu, even at lower concentrations of individual ions. The Na/Ca ratio and fluoride combination in potable water, has been identified as one of the plausible causes of CKDu.

The toxicity of potable water from CKDu prevalent areas could be minimized, if the fluoride level of the CKDu prevalent areas can be brought below 0.4 mg/L, to overcome the synergistic effect between Na/Ca ratio and fluoride. The effects of solution Na/Ca ratio, on the adsorption of fluoride onto functionalized modified fly ash (FMFA) were investigated in this work. $(FMFA)_{opt}$ was selected as the optimized FMFA from a series of synthesized adsorbents, with varying degrees of functionalization with CaO, MgO and Al_2O_3. It was found that the maximum adsorption took place at pH 6.8 and the maximum monolayer adsorption (Q_m) increased from 0.452 mg/g to 0.755 mg/g when the Na/ Ca ratio of the solution was changed from 01 to 07. The adsorption studies confirm that the Ca^{2+} ions in the solution were rejected by $(FMFA)_{opt}$ while giving preference to F- ion adsorption, according to the Donnan coion exclusion rule. The defluoridation reaction fits the Langmuir Model and pseudo second order kinetics. NaOH was identified as the best desorbent for $(FMFA)_{opt}$. regeneration. (FMFA)opt is a low cost, an effective and efficient adsorbent to remove fluoride irrespective of the Na/Ca ratios present in CKDu prevalent areas.

Keywords: CKDu, fluoride, Na/Ca ratio, functionalized modified fly ash, defluoridation.

Acknowledgement

First of all, I would like to extend my heartfelt gratitude to my supervisor Prof. Mahesh Jayaweera, for giving me the opportunity to complete the research. Your guidance and encouragement given at every step of the way in the research helped me to achieve the goals. Your support was immense, and I am very fortunate to have you as my supervisor. I extremely appreciate the advice given in experiments, writings and moral assistance given to complete this research.

I am very grateful to my co-supervisor Dr. Buddhika Gunawardana, for providing her guidance and support for the research project. Your advice and assistance given are very much appreciated. Furthermore, I would like to extend my gratitude to Prof. Jagath Manatunge for guiding me to conduct fruitful and successful research. Your feedback on my experiments, writing, helped me to complete a very productive study.

I wish to express my sincere thanks to the laboratory staff of Environmental Engineering Laboratory, Department of Civil of Engineering, University of Moratuwa; Ms. Nilanthi Gunathilake Mr. Kasun Zoysa, Mr. Justin and Mr.Dhananjaya for the assistance received to conduct my research experiments successfully in the Environmental engineering laboratory. My special thanks go to Ms. Nipuni for helping me with the lab work.

I would like to thank head and the staff of Analytical Laboratory, Department of Materials Science and Engineering, University of Moratuwa for allowing me to use laboratory equipment.

I would like to thank Ayomi, Thilini, and Gimhani for their friendship, guidance, strength and assistance given in the period of the research study. Thank you, Madhusha for being my research partner and helping me in various ways to complete the research and giving me the moral support for the completion.

I am grateful to my family for being there for me, giving their unconditional love and support to fulfill my aims. Finally, I would like to thank my husband, Roshan for supporting, encouraging and understanding me in my quest.

Table of contents

List of figures

List of Tables

List of abbreviations

Abbreviation	Description
$(FMFA)_{opt}$	Optimized Functionalized modified Fly Ash
CFA	Coal Fly Ash
CKD	Chronic Kidney Disease
CKDu	Chronic Kidney Disease of unknown etiology
EDX	Energy-Dispersive X-ray Spectroscopy
ESEM	Environmental Scanning Electron Microscopy
FMFA	Functionalized modified Fly Ash
FTIR	Fourier Transform-Infrared Spectroscopy
GFR	Glomerular filtration rate
IC	Ion Chromatography
MFA	Modified Fly Ash
XRD	X-ray Powder Diffraction

1. INTRODUCTION

1.1 Introduction

Chronic kidney disease (CKD) is pervasive worldwide and has been a profound cause of morbidity and mortality (Jha et al., 2013), and largely attributed to traditional risk factors such as diabetes and hypertension (Vos et al., 2015). A significant proportion of CKD remains globally unidentifiable and is, therefore, termed as CKD of unknown etiology (CKDu). CKDu is considered to be triggered in the absence of a past history of diabetes mellitus, chronic or severe hypertension, snake bite, glomerulonephritis or urological diseases (Wanigasuriya, 2012). CKDu is slowly progressive, probably starting in the second decade of life, asymptomatic in its early stages and peripheral edema and hypertension are reported to be delayed symptoms (Jayatilake et al., 2013). Nephrotoxins play a key role in the etiology of CKDu, and the main histopathological features of CKDu include tubular atrophy with or without nonspecific interstitial mononuclear cell infiltration, and interstitial fibrosis (Nanayakkara, 2012). CKDu has been globally manifested in many individuals for a few decades (Jayasekara et al., 2015). CKDu has been reported in many countries, including El Salvador (Peraza et al., 2012) Costa Rica (Cerdas, 2005), Nicaragua (O'Donnell et al., 2011), Tunisia (Abid et al., 2003), Egypt (El-Minshawy and Kamel, 2011), India (Machiraju et al., 2009), Tunisia (Gifford et al., 2017), and Sri Lanka (Noble et al., 2014).

Chronic kidney disease of unknown etiology appears to have evolved in the mid-sixties in agricultural areas of dry zones around the equator (Wimalawansa, 2014) and now had spread beyond those zones.CKDu has been often reported in areas of agricultural lands with poor drainage, prolonged droughts leading to inadequate water supply, and seasonal fluctuations on groundwater quality (Wimalawansa 2014). Nephrotoxic contaminants geochemically originate mainly from the dissolution of minerals and potable water is often considered to be a major source of such contaminants. Heavy metals, fluoride, cyanobacterial and algal toxins, agrochemicals, salinity, and ionicity in water have been implicated in the disease; but no precise source or causative factor has been identified yet (Wimalawansa, 2015). The synergistic and antagonistic effects of co-contaminants

that are ever-present even at lower exposure levels in potable water, and have been postulated to have triggered the disease (Wimalawansa, 2015). When considering the identified plausible causal factors, fluoride ions in water, individually or in combination with other constituents, have been suspected to be a major cause for the disease.

Based on the geographical distribution of groundwater fluoride levels in the dry zone of Sri Lanka, Dissanayake and Chandrajith (2017) suggest that fluoride and its interactions with other ions or elements could be associated with CKDu. Studies from several other countries have clearly shown the importance of groundwater fluoride levels as a significant risk factor for kidney diseases (Bober et al., 2006; Chouhan and Flora, 2008). Fluoride, as an individual ion, does not act alone, but its extreme reactivity makes it combine easily with metal ions such as Ca, Mg, Na and with metalloids such as Al (Noble et al., 2014). Fluoride is, therefore, an excellent geochemical carrier and a marker for many possible multi-faceted causative agents. It is apparent that, except for the pineal gland (Luke, 2001), it is the kidney that accumulates fluoride most in the human body (Ileperuma and Dharmagunawardhane, 2009). The role of fluoride and its combinations with other ions or constituents for the persistence of the CKDu has been inadequately investigated or sparingly reported.

This study, focuses on investigating one of the fluoride-related postulate, the Na/Ca ratio, in the presence of fluoride. In areas with high Ca^{2+} activity and resulting lower Na/Ca ratios with increased fluoride in groundwater, there seems to have an elevated incidence of CKDu (Chandrajith et al., 2011); hence, defluoridation of water is of utmost importance to reduce the synergistic effect of fluoride when present with different Na/Ca ratios. The identification of the role of fluoride and Na/Ca ratio in CKDu persistence and the biochemistry that is altered to inflict the disease are delineated in this study.

Interestingly, there have been numerous investigations worldwide on the defluoridation efforts when fluoride alone (Vithanage and Bhattacharya, 2015), but its removal in the presence of other reactive ions or constituents has been poorly investigated. The behaviour of fluoride in the presence of other ions in potable water warrants synergistic or antagonistic effects on the pervasiveness of CKDu and is, therefore, crucial to study

the possible defluoridation efforts under such, perhaps deleterious conditions.

Identification of a novel material to curtail the above problems was one of the main focuses of this study. Coal fly ash (CFA) was used as a raw ingredient to synthesize modified fly ash (MFA), which is again impregnated with metal oxides in order to modify the adsorbent surface for effective and efficient defluoridation. The optimized functionalized modified fly ash $(FMFA)_{opt}$ obtained expects to eliminate the synergistic effect of fluoride and calcium by exclusively removing fluoride up to the level of 0.4 ppm or below. Therefore, the permeate water will not pose any threat to the CKDu community due to the low levels of fluoride present in the potable water. The new material synthesis giving cost-effective fluoride adsorbent is a timely need for the potable water purification in the CKDu prevalent area.

The overall objective of the present research study is the defluoridation of potable water in CKDu prevalent areas, minimizing the synergistic effects of different Na/Ca ratios in the presence of high Ca and varying Na levels

Specific objectives

1. Establishment of the distribution of fluoride and Na/Ca ratios of potable water for different geographical locations in CKDu affected areas, and studying the linkage between different Na/Ca ratios in the presence of fluoride on CKDu prevalence

2. Development of a suitable material for effective defluoridation in CKDu prevalent areas, overcoming the synergistic effect caused by fluoride with different Na/Ca ratios in the presence of high Ca and varying Na levels

1.2 Approach

Chapter 1 presents the introduction to the research study with narrative on CKDu, its prevalence in Sri Lanka, the synergistic effect of Na/Ca ratio with fluoride in potable water that can be attributed to CKDu prevalence, unavailability of a reliable treatment method for defluoridation to overcome the synergistic effects, and the importance of developing a new adsorbent to overcome this effect. Chapter 1 contains the overall

objective and specific objectives of the research study.

Chapter 2 provides a summary of literature available on CKDu, global and local distribution of CKDu, potable water, and CKDu, nephrotoxicity inflicted by fluoride alone and in combinations, nephrotoxicity of fluoride without multiple ion interactions, nephrotoxicity of fluoride with multiple ion interactions, combined effect of fluoride and Na/Ca ratio, defluoridation in the presence of fluoride, and MFA functionalization enhancing its affinity towards anions.

Chapter 3 describes the materials and methods used in this research project. Experimental procedures followed to achieve each objective are described in detail. Especially, experimental setups for each objective, methods followed to obtain chemical characteristics of adsorbent are illustrated. Further, analytical methods used for analysis of fluoride and the details of batch studies, isothermal and kinetic studies are explained.

Chapter 4 presents the results and discussion of each objective considered in the research project. The distribution of fluoride and Na/Ca ratios of potable water for different geographical locations in CKDu affected areas was established, and the linkage between different Na/Ca ratios in the presence of fluoride on CKDu prevalence was interpreted. Suitable material for effective defluoridation in CKDu prevalent areas, overcoming the synergistic effect caused by fluoride with different Na/Ca ratios in the presence of high Ca and varying Na levels was achieved using $(FMFA)_{opt.}$

Chapter 5 concludes the major findings of each objective and recommendations for future research.

2. LITERATURE REVIEW

2.1 . What is CKDu?

The last two decades marked a progressive increase in an epidemic of Chronic Kidney Disease of unknown ('u') origin (CKDu) among the farming communities in Sri Lanka. Therefore, the health sector of the country experiences a burden in investigating and providing free services to the CKDu patients (Nanayakkara et al., 2012; Wanigasuriya, 2012). CKDu is asymptomatic in the early stages, but then patients experience impairment in the proximal tubules and the interstitium, followed by renal failure at the latter stages (Athuraliya et al., 2014; Chandrajith et al., 2011; Nanayakkara et al., 2012). The main occurrence of the disease is in the dry zone of the country, especially the North Central Province (NCP) of Sri Lanka. CKDu is common among males from poor socioeconomic backgrounds who are engaged in paddy rice farming (Senevirathna et al., 2012; Jayasekara et al., 2013).

2.2 Global distribution of CKDu

The rates of chronic kidney disease (CKD) are in the rising in an alarming manner within the developing world (Barsoum, 2006; Hossain et al., 2009). Various authors have defined CKDu differently. While there is no internationally accepted case definition, common characteristics across studies include asymptomatic and progressive CKD, absent or sub-nephrotic proteinuria, absence of hematuria, absence of diabetes, chronic or severe arterial hypertension, HIV, snake bite, glomerulonephritis or other urinary tract disease, normal glycosylated haemoglobin (<6.5%), blood pressure <160/100 mmHg in untreated patients, and <140/90 mm Hg in patients receiving up to 2 antihypertensive drugs (Vos et al., 2015; Rajapurkar et al. 2012; Martín-Cleary and Ortiz., 2014)

An epidemic of chronic kidney disease of unknown origin, emerged in the Central America has been named Mesoamerican nephropathy. Mesoamerican nephropathy (MeN) has emerged as a leading cause of morbidity and mortality in low altitude coastal areas of Nicaragua and El Salvador, with additional foci in Costa Rica and Guatemala (Sanoffet al., 2010). This form of chronic kidney disease is present primarily in young male agricultural workers from communities along the Pacific

coast, especially workers in the sugar cane fields. In general, these men have a history of manual labor under very hot conditions in agricultural fields (Correa-Rotter et al., 2014). Roncal-Jimenez et al., (2016) proposed that dehydration coupled with heat stress, rhabdomyolysis and hyperuricemia are likely factors responsible for this epidemic.

Contemporaneous to the MeN epidemic, a dramatic rise in CKDu, occurred in the North Central Province of Sri Lanka (NCP) and has been subjected to extensive research at local level (Giffored et al., 2017).

2.3 CKDu in Sri Lanka

In the rural areas of Sri Lanka CKDu has been reported over the past few decades. The North Central Province (NCP) has the highest occurrence of CKDu reported, where hot and dry weather prevails (Wanigasuriya, 2014; Jayasekara et al., 2013). Mostly men were diagnosed with the disease when compared to women. (Athuraliya et al, 2011). Exact prevalence and geographic scope of the problem is unclear. Some estimates suggest 2 to 3% prevalence rate among those older than 18 years of age (Chandrajith et al.,2011), while other recent work suggests a prevalence closer to 15% (Jayatilake et al., 2013).

Though several hypotheses have been postulated concerning the underlying causes of the CKDu epidemic in Sri Lanka and elsewhere, evidence in support of them remains limited. Existing research has reported that risk factors such as hypertension and diabetes are not the cause of the disease (Nanayakkara et al., 2012). Another hypothesis concerns the role of environmental exposures to high concentrations of nephrotoxicants (such as As, Cd, Pb, and U), which may accumulate and cause functional and structural damage in the proximal tubule cells of the kidney (Sabolic, 2006).

In Sri Lanka, previous studies using case–control methodologies have reported that CKDu is related to biomarkers for As (Jayasumana et al., 2013) and Cd (Wanigasuriya et al., 2011), and have identified farming and the use of fertilizer or other agrochemicals as risk factors (Chandrajith et al., 2011; Jayatilake et al., 2013). Jayasumana et al. (2013) also report that high levels of As exposure in CKDu patients coincide with observable skin lesions.

Athuraliya et al,. (2009) is one of the first published reports, which addresses the extent of the CKDu endemic. The study evaluated 492 clinical records of CKDu cases and found that it cannot be correlated to diabetes mellitus, hypertension or other known causes. In general, comprehensive epidemiological data about the CKDu endemic and detailed clinical descriptions of patients with CKDu in Sri Lanka are lacking. Most of the studies that have been conducted in Sri Lanka focus on identifying risk factors and possible etiologies.

2.3.1. CKDu prevalence in different regions of Sri Lanka

In a publication of Chandrajith et al., (2011) it was concluded that CKDu was reported in the range 2-5% in different regions among the people having CKD. This observation is not very significant, but, in NCP the 84% of the patients with CKD had CKDu compared to a much lower CKDu prevalence in non-endemic regions. The CKDu prevalence in Sri Lanka is given in Figure 2.1

A more comprehensive work done by Athuraliye et al., (2011) studied the inhabitants from three different regions, the North Central, the Central, and the Southern regions. In the three regions CKD occurrence was 5%, 10%, and 2%, respectively, but in the North Central region, 87% of the CKD cases were of unknown etiology. In the other two regions diabetes and hypertension were the main risk factors of CKD. Jayasekara et al., (2015) have reported that the male to female ratio was 2.4:1 and that the CKDu prevalence was 70% in the NCP.

2.4 Potable water and CKDu

Potable water is often considered to be a major source of nephrotoxic contaminants that causes CKDu, and the contaminants of concern often come from natural (e.g., local geological materials) sources. In addition to the possibility of natural contamination, intensive use of agrochemicals in Sri Lanka since the 1960s may have polluted local water sources. Data on the distribution of such inorganic nephrotoxic elements (such as As, Cd, Pb, and U) in water supplies are rather limited. Moreover, the geographic data coverage is patchy or limited to a few selected elements (Jayatilake et al., 2013).

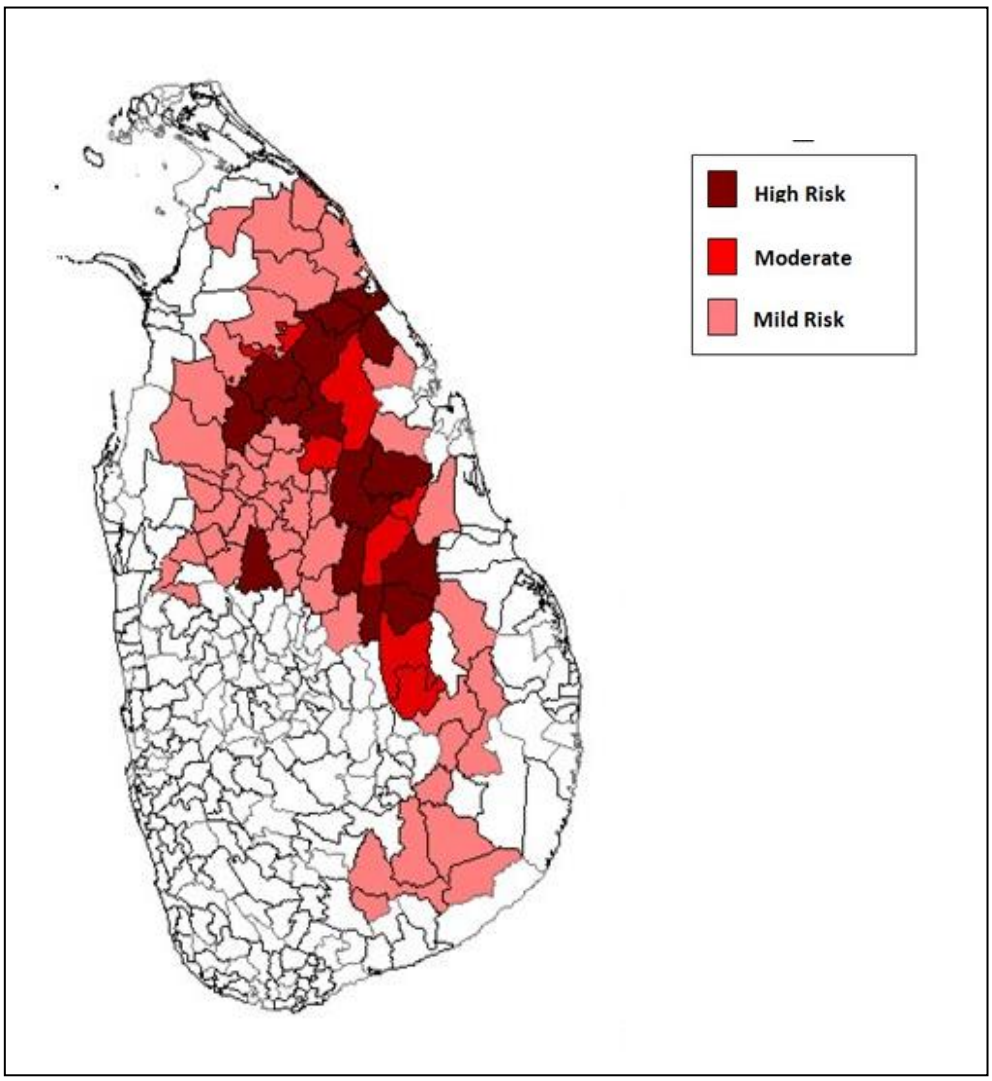

Figure 2.1: CKDu prevalence in Sri Lanka (Source; Official web page of Presidential Task force on Prevention of Kidney Disease of uncertain etiology)

A systematic assessment of water quality is, therefore, needed, and should be linked with biomonitoring (e.g., in urine) of the potential elements of concern, in order to fully understand exposures, including the potential role of food sources of these contaminants and assess their potential health effects (Wilhelm et al., 2004; Aguilera et al., 2008; Calafat, 2012; Karagas et al., 2001).

The villagers who consume spring water even within the CKDu prevalent areas are unaffected by the disease. CKDu was found to be more prevalent in individuals drinking water from shallow wells compared to natural springs (Jayasekara et al., 2015). The spring water consists of relatively lower concentrations of most of the elements; therefore the synergistic effect due to multiple elements is not pronounced (Wasana et al., 2015)

Groundwater in the CKDu endemic area is found to be either hard or very hard and contain Ca, Mg, Fe, and Sr ions (Jayasumana, et al., 2012). The geochemistry of soils from the Madirigiriya, Talawa, and Padaviya districts in NCP suggests that fluoride is not readily retained in sediments, leading to high values in groundwater. The high mobility of fluoride from soil to water is facilitated by immature soils, which have a sandy clay loam texture containing some primary minerals and rock fragments (Jayawardana et al., 2012).

The fluoride level of well water in both prevalent and non-prevalent areas reported values, which were above the WHO-recommended level of 0.6 mg/L. Ca-bicarbonate type water is predominant in prevalent CKDu areas, whereas Na–K dominant anion type water is common in non-prevalent areas. These observations by Chandrajith et al., (2011) provided a baseline for the fluoride related Na/Ca ratio hypothesis.

2.4.1. Nephrotoxicity inflicted by fluoride alone and in combinations

Fluoride in conjugation with other ions inflict more profound neprotoxicity when compared to the individual ion. The complex chemical behavior inflicting unfavorable effects on humans is poorly investigated. The underlying hydrogeochemistry, physical chemistry, ecotoxicology, and biochemistry of the potable water cycle, imposing adverse effects in the areas of CKDu prevalence, are vital expanses that needs to be discussed.

2.4.2. Nephrotoxicity of fluoride without multiple ion interactions

The hydro-geochemistry of fluoride, plays a vital role in neprotoxicity. In the tropical and arid regions, the primary source of drinking water is from groundwater, where the neprotoxicity can be pronounced. Fluorine compounds usually dissociate to release fluoride in the groundwater. The radius of the fluoride ion (0.133 nm) is almost the same as that of the hydroxyl ion (~0.110 nm) thus, fluoride becomes an excellent aquaphile (Dissanayake and Chandrajith, 2017). Chandrajith et al. (2010) have highlighted the presence of fluoride in potable water as a possible contributor to the etiology of chronic kidney disease. According to the authors there is a possible replacement of hydroxide ion with fluoride ion in dental and bone tissues. Fluoride

ions may biochemically affect several essential enzyme-related metabolic functions. Fluoride ions often pass cell membranes by simple diffusion, enter soft tissues and cause their impairment (Carlson et al., 1960). A kidney when damaged for whatever the reason tends to accumulate fluoride ions aggravating the kidney damage fast towards the final stages. Fluoride is more genotoxic at lower doses than at higher doses when ingested through drinking water (Podder et al., 2011).

Fluoride ion exposure of human collecting duct cells induces major impairment of the sodium pump known as basolateral Na-K-ATPase, in addition to nonspecific cell injury (Cittanova et al., 1996). Zager and Iwata (1997) have carried out some experiments to characterize some subcellular determinants of fluoride cytotoxicity and to determine whether sub-toxic fluoride exposure affects tubular cell vulnerability to superimposed ATP depletion and nephrotoxic attack. The study concluded that, (a) fluoride induces dose-dependent cytotoxicity in cultured human proximal tubular cells, (b) this occurs via Ca^{2+} and phospholipase A2 (PLA2s) dependent mechanisms, (c) partial cytosolic PLA2 depletion subsequently results, and (d) sub-toxic fluoride exposure could acutely increase cell resistance to attack further.

Dharma-wardana et al., (2015) have highlighted the importance of groundwater ionicity, describing the contribution of fluoride towards CKDu, by denaturing kidney membrane proteins in accord to the Hofmeister series. Interestingly, adult male Wistar rats on oral administration of fluoride (5 and 20 mg/L), exhibited impaired hepatocytes and hepatic function. This observation is strongly supported by the histopathological observation of necrosis and portal inflammation with increased serum alanine aminotransferase (ALT), aspartate aminotransferase (AST), and alkaline phosphatase (ALP) activities (Perera et al., 2018). In the same study, elevated creatinine levels were observed, when exposed to a longer period (60 days) of oral administration indicating renal damage. In contrary, Nanayakkara et al., (2014) states that higher serum fluoride is a result of lowered eGFR (impaired renal function) and fluoride ingestion cannot be considered as the primary cause of CKDu.

Fluoride causes excessive production of oxygen free radicals, nitric oxide (NO) and lipid peroxides (LPO), leading to the reduced capability of scavenging free radicals

in BV-2 Microglia cells (Shuhua et al., 2012). This phenomenon severely Damages to the biological membrane structure, functions of cells, and bio-macromolecules, such as proteins and nucleic acids, and even the entire soft tissues are pronounced due to toxicant production (Shuhua et al., 2012). The stimulation of gamma-glutamyltransferase (γ-GT) activity by fluoride ingestion contributes to the renal morphological damage in ischmic rats, at the level of proximal tubular cells (Cutrín et al., 2000).

In the Netherlands, where the water fluoridation was banned many decades ago, the fluoride retention in patients with renal insufficiency was 3.25-fold higher as in healthy individuals at similer oral intake levels (NIHEP, 1989). Human kidneys concentrate fluoride as much as 50-fold when filtering from plasma to urine (Carton, 2006) making kidney cells a target for fluoride toxicity (Collins et al., 1995). People with renal failure can have a four-fold increase in skeletal fluoride content (Marier, 1977), and have a higher risk of spontaneous bone fractures, at 25 mg/day fluoride in drinking water (Inkovaara, 1975). Fluoridated water in the areas of chronic renal failure induces activated osteoblasts to produce excessive osteoid in which the collagen fibrils are disarrayed (Lough et al., 1975). Children consuming water with fluoride level higher than 2 mg/L have exhibited increased levels of lactic dehydrogenase in their blood and increased levels of N-acetyl-beta-glucosaminidase (NAG) and gamma-glutamyltransferase in their urine (Xiong et al., 2007).

In contrary to all the above studies done on individual effect of fluoride on nephrotoxicity, Wasana et al., (2017) using Sparague-Dewley male rats implicate no effect on kidney tissues even when the fluoride alone in potable water was in 6.7-fold increase than that of WHO maximum guideline level (1.5 mg/L).

Dissanayake and Chandrajith, (2017) suggest that environmental or occupational fluoride exposure is associated with fluoride toxicity. Renal toxicity could be a consequence of acute or chronic fluoride exposure in both animals and humans (Dote et al., 2000). Climate change has a marked effect on the elevated concentrations of fluoride in groundwater in tropical countries over the last two decades (Dissanayake and Chandrajith, 2017). Therefore, the farmers who are severely dehydrated in the dry zones tend to consume more fluoride-rich water, inflicting the disease (Ileperuma and Dharmagunawardhane, 2009).

Recent investigations show that even within a few years, groundwater wells in the dry zone of Sri Lanka have manifested a marked increase in fluoride levels changing from safe levels (WHO recommended maximum guideline level of 1.5 mg/L) to deleterious levels of drinking (Chandrajith et al., 2012). Nevertheless, to date, there is no guideline value of fluoride when present either alone or in combination with other ions developed for nephrotoxic effect.

2.4.3. Nephrotoxicity of fluoride with multiple ion interactions

No single geochemical parameter is found to have a clear and direct relation to CKDu. The unique hydrogeochemistry of potable water can be closely associated with the incidence of disease Chandrajith et al., (2017). The current WHO guideline levels of fluoride for drinking are based on the toxicity acting alone. The presence of many types of ions leads to a reduction in the toxicity of the multiple-ion system. However, the interaction of fluoride with other ions in combination to trigger CKD has not been well documented. In a multi-ion system, there are many possible pairing processes, most of which do not warrant the toxicity (Dharma-wardana, 2017). Chronic dehydration and oxidative stress could trigger the renal damage (Roncal-Jimenez et al., 2015) and in the presence of the combination of fluoride with other potential nephrotoxic ions or constituents can lead to the development of CKDu, even at lower concentrations of individual ions.

2.4.4. Combined effect of fluoride and Na/Ca ratio

The Na/Ca ratio in potable water with high levels of fluoride, is another plausible cause of CKDu implicated by Chandrajith et al., (2011). The regulation of Ca^{2+} due to high intake of Na^{+} was observed by Spencer et al., (1969), where a 30% decrease of plasma Ca^{2+} levels occurred during the intake of sodium fluoride in human subjects. Fluoride shows more affinity towards Ca^{2+} in endemic CKDu regions where Ca^{2+} activity is more prominent compared to the sodium activity (Chandrajith et al., 2011). Similarly, as exemplified by Simon et al., (2014), in areas with Ca^{2+} deficiency and with high contents of fluoride, even skeletal fluorosis is very common. In areas with high Ca^{2+} activity, resulting lower Na/Ca ratios with

increased fluoride in groundwater, there seems to have an elevated incidence of CKDu (Chandrajith et al., 2011). On the other hand, with high calcium levels in the presence of fluoride, CaF_2 is said to form with an insoluble precipitate in potable water, causing kidney tubular damage. High sodium levels in the presence of fluoride in potable water are said to form NaF, which is soluble in water with no prospective kidney tubular damage (Chandrajith et al., 2011).

Biochemical pathways and mechanisms by which fluoride acts, are strongly influenced by the presence of Ca^{2+} and Na^{+} ions. Fluoride induces dose-dependent cytotoxicity in cultured human proximal tubular cells occurs via Ca^{2+} with phospholipase-A2 (PLA2) dependent mechanisms. NaF, for example, could protect against cell injury by demonstrating a cytoprotective effect (Zager and Iwata, 1997). The dual role of fluoride as both a cytoprotective and a cytotoxic agent is heavily dose-dependent (Zager and Iwata, 1997). Borke and Whiteford, (1999) have recorded negative effects on several Ca-dependent processes, including kidney glomerular and tubular function with both acute and chronic exposures to elevated levels of fluoride.

It has been reported that Na/Ca ratios were in a range of 1.6–6.6 and 350–469 in the CKDu endemic areas and the non-endemic regions, respectively (Chandrajith et al., 2011). Paranagama, (2014) reported the average Na/Ca ratio to be 2.36 to 0.17 in CKDu prevalent areas and followed the same pattern as given in Chandrajith et al., (2011), where the CKDu non prevalent areas had a higher Na/Ca ratio respect to the prevalent areas.

In summary, with the onset of dry seasons, high levels of calcium could be pronounced compared to those of sodium. In coastal areas where the sodium levels are too elevated because of salinity intrusions, CKDu is often not endemic. Though this hypothesis is supported by a couple of researchers, concrete evidence is yet to be published with more toxicological studies.

2.5 Standards for potable water fluoride regulation

The optimal fluoride level in drinking water for general good health set by the World Health Organization (WHO) is 1.5 mg/L. In Sri Lanka the regulation the optimum fluoride level is 1.0 mg/L (SLSI, 2013). In 1.0 mg/L optimal level allocation, the neprotoxicity levels of fluoride alone is considered. Neprtoxicity can be pronounced due to synergistic effects when multiple ions are present with fluoride. The toxicity will be pronounced at lower levels of fluoride, therefore it is important to establish a limit, at which the synergistic effect would be of minimum.

In Table 2.1, the fluoridation levels of potable water levels adopted by different countries are given. When present in drinking water at the optimum level, or used in dental treatments, fluoride can promote dental health by helping to prevent tooth damage and decay.

Table 2.1: The fluoridation levels of potable water

Country	Levels (mg/L)	Reference
Egypt	Fluoridation 0.4 max Tap water – 0.36	Abu Zeid and Elhatow, (2007)
Nigeria	Fluoridation 0.3–0.6	Akpata et al., (2009)
Hong Kong	Fluoridation 0.48 - 0.69	Water Supplies Department, The Government of Hong Kong Special Administrative Region, (2014)
Singapore	Fluoridation 0.4-0.6	Luan, (2010)

According to Table 2.1 it is evident that for most of the countries the fluoridation level is below 0.4 mg/L. There is no guideline value of fluoride when present either alone or in combination with other ions, developed for nephrotoxic effect. In accordance with above fluoridation levels, health aspects and neprotoxic effects, it is advisable to maintain the fluoride level in potable water below 0.4 mg/L.

2.6 Defluoridation in the presence of Fluoride

Numerous attempts have been reported on implementing economical and efficient new technologies, for the removal of excess fluoride from potable waters. Adsorption (Bhatnagar et al., 2011), ion exchange (Yu et al., 2015), chemical precipitation (Gogoi et al., 2015), membrane filtration (Oshima et al., 1996), reverse osmosis (Sehn, 2008), and electrodialysis (Ergun et al., 2008) are the most commonly used methods in the current process of water purification.

However, it is apparent that most of these methods have been successfully adopted to investigate the removal capacities of fluoride alone, not taking into consideration the combined effects with other ions. Vithanage and Bhattacharya, (2015) have reviewed critically the available defluoridation techniques with their merits and demerits. In that study, the effects, when combined with other ions have not been discussed. Table 2.2 gives the defluoridation method with advantages and limitations

The technologies that allow simultaneous removal of fluoride and arsenic are investigated using adsorption (Jing et al., 2012), membrane filtration (Padila and Saitua, 2010) and coagulation (Ingallinella et al., 2011; Pinon–Micromontes et al., 2013). There have been, however, no proper investigations of promising techniques that simultaneously remove fluoride and other ions that are supposed to inflict synergistic effect on CKDu. Masking effects on defluoridation inflicted by other ions in the solution are not convincingly elucidated in the literature.

Table 2.2: Available defluoridation methods with advantages and limitations

De fluorination method	Reference	Advantage	Limitations
Adsorption Adsorptive materials: activated alumina, activated carbons, and other natural and synthetic adsorbents.	Bhatnagar, et al., (2011) and Zhao et al., (2017)	Cost effective Removes 90% of fluoride Greater accessibility, low cost, simple operation, availability of wide range of adsorbents	The process is highly pH dependent. High concentration of total dissolved solids causes fowling presence of other anions competes on adsorbance.
Ion exchange	Biswas et al., (2009) and Popat et al., (1994)	High productivity (90-95 % fluoride removal).	Efficiency is reduced in the presence of other ions and alkalinity.
Membrane filtration: Nano filtration reverse osmosis	Pontie et al., (2008)	High productivity. It lives up to expectations under wide pH range. Interference because of the presence of other ion is not observed.	Highly expensive technique when contrasted with other defluoridation techniques. Prone to fouling, scaling or membrane degradation
Coagulation/precipitation: Activated alumina	Ghorai and Pant, (2005)	High efficiency; commercially available chemical	Efficiency depends on the pH and the presence of co-ions in the water, adjustment and readjustment of pH is required.

2.7 Zeolite as a deflouridation material

Zeolites are crystalline microporous alumino-silicates, built up of a 3-dimensional framework of $[SiO_4]^{4-}$ and $[AlO_4]^{5-}$ tetrahedral, linked by sharing oxygen atoms (Apak et al., 1998).and weakly bonded [readily exchangeable] cations and water molecules in the pores and voids of the structure.

The cation exchange capacity is determined by the negative charge, resulting from the substitution of Si (IV) by Al (III) in the tetrahedral. Cation exchange capacity (CEC) is a measure of the number of cations per unit weight available for exchange, usually expressed as milli-equivalent per gram of materials. As a rule, the greater the Al content [i.e. the more extra framework cations needed to balance the charge], the higher the CEC of the zeolite (Ramesh and Reddy, (2011).

The composition of the zeolite framework is generally determined by the synthesis conditions of the zeolite, but can also come from post synthetic modification. In particular, a lower Si/Al ratio is very important for creating ion exchangeable zeolite species and determines the concentration and strength of acidic sites present. A higher Si/Al ratio also forms more hydrophobic and hydrothermally stable zeolite species (Auerbach et al., 2003).

Figure 2.2: Naturally occurring zeolite Clinoptilolite

Natural zeolites different deposits may vary widely in purity (from 15 -20 up to 90-95%), chemical composition, crystal size, porosity, pore diameter and other properties determining their sorption and ion exchange capacity. The main advantages of natural zeolites are their low price and availability (Lydon, 2013).

Synthetic zeolites are generally produced by alkali treatment of silica and alumina-bearing raw materials of synthetic, natural or waste origin. Synthetic Zeolite from waste material has been used as a solution for the increasing by products of different processes. Municipal solid waste incineration ash, Coal fly ash, oil shale ash, rice husk ash and other wastes are used in synthetic zeolite synthesis (Lydon, 2013)

2.6.1. Zeolites from Coal Fly Ash (CFA)

Over 500 million tonnes of Coal Fly Ash (CFA) are generated every year in the world as a by-product of coal combustion in thermal power plants. More than 65% of this fine powdered waste is disposed of in landfills and ash ponds creating serious problems with air and water pollution. A large number of scientific articles have been devoted to the development and optimization of hydrothermal methods for CFA zeolitization. These methods generally are based on alkaline activation of CFA aiming at the dissolution of Al and Si- bearing phases and precipitation of zeolite (Lydon, 2013).

2.6.2. Modified Fly Ash (zeolite) and Functionalization

Zeolite is generally mixtures with different compounds and ligands, therefore, it needs to be modified prior to use. Modification improves the function of zeolite as an adsorbent (Ertan and Çakicioğlu-ÖZKAN, 2005). Functionalization is performed to bring about favorable characteristics to the synthesized zeolite. There are many metal oxides that can be incorporated into the zeolite. The functionalization should be done with materials that exhibit high defluoridation ability.

Zeolite loaded with CaO will increase the strength and the content of the base. The formation of Si-O-Ca could enhance the basicity of the zeolite catalyst (Xu et al., 2008) MgO nanoparticles can be used as an adsorbent for defluoridation (Devi et al., 2014) so

it can be easily incorporated into modified fly ash. Activated alumina and metal/metal oxide impregnated alumina have been identified as effective fluoride adsorbents (Ku and Chiou, 2002; Ghorai and Pant, 2005; Pietrell, 2005; Shimelis et al., 2006; Puri and Balani, 2000; Tripathy et al., 2006). Therefore could be effectively used for defluoridation of drinking water.

MgO, CaO and Al_2O_3 could be directly dispersed onto zeolite molecular sieve by microwave irradiation (Wang, et al., 1998; Wu et al., 2013; Kovacheva et al., 2001) and also by metal nitrate solution method. The incorporation of the metal oxides on to zeolite framework will enhance its adsorption capacity of fluoride as well as modify zeolite surface for a high affinity towards anions.

3. MATERIAL AND METHODS

3.1 Establishment of the distribution of fluoride and Na/Ca ratios of potable water for different geographical locations in CKDu affected areas

There have been many research published regarding plausible factors causing CKDu when high levels of fluoride present in the potable water. The lower Na/Ca ratio identified by Chandrajith et al., (2017) and Paranagama, (2014) has been one of the main characteristic in the CKDu prevalent areas. According to them the Na/Ca ratio of all CKDu prevalent areas are lower than value 7. The above-mentioned studies were restricted to a few CKDu prevalent areas in the country; therefore, the potable water quality data of the CKDu prevalent areas and of non-prevalent areas, recorded in literature were analyzed to identify linkage between different Na/CA ratios in the presence of fluoride on CKDu prevalence.

Thus the data on potable water quality, were used to identify the distribution of Na/Ca ratios in the CKDu prevalent areas and to identify the water quality parameters that should be of importance in defluoridation. The data were analyzed using SPSS software (IBM-SPSS-2018) to obtain the correlations between different water quality parameter. The data obtained through literature are given in Annexure 1.

3.2 Optimization of fluoride removal efficiency of Modified Fly Ash (MFA)

3.2.1. Synthesis and characterization of MFA (Zeolite)

Coal fly ash (CFA) was taken and soaked in 10% HNO_3 for 24 hours. Soaked fly ash was washed with distilled water until the pH reached pH 4 and then dried at 60 °C for 12 hrs. 140 g of dried fly ash was mixed with 2M NaOH (350 ml) and refluxed at 90 ^{o}C for 96 hours. Then the mixture was filtered and washed three times with DI water, then dried at 70^{o}C for 24 hours. Figure 3.1 gives the MFA synthesis procedure.

CFA was taken and soaked in 10% HNO_3 for 24 hours.

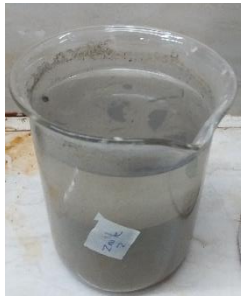

Soaked FA was washed with distilled water until the pH reached pH 4

FA was dried at 60 °C for 12 hrs and crushed

A weight of 140 g of dried fly ash was measured.

FA was transferred into a round bottom flask

FA was mixed with 2M NaOH (350 ml)

The mixture was refluxed at 90^{o}C for 96 hours.

Figure 3.1 : MFA synthesis procedure

3.2.2. Characterization of MFA (zeolite) using SEM, EDX, XRD and FTIR

Morphology and elemental composition of the Zeolite were analyzed, before and after the experiments using Environmental Scanning Electron Microscopy (ESEM- Carl Zeiss, EVO 18, Secondary Electron Microscope, Germany) coupled with Energy-Dispersive X-ray Spectroscopy (EDX Z1 analyser, USA). The phase identification of the Zeolite was performed by the X-ray Powder Diffraction (XRD-D8, ECO, Advance Bruker Diffractometer with filtered Cu Kα radiation, Germany). Fourier Transform-Infrared Spectroscopy (FTIR, ALPHA Bruker, Germany) was performed in the adsorption mode at ambient temperature in the spectral range of 500–4,000 cm^{-1} to identify the functional groups of the Zeolite.

3.3 Synthesis and characterization of MFA

3.3.1. The impregnation of MgO, CaO and Al_2O_3 in the MFA (zeolite)

The 0.05M Nitrate solutions ($Mg(NO_3)_2$, $Ca(NO_3)_2$, $Al_2(NO_3)_3$ were mixed according to the given volume ratios (Table 3.1) with 10 g of coal fly ash zeolite to obtain an array of functionalized modified fly ash (FMFA).

Table 3.1: Mixing ratios of nitrate solutions for the functionalization of MFA

Material	$Al_2(NO_3)_3$	$Mg(NO_3)_2$	$Ca(NO_3)_2$
FMFA1	1	1	1
FMFA2	2	1	1
FMFA3	3	1	1
FMFA4	1	2	1
FMFA5	1	1	2

The final volume of the nitrate solution mixture was 200 mL. FMFA1 was used as the control for the modification experiment. Vithanage and Bhattacharya, (2015) pointed

that Al_2O_3 is the most efficient in fluoride removal; therefore, different ratios of aluminium nitrate solutions were used for FMFA2 and FMFA3 as given in Table 3.1. FMFA4 had higher $Mg(NO_3)_2$ volume while FMFA5 had higher $Ca(NO_3)_2$ volume.

The mixtures were kept in the mechanical shaker for 24 hours and then was kept in the sonicator for 90 minutes. The sonication was programmed to the highest intensity with the normal pulse at 70 ^oC. The mixture was then transferred to an evaporating dish and then evaporated in the oven at 90 ^oC till dry. The resultant powder was then calcinated at 550 ^oC. The final product is then added with 100 mL of DI water and sonicated for 15 minutes twice. The FMFA were then dried, crushed and sieved. The synthesis procedure is given in Figure 3.2. The synthesized FMFA is referred to as FMFA1, FMFA2, FMFA3, FMFA4, and FMFA5 according to the ratios of the nitrate mixtures used in the modification process.

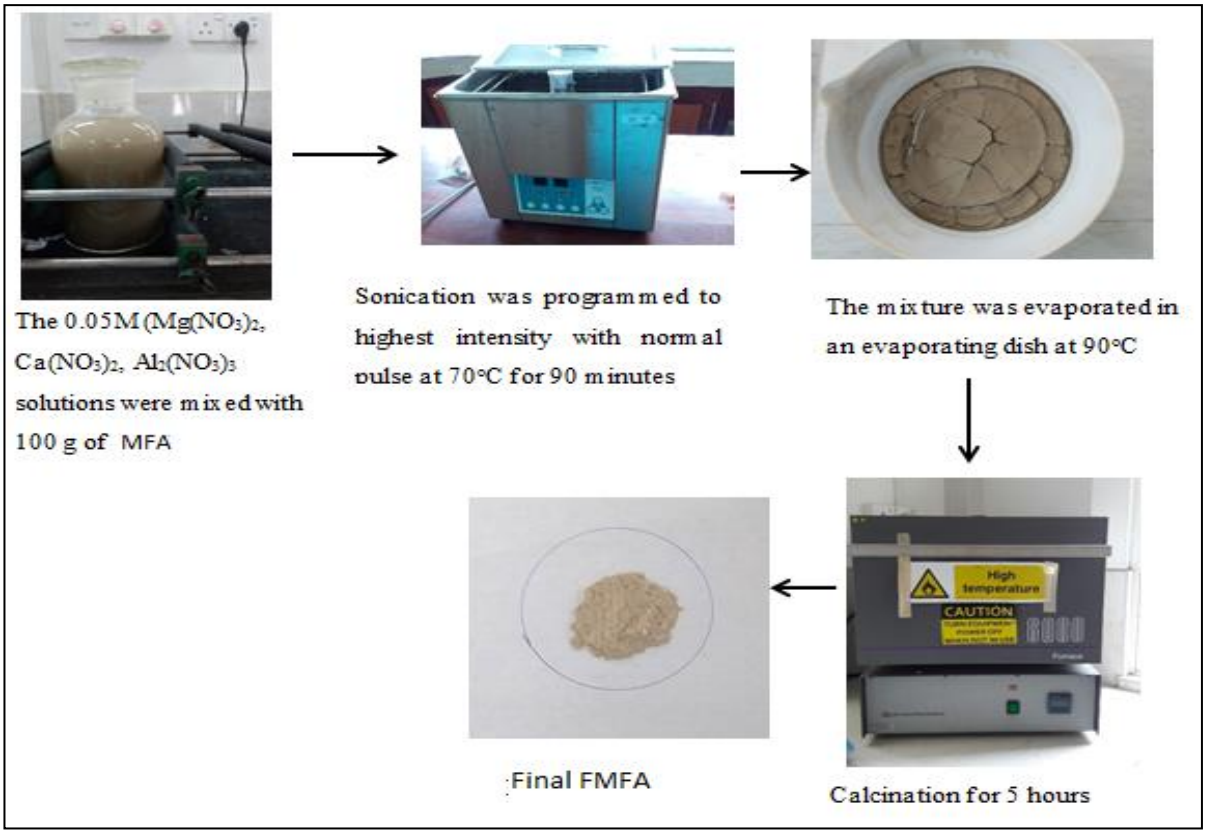

Figure 3.2: The array of FMFA synthesis procedure

3.3.2. Defluoridation efficiency evaluation for the of different arrays of FMFA

3.3.2.1. Single-solute studies for removal of Fluoride

Single-solute batch experiments were carried out using FMFA1-FMFA5 and zeolite to study the fluoride adsorption isotherms. Anhydrous sodium fluoride (from Merck, Darmstadt, Germany) was used to prepare fluoride solutions. All chemicals used in the study were of analytical reagent grade. The fluoride removal was studied with the fluoride concentrations of 5 ppm, 3 ppm and 2 ppm for FMFA dosages of 0.5 g in 100 ml of the fluoride solution with the contact time of 24 hours. The initial solution pH was maintained between 6 and 6.5. The fluoride concentration was measured using the Ion Chomotagraphy (930 compact IC Flex1). The FMFA with the highest fluoride removal was identified and it was identified as $(FMFA)_{opt}$. The setup for the batch studies on the mechanical stirrer is given in Figure 3.3.

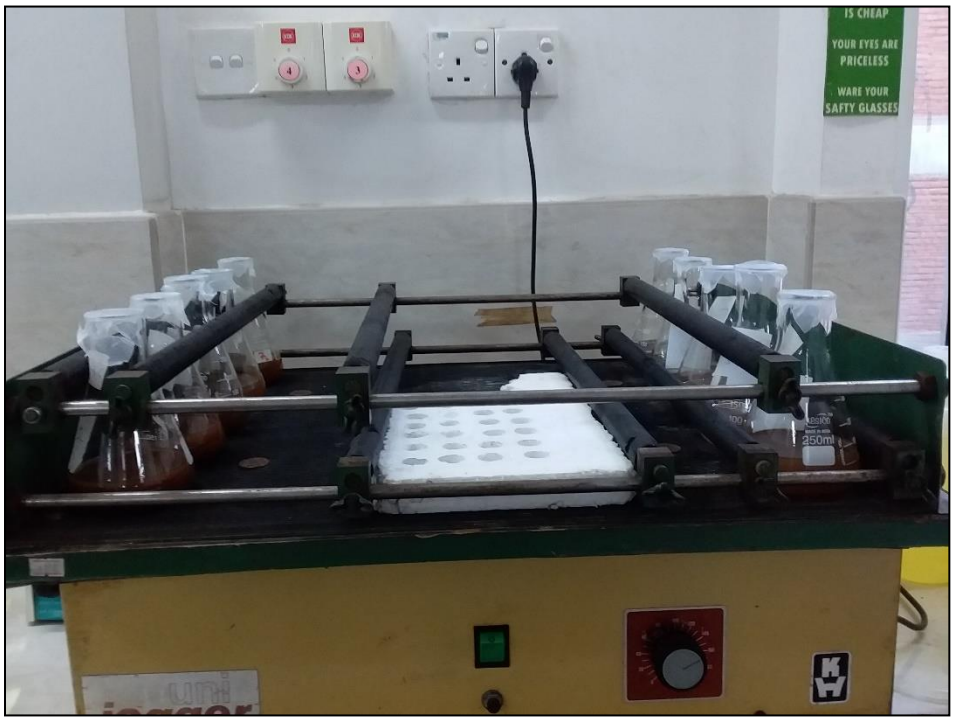

Figure 3.3: The setup for the batch studies on the mechanical stirrer

3.3.2.2. Single-solute studies for removal of calcium

The calcium removal of the different materials was studied to identify a suitable material for the exclusive removal of fluoride when Ca is present in the potable water. Calcium Nitrate (from Merck, Darmstadt, Germany) was used to prepare a 200 ppm calcium solution. All chemicals used in the study were of analytical reagent grade. The calcium removal was studied for FMFA1-FMFA5 and zeolite with 0.5 g in 100 ml of the solution with the contact time of 24 hours. The initial solution pH was 6. EDTA titration was used to measure the calcium concentration of the filtrate following adsorption. The material with the lowest calcium removal and highest fluoride removal was selected for further studies.

3.4 Characterization of $(FMFA)_{OPT}$ using SEM, EDX, XRD and FTIR

$(FMFA)_{opt}$ was identified as the best material for the removal of fluoride when compared with zeolite and other modified zeolites. Morphology and elemental composition of $(FMFA)_{opt}$ was analyzed, after the modification using Environmental Scanning Electron Microscopy (ESEM- Carl Zeiss, EVO 18, Secondary Electron Microscope, Germany) coupled with Energy-Dispersive X-ray Spectroscopy (EDX Z1 analyser, USA). The phase identification of the $(FMFA)_{opt}$ was performed by the X-ray Powder Diffraction (XRD-D8, ECO, Advance Bruker Diffractometer with filtered Cu Kα radiation, Germany). Fourier Transform-Infrared Spectroscopy (FT–IR-ATR, ALPHA Bruker, Germany) was performed in the adsorption mode at ambient temperature in the spectral range of 500–4,000 cm^{-1} to identify the functional groups of the $(FMFA)_{opt}$.

3.5 Optimization of experiment condition for the $(FMFA)_{opt}$ for defluoridation

3.5.1. Optimum dosage

A volume of 100 ml of Ca^{2+} (200 ppm) and Sodium Fluoride (2 ppm) was used for the dosage selection. The initial solution pH was 6, the temperature was 28 ºC, and the

stirring speed was 100 rpm. The contact time was 24 hrs. The $(FMFA)_{opt}$ dosage giving the maximum adsorbance of fluoride was selected as the optimum dosage.

3.5.2. Optimum contact time

A volume of 100 ml of Ca^{2+} (200 ppm) and Sodium Fluoride (2 ppm) was used for the optimum contact time selection with the optimum dosage of 2.2.g. The initial solution pH was 6.7, the temperature was 28 ºC, and the stirring speed was 100 rpm. The contact time was varied from 2 minutes to 5 hours. The contact time giving the maximum adsorbance of fluoride was selected as the optimum contact time.

3.5.3. Optimum pH

A volume of 100 ml of Ca^{2+} (200 ppm) and Sodium Fluoride (2 ppm) was used for the optimum pH selection with the optimum dosage of $(FMFA)_{opt}$ (2.2.g). The optimum contact time of two hours was used as the mixing period, the temperature was 28 ºC, and the stirring speed was 100 rpm. The contact pH of the mixture was changed from pH 2 to 12 using 20% HCl and 20% NaOH. The pH value giving the maximum adsorbance of fluoride was selected as the optimum pH.

3.6 Removal of different fluoride levels with different Na/Ca ratios using $(FMFA)_{opt}$

Based on the Secondary data collected under the first objective, the Na/Ca ratio was below 7 for all the CKDu prevalent areas that were recorded. Therefore, three values of Na/Ca ratio were selected for the analysis. Initial Calcium ion concentration was kept constant at 200 mg/L and the initial sodium ion concentration was varied as given below;

Na/Ca ratio 01 – initial sodium ion concentration -200 mg/L (eg: Giradrukotte)
Na/Ca ratio 03 – initial sodium ion concentration 600 mg/L (eg: Nikawewa)
Na/Ca ratio 07 – initial sodium ion concentration 1400 mg/L (eg: Huruluwewa)

The initial fluoride concentration was varied from 1.5 mg/L to 4 mg/L for all 3 Na/Ca ratios. A volume of 100 ml of the above-mentioned mixtures was used with 2.2 g of $(FMFA)_{opt}$ to determine the percentage fluoride and calcium removal. The optimum pH of 6.8, optimum contact time of 2 hrs was used for the experiment. The temperature was kept at 28 ºC throughout the experiment with a stirring speed of 100 rpm.

The removal of fluoride was measured to determine the effect of Na/Ca ratio in the removal of Fluoride from potable water. The removal of calcium was measured to determine the effect on Na/Ca ratio during defluoridation.

3.7 Adsorption Isotherms and kinetic studies for $(FMFA)_{opt}$

3.7.1. Adsorption Isotherms

A series of batch experiments were conducted to determine the adsorption isotherm and kinetic behaviour of the adsorbent. The amount of fluoride removed per unit mass of the $(FMFA)_{opt}$ (Q_e) in mg/g was calculated using Eq. 1:

$$Q_e = (C_o - C_e) \times \frac{V}{W} \quad (1)$$

Where C_o and C_e are the initial and the equilibrium concentrations of fluoride in the solution (mg/L) respectively, V is the volume of solution (L), and W is the mass of the adsorbent (g) added.

The Langmuir adsorption isotherm model was used to study fluoride removal and to describe the amount of adsorbate adsorbed per unit weight of adsorbent at equilibrium. The Langmuir adsorption isotherm model assumes that the adsorbent surface is homogeneous with equal sorption sites, only monolayer adsorption occurs with no interaction between adjacent adsorbed ions, and adsorbate ions tend to either adsorb or desorb. Langmuir adsorption isotherm (Langmuir, 1938) is given by Eq. 2:

$$\frac{1}{Q_e} = \frac{1}{Q_m} + \frac{1}{Q_m K_L C_e} \quad (2)$$

Where C_e is the equilibrium concentration of adsorbate (mg/L), Q_e is the amount of adsorbate adsorbed per unit mass of the adsorbent at equilibrium (mg/g), Q_m is maximum monolayer coverage capacity (mg/g), and K_L is the Langmuir isotherm constant (L/mg).

Essential characteristics of Langmuir adsorption isotherm can expressed using a dimensionless constant separation factor or equilibrium parameter, R_L given in Eq. 3; where C_o is initial concentration (mg L^{-1}), and K_L is Langmuir isotherm constant. R_L value describes the adsorption mechanisms, which is unfavorable ($R_L > 1$), linear ($R_L = 1$), favorable ($0 < R_L > 1$), or irreversible ($R_L = 0$) (Weber and Chakravorti, 1974).

$$R_L = \frac{1}{[1 + (1 + K_L C_o)]} \quad (3)$$

Freundlich model was applied for fluoride removal to ascertain the adsorption characteristics, assuming the heterogeneous surfaces where fluoride or calcium could bind by multi-layer formation, and there exists an interaction among adsorbed ions. Freundlich adsorption isotherm (Freundlich, 1906) is given by Eq. 4:

$$\log\left(Q_e\right) = \log\left(K_f\right) + \frac{1}{n}\log\left(C_e\right) \quad (4)$$

Where K_f is Freundlich isotherm constant (mg/g), n is adsorption intensity, C_e is the equilibrium concentration of adsorbate (mg/L), and Q_e is the amount of adsorbate adsorbed per gram of the adsorbent at equilibrium (mg/g). The Freundlich constant (n) indicates the adsorption mechanism and when $2 < n < 10$, adsorption is favorable, between $1 < n < 2$ moderately difficult and $n < 1$ poor adsorption (Kakavandi et al., 2013).

3.7.2. Kinetic studies

Kinetics of fluoride adsorption were analyzed using Lagergren's pseudo-first-order kinetic model (Lagergren, as cited in Yuh-Shan, 2004), which describes the adsorption of one ion of adsorbate to one adsorption site and the pseudo-second-order kinetic model, which describes the adsorption of one ion of adsorbate to two adsorption sites (Ho and McKay, 1999). These two models identify kinetics of DEHP adsorption processes to be fitted either to chemisorption or physisorption. The pseudo-first order kinetic model and the pseudo-second-order kinetic models expressed in Eq. (5) and (6):

$$\log\left(q_e - q_t\right) = \log q_e - \left(\frac{K_1}{2.303}\right) t \tag{5}$$

$$\frac{t}{q_t} = \frac{1}{\left[K_2 \left(q_e\right)^2\right]} + \left(\frac{1}{q_e}\right) t \tag{6}$$

Where q_e is the amount of adsorbate adsorbed on adsorbent (mg/g) at equilibrium, q_t is the amount of adsorbate adsorbed on adsorbent (mg/g) at time t (minutes), K_1 is the rate

constant (min^{-1}) for pseudo-first order kinetics, and K_2 is the rate constant (gm/g/ min) for pseudo-second-order kinetics.

3.8 Regeneration studies for $(FMFA)_{opt}$

The regeneration was done to identify a regenerating reagent for $(FMFA)_{opt}$. The regeneration was studied using HCL, NaCl and NaOH solution with pH 4, 7 and 12, respectively. The batch experiments were conducted using 2.2 g of $(FMFA)_{opt}$ in 100 mL of fluoride solution with a Na/Ca ratio of 7. The contact time was 2 hours and the optimum pH of 6.8 was maintained throughout the experiment. After the adsorption cycle $(FMFA)_{opt}$ was allowed to settle at the bottom of the conical flask before decanting the supernant. A volume of 50 ml of regenerating reagent was then added to $(FMFA)_{opt}$ containing flask and kept in the mechanical shaker at 100 rpm for an hour. The regeneration reagent was decanted. Then the $(FMFA)_{opt}$ solid was washed with DI water two times and decanted. The $(FMFA)_{opt}$ containing conical flask was kept in the oven until a steady weight is reached. The weight of the flask was recorded and then another adsorption and desorption cycle was carried out. The weight loss of $(FMFA)_{opt}$ at each step was kept to a minimum (less than 0.05 g). The fluoride adsorption was measured after every adsorption cycle. This was repeated for 4 regeneration cycles.

4. RESULTS AND DISCUSSION

4.1 Establishment of the distribution of fluoride and Na/Ca ratios of potable water for different geographical locations in CKDu affected areas

The low quality of potable water, in CKD prevalent areas have been identified as the main culprit in CKDu prevalence. Annex 01 comprises of the literature used to obtain secondary water quality data of CKDu prevalent and non-prevalent areas. The summarized secondary data of Annex 01, for the CKDu prevalent and non-prevalent areas are presented in Table 4.1 and Table 4.2.

Table 4.1: The potable water quality of CKDu prevalent areas

Parameter	Max	Min
Average Na	221.41 mg/L	5.85 mg/L
Average Ca	690.90 mg/L	8.00 mg/L
Average Na/Ca ratio	6.60	0.07
Average F	10.57 mg/L	0.12 mg/L

Average sodium ion concentration was in the range of 5.85−221.41 mg/L, while the average calcium ion concentration was 8.00−690.90 mg/L. The distribution of calcium in potable water indicates that the CKDu prevalent areas comprise of hard and soft waters. Average Na/Ca vary between 0.07−6.60, while the fluoride ion concentration range between 0.12−10.57 mg/L.

The distribution of average Na/Ca ratios in CKDu prevalent areas with the respective fluoride levels is illustrated in Figure 4.1.

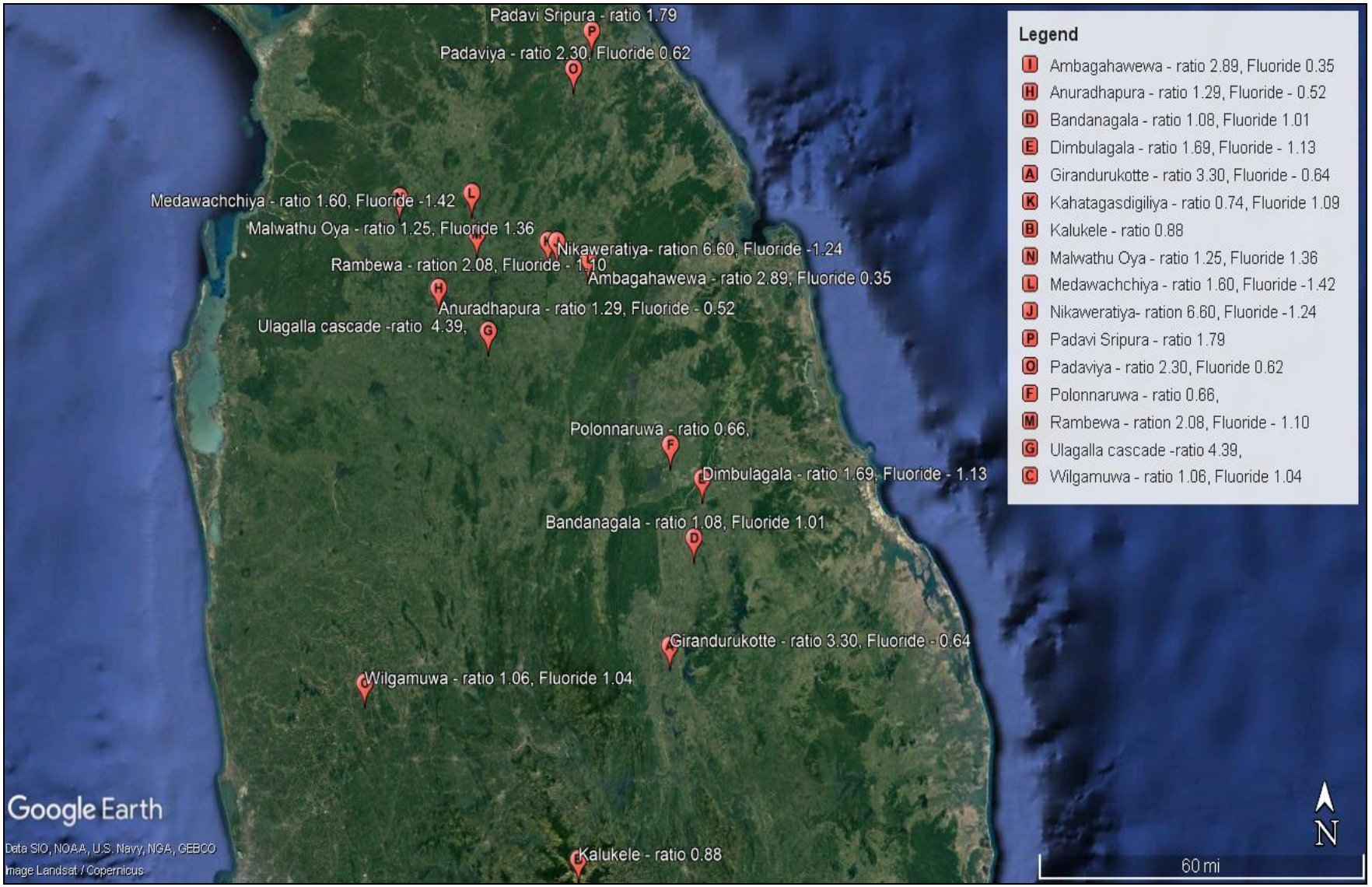

Figure 4.1: The distribution of Na/Ca ratios in CKDu prevalent areas.

Table 4.2: The potable water quality of CKDu non prevalent areas

Parameter	Max	Min
Average Na	561.00 mg/L	2.50 mg/L
Average Ca	66.81 mg/L	0.60 mg/L
Average Na/Ca ratio	469.10	0.37
Average F	1.05 mg/L	0.08 mg/L

Average sodium ion concentration was in the range of 2.50−561.00 mg/L, while the average calcium ion concentration was 0.60−66.81 mg/L The distribution of calcium in potable water indicates that the potable water in CKDu prevalent areas are mostly soft water. Average Na/Ca ratio vary between 0.37−469.10, while the average fluoride ion concentration range between 0.08−1.05 mg/L.

According to the secondary data given in Annex 01, it is evident that the Na/Ca ratio is distribution is lower across the CKDu prevalent areas. The distribution of average Na/Ca ratio with the respective fluoride values for CKDu prevalent and non-prevalent areas are given in Figure 4.2. The data show a close match with Paranagama, (2014) range of 0.17-2.63 given for CKDu prevalent areas. The critical area for the CKDu prevalence was identified to be within the area demarcated within the red box.

The majority of the water quality data of CKDu prevalent areas are located within the red box. There are some data points which have fluoride levels below 0.4 ppm value. The data points where fluoride levels are below 0.4 ppm were analyzed, it is evident that the calcium concentration in these areas are very high compared to sodium concentrations. The water quality data represent the mean values for both Na/Ca ratio and fluoride concentration. Therefore, extreme values reported in the areas may have contributed to the final water quality, making those data points appear as outliers. During this study the fluoride level of the CKDu prevalent areas is brought below 0.4 mg/L, as a solution to overcome the synergistic effect between Na/Ca ratio and fluoride.

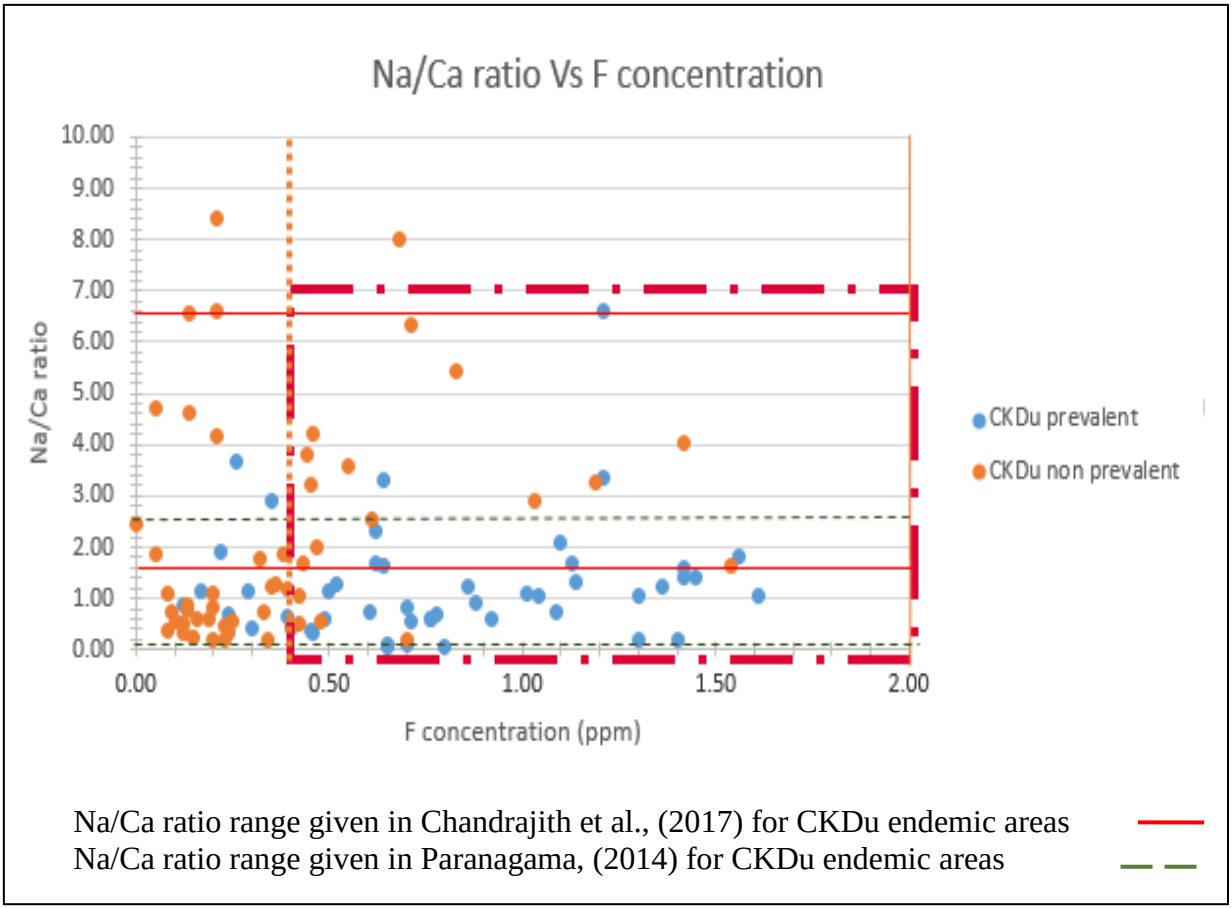

Figure 4.2: Critical ranges for Na/Ca ratio in CKDu prevalent areas

The correlation between the different water quality parameters in CKDu prevalent areas are given in Table 4.3. According to the correlation analysis, there is a weak positive correlation between Na concentration and Na/Ca ratio. A weak negative correlation between Ca concentration and Na/Ca ratio is also evident through the analysis. Weak positive correlation is there between Ca concentration and F concentration. A final conclusion on the correlation cannot be made due to the weak correlations the parameters exhibit between each other.

The correlation between the different water quality parameters for CKDu non-prevalent areas are indicated in Table 4.4. A strong positive correlation is between Na concentration and Ca concentration in CKDu non-prevalent areas.

Table 4.3: The correlation between the water quality parameters in CKDu prevalent areas.

		NaCKDu	CaCKDu	ratioCKDu	FCKDu
NaCKDu	Pearson Correlation	1	.174	.540**	.125
	Sig. (2-tailed)		.203	.000	.403
	N	55	55	55	47
CaCKDu	Pearson Correlation	.174	1	-.428**	.339*
	Sig. (2-tailed)	.203		.001	.020
	N	55	55	55	47
ratioCKDu	Pearson Correlation	.540**	-.428**	1	-.106
	Sig. (2-tailed)	.000	.001		.460
	N	55	55	61	51
FCKDu	Pearson Correlation	.125	.339*	-.106	1
	Sig. (2-tailed)	.403	.020	.460	
	N	47	47	51	51

**. Correlation is significant at the 0.01 level (2-tailed).

*. Correlation is significant at the 0.05 level (2-tailed).

Table 4.4: The correlation between the water quality parameters in CKDu non-prevalent areas.

		NaNonCKDu	CaNonCKDu	ratioNonCKDu	FNonCKDu
NaNonCKDu	Pearson Correlation	1	.774**	.025	.028
	Sig. (2-tailed)		.000	.839	.826
	N	68	68	68	65
CaNonCKDu	Pearson Correlation	.774**	1	-.125	-.041
	Sig. (2-tailed)	.000		.308	.744
	N	68	68	68	65
ratioNonCKDu	Pearson Correlation	.025	-.125	1	.014
	Sig. (2-tailed)	.839	.308		.914
	N	68	68	73	65
FNonCKDu	Pearson Correlation	.028	-.041	.014	1
	Sig. (2-tailed)	.826	.744	.914	
	N	65	65	65	65

**. Correlation is significant at the 0.01 level (2-tailed).

4.2 Optimization of fluoride removal efficiency of MFA

4.2.1. Synthesis and characterization of MFA (zeolite) using SEM, EDX, XRD and FTIR

The synthesized MFA (zeolite) was characterized using SEM, EDX, XRD and FTIR to analyze the different characteristics which will enable us to predict its morphology and structure. Table 4.5 gives the analyzing method with the relevant analysed characteristics.

Table 4.5: The Analyzing method with the relevant analyzed characteristics

Analyzing method	Analyzed character
ESEM-EDX	Morphology
	Chemical composition
XRD	Crystal structure
	Unit cell dimensions
	Sample purity
FTIR	Bonding pattern
	Functional groups

4.2.1.1. ESEM and EDX analysis (FA and MFA)

Morphology and elemental composition of FA and MFA (zeolite) was analyzed, using Environmental Scanning Electron Microscopy.

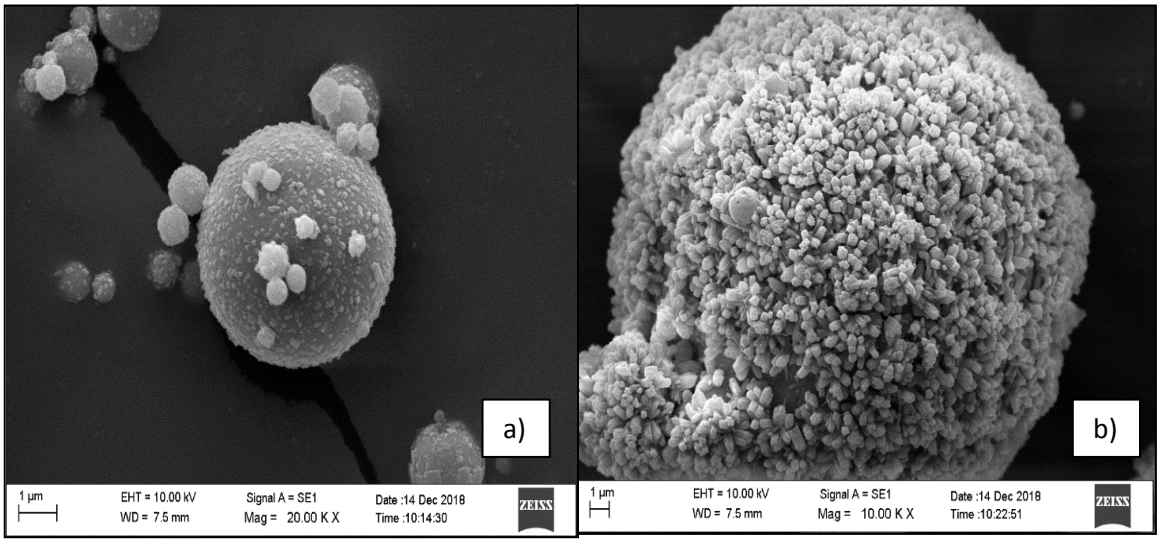

Figure 4.3: a) ESEM image of Coal fly ash (x50000), b) ESEM Image of Modified fly ash (zeolite) (x 50000)

Fly ash ESEM image as illustrated in Figure 4.3, appears in a spherical shape. The surface is smooth and dotted with small flecks. The ESEM image of MFA illustrates that the surface comprised with elongated sharp edged solid prisms. The surface is fully covered with these prisms, which are perpendicular to the surface.

The summary of the EDX analysis is given in Figure 4.4 and Table 4.4

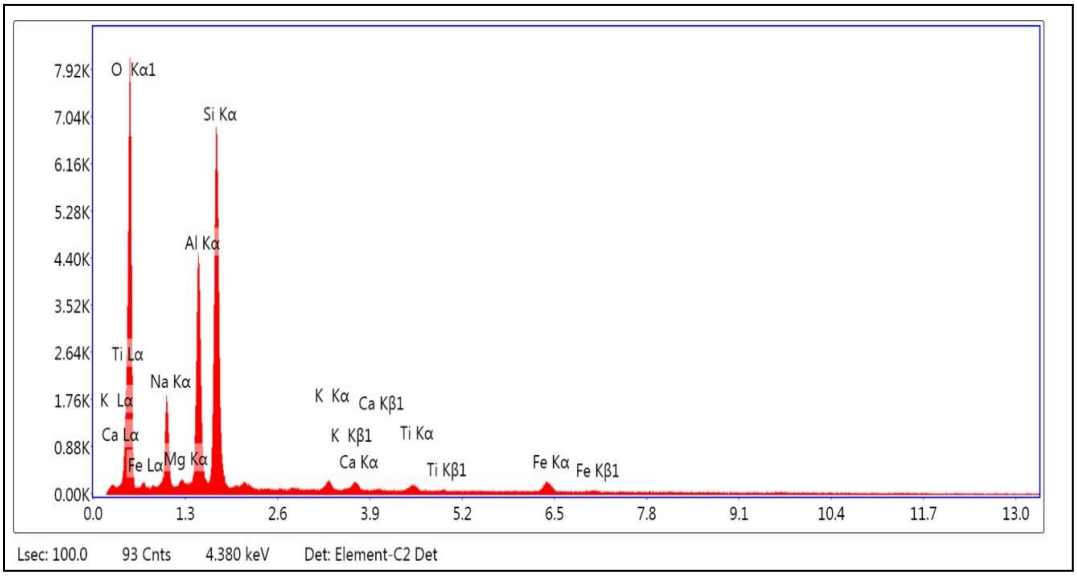

Figure 4.4: The EDX image of MFA

Table 4.6: The weight and atomic composition of the MFA (zeolite)

Element	Weight %	Atomic %
O	45.53	59.39
Al	14.54	11.25
Si	24.44	18.16
Na	9.14	8.3
Mg	0.35	0.3
K	0.91	0.49
Ca	1.06	0.55
Ti	0.97	0.42
Fe	3.05	1.14

The EDX analysis of MFA given in Table 4.6 confirms that the surface was composed of Si, O and Al without any other dominant impurities, while the diffraction narrow peaks confirmed the crystalline structure of MFA without any impurities. Similar observations on agglomeration and the formation of the crystalline structure of MFA have been reported by Manafia and Joughehdoustb, (2005) and Ferrarini et al., (2016).

4.2.1.2. XRD analysis of MFA

The XRD peak analysis of MFA is illustrated in Figure 4.5

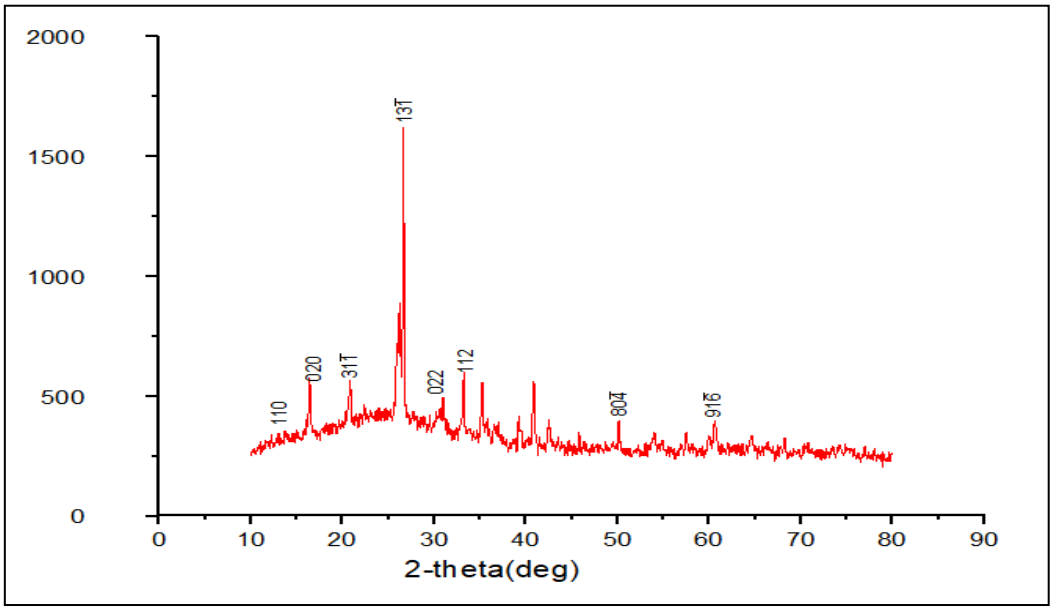

Figure 4.5: X-ray Powder Diffraction of MFA

Table 4.7: Peak list given for modified coal fly ash (zeolite) in XRD analysis

2-theta (deg)	d (ang.)	Phase name
12.397	7.134	Zeolite P, (Na)(1,1,0)
17.630	5.027	Zeolite P, (Na)(0,2,0)
21.64	4.102	Zeolite P, (Na)(3,1,-1)
28.031	3.180	Zeolite P, (Na)(1,3,-1)
30.98	2.884	Zeolite P, (Na)(0,2,2)
33.28	2.690	Zeolite P, (Na)(1,1,2)
51.38	1.776	Zeolite P, (Na)(8,0,-4)
62.80	1.478	Zeolite P, (Na)(9,1,-6)

Table 4.7 shows the X-ray diffraction (XRD) pattern of synthesised MFA, exhibiting peaks at 12.39°,17.63°,21.64°, 28.03°, 30.98°, 33.28°,51.38°, and 62.80°, which can be assigned to diffraction planes of (110), (020), (3-11), (13-1), (022), (112), (80-4), and (91-6), respectively. $Na_8(Al_8Si_8O_{32})(H_2O)_{15.17}$ is the formula given to P zeolite (Na). Querol et al., (2002) have reported the same observations, while the XRD library correctly matched the data with database card number 01-089-6322.

The average crystalline size of the MFA was calculated from the XRD spectrum using Scherrer Formula as given in Eq. 6 (Chekli et al., 2016).

$$D = \frac{0.9\lambda}{\beta \cos \Theta} \quad (6)$$

Where D is the average crystalline size, λ is the wavelength of the X-ray radiation, β is the full width of half maximum of a diffraction peak, and Θ is the angle of diffraction. The average crystalline size obtained from XRD data was 0.318 nm, which confirms that synthesised MFA was within the nano-scale.

4.2.1.3. FTIR analysis of MFA

The FTIR spectrum of MFA was obtained in order to verify the bond pattern and the functional groups. The FTIR image of MFA is illustrated in Figure 4.6 and the specific bands recorded are given in Table 4.8.

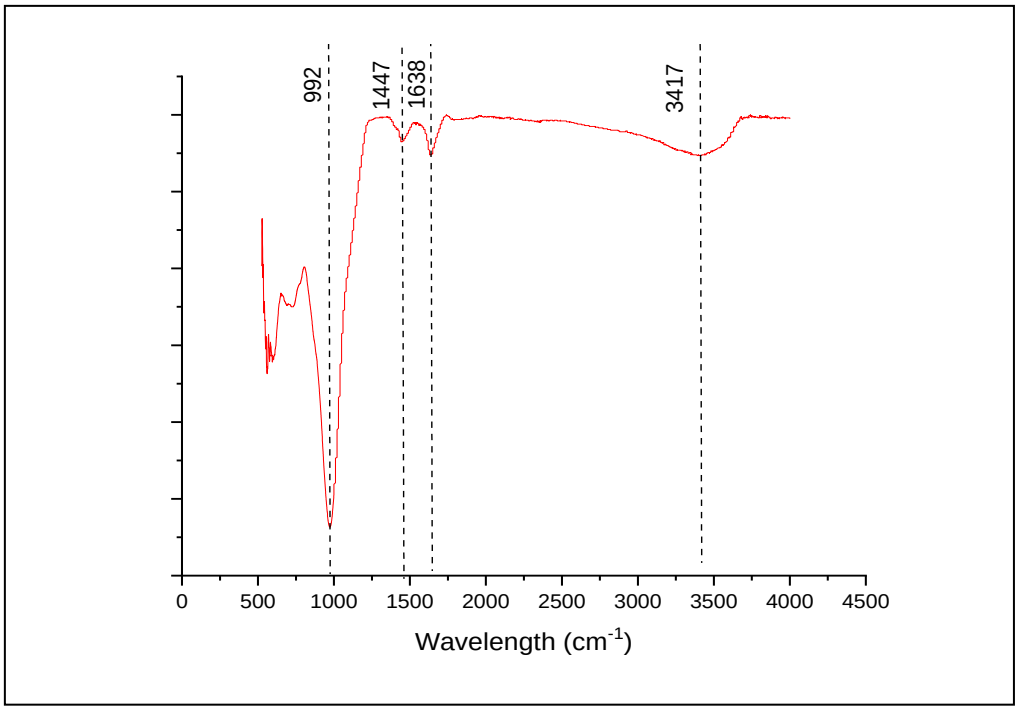

Figure 4.6: FTIR spectrum of MFA (zeolite)

Table 4.8: The specific bands recorded in FTIR spectrum and their corresponding bonds

Band	Corresponding bond
3417.07	O-H stretching vibration
1635.83	Bending vibration of water
1447.83	O-H stretching vibration
992.31	Si-O sym.stretching
595.17	Al-O stretching
576.00	Al-O stretching
560.33	Al-O stretching

Source: Mozgawa et al., (2011); Zholobenko et al., (1998); de Peña and Rondón, (2013)

The FTIR spectrum of MFA shows the specific peaks which reflect the surface functional groups, and the complex nature of the surface of MFA. MFA shows broad bands around the wavelengths given in Table 4.8. According to band analysis, it could be inferred that the structure that was proposed by XRD analysis, is compatible with the FTIR results obtained.

According to all structural and morphological analysis, MFA, that is synthesized is identified to have the structure of P zeolite. This is one of the structures that could be synthesized using a coal fly ash modification. The structure of P zeolite (modified from Ramírez, et al., 2013) is illustrated in Figure 4.7.

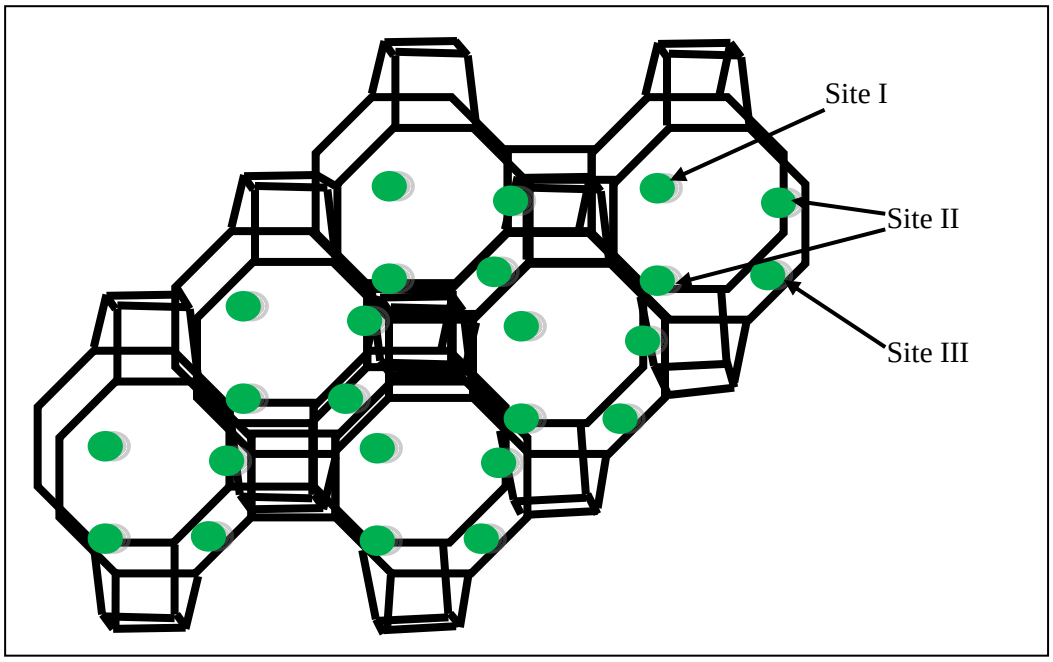

Figure 4.7: The structure of P zeolite and available sites for modification (modified from Ramírez, et al., 2013)

P zeolite has a similar structure to that of Gismondine. This zeolite's framework is characterized by perpendicular double crankshaft chains of tetrahedra. These tetrahedra are connected at all corners, thus forming pore systems that consist of two eight-membered ring (8 MR) channels connected by four-membered rings (4 MRs). This topology has a high framework flexibility, which allows the accommodation of a wide range of extra- framework cations (Celestian et al., 2003; Tripathi, et al., 2000).

There are three sites for cations; sodium ions are located on both sides of the eight-ring channels, coordinated to the walls of both 8 MR channels, allowing passage through the channels (Tripathi, et al., 2000).

P zeolite comprise of Si/Al ratio of 1.46, with a specific surface area of 51.58 gcm^{-3} as determined by BET method (S_{BET}). P zeolite has a total pore volume of 0.124 cm^3g^{-1} (Ramírez et al, 2013), therefore is used as a gas adsorbent.

4.2.2. Synthesis and characterization of FMFA

4.2.2.1. The incorporation of MgO, CaO and Al_2O_3 in to MFA (zeolite)

The modification of MFA is done through the use of different volume ratios of $Mg(NO_3)_2$, $Ca(NO_3)_2$, $Al_2(NO_3)_3$ solutions. The modification process does not exactly produce the FMFA with the original amount of metal nitrate composition. In some embodiments, the amount of impregnated metal in metal exchanged and impregnated MFA may fully occupy the metal exchange sites or might not occupy at all.

The final products (FMFA1-FMFA5) were sonicated for 15 minutes prior to use, to remove the excess metal oxides hindering the adsorption sites. The initial adsorption studies devoid of the washing step resulted in low adsorption levels, therefore, the washing step was opted to remove the excess metal oxides deposited on the adsorbent surface. Array of FMFA was crushed and sieved before it was used in the experiment to increase the active surface area of the adsorbent.

The array of FMFA is illustrated in Figure 4.8. The colour of MFA has changed from grey to light brown when modified. It can be inferred that the oxide formation on the surface of MFA structure was responsible for the colour change.

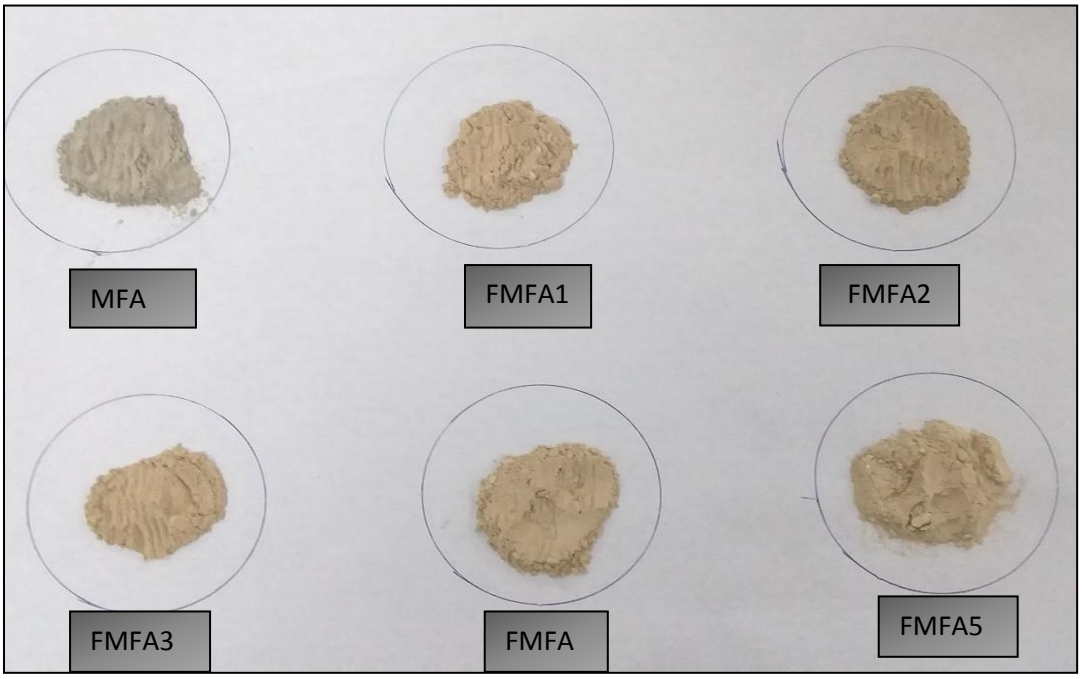

Figure 4.8: The array of functionalised MFAs

According to Vithanage and Bhattacharya, (2015) alumina was recognized as the major oxide which could remove the fluoride from water, therefore different ratios of aluminium nitrate solutions was used for Z2 and Z3 as indicated in Table 3.1. Z4 had higher $Mg(NO_3)_2$ volume ratio and was used for in defluoridation. The major focus of this study was to minimize or eliminate Ca^{2+} ion adsorbed using a CaO embedded adsorbent surface. All three oxides were used to maximize the efficiency of the defluoridation. These three oxides have been individually used in defluoridation but modification of MFA using all three oxides has not been attempted.

The proposed structure for FMFA and the proposed modification process is shown in Figures 4.9 and 4.10 respectively.

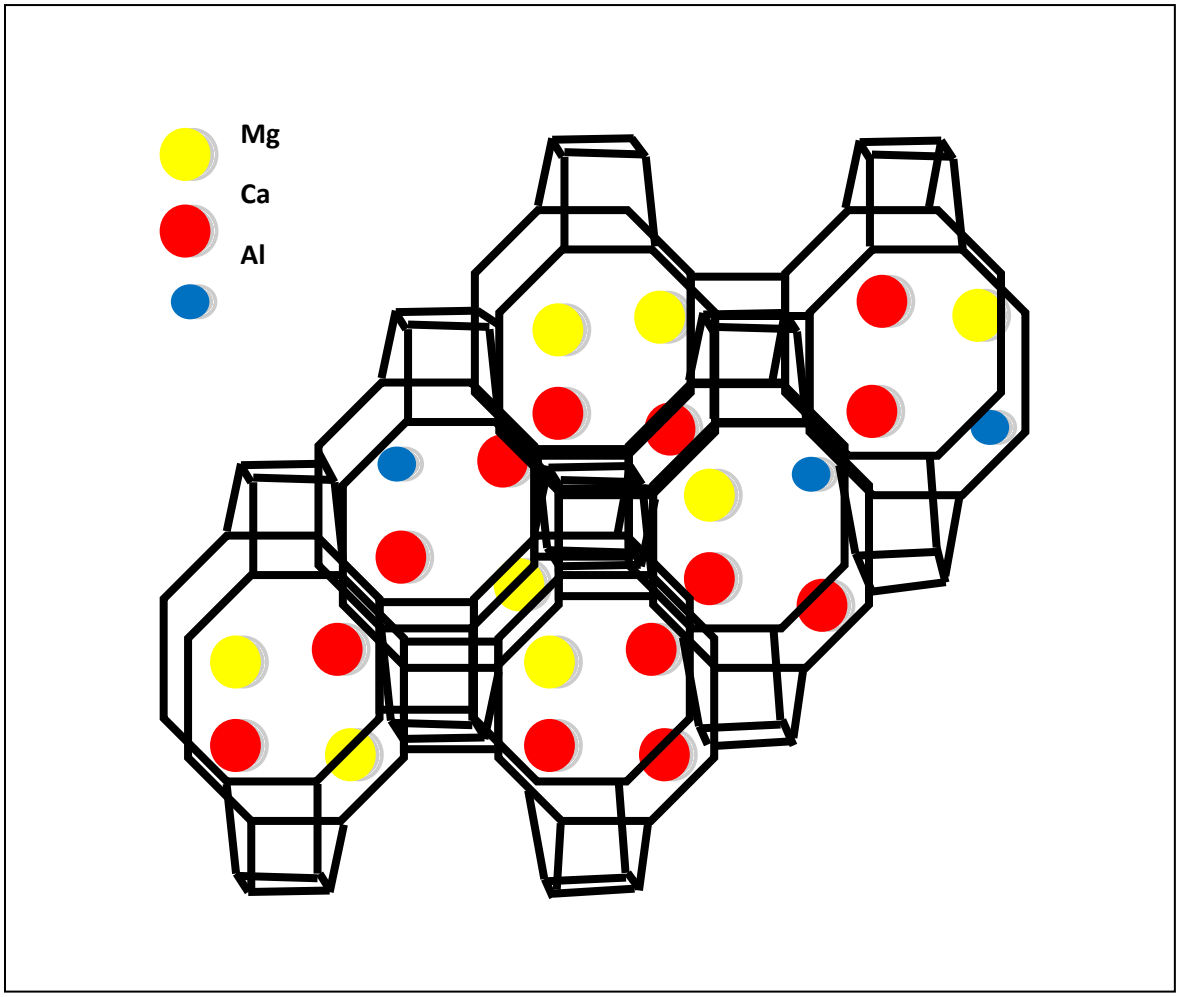

Figure 4.9: The proposed FMFA structure

The FMFA synthesis was a result of trial and error, in an attempt to obtain a new defluoridation material. As MFA is a low cost adsorbent, modification of it with metal oxides have improved its defluoridation efficiency. The increase in efficiency was evident in the batch studies that were conducted following the synthesis.

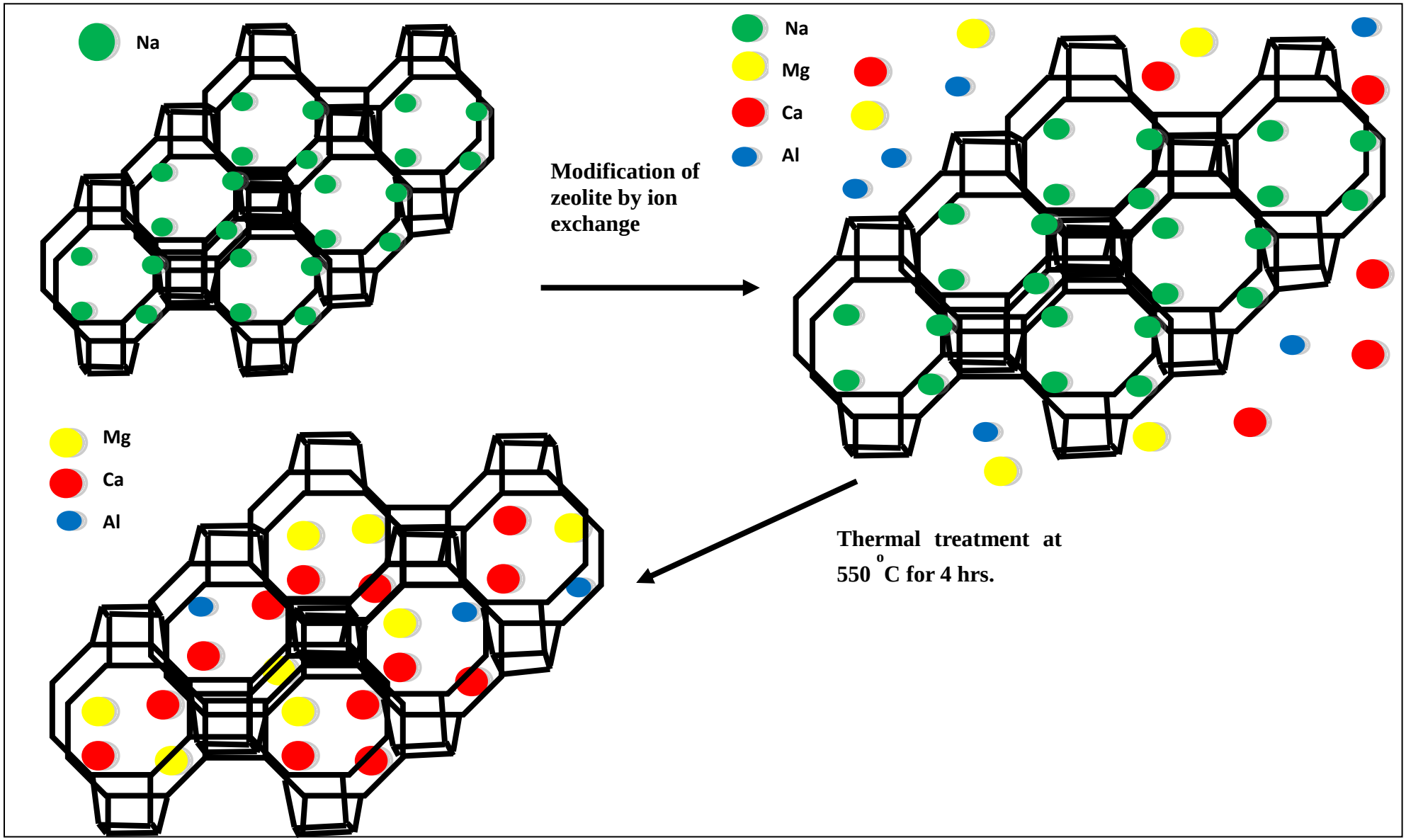

Figure 4.10 : The proposed mechanism for the functionalization of MFA

4.3 Evaluate the efficiency of different arrays of FMFA for the removal of Fluoride

4.3.1. Single-solute studies for removal of Fluoride

The defluoridation was carried out using synthesised MFA and FMFAs. A mass of 0.5 g of all materials was used in the defluoridation studies. The concentrations of 5 ppm, 3 ppm and 2 ppm were used to evaluate the defluoridation of the material. The final fluoride concentrations reached and defluoridation percentage for all materials are given in Table 4.9 and Table 4.10.

Table 4.9: The final fluoride concentrations reached by each material following defluoridation with respect to changes in initial concentrations (5 ppm, 3 ppm, 2 ppm)

Material	**5 ppm**		**3 ppm**		**2 ppm**	
	Final F^- concentration (ppm)	**SD**	**Final F^- concentration (ppm)**	**SD**	**Final F^- concentration (ppm)**	**SD**
FMFA5	4.199	0.071	0.830	0.035	0.439	0.009
FMFA4	4.526	0.007	1.202	0.212	0.517	0.007
FMFA3	4.448	0.014	1.350	0.007	0.639	0.007
FMFA2	4.823	0.007	0.961	0.007	0.665	0.014
FMFA1	4.862	0.014	1.110	0.014	0.555	0.015
MFA	5.048	0.074	1.495	0.007	0.660	0.001

Table 4.10: The defluoridation percentage of MFA and FMFAs at different initial fluoride concentrations

Material	5 ppm	SD	3 ppm	SD	2 ppm	SD
FMFA5	28.18	1.06	74.78	0.14	80.07	1.56
FMFA4	21.57	1.16	63.58	5.11	76.56	0.98
FMFA3	22.83	1.14	58.81	1.51	71.08	1.21
FMFA2	16.43	1.24	70.94	1.07	70.59	1.23
FMFA1	19.03	6.01	66.56	1.23	75.57	1.02
MFA	11.72	1.31	54.40	1.68	70.41	1.24

According to Table 4.10 it can be clearly seen that MFA exhibits lowest adsorbance capacity at all concentration levels. The concentration of 5 ppm showed the lowest defluoridation for all materials (Figure 4.11). The highest concentrations were used to determine whether the materials are capable of defluoridation at high levels of fluoride, if such levels were present in potable water. These materials showed very low absorbency indicating that the materials cannot be used when high concentration fluoride is present in potable water.

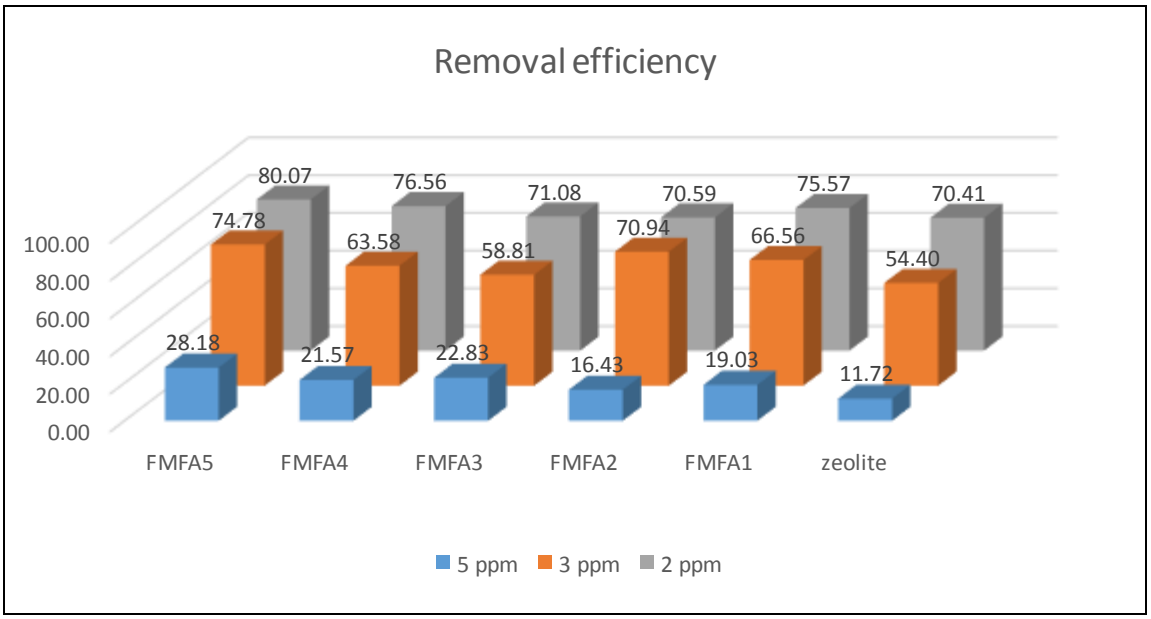

Figure 4.11: The removal efficiency of the adsorbents MFA and FMFAs

The concentration of 3 ppm and of materials. FMFA5 and FMFA2 showed significantly higher fluoride adsorbance at 3 ppm, but this was not adequate for to be used as a good adsorbent. All material exhibited high adsorbance at the concentration of 2 ppm. When material were compared, FMFA5 was identified as the most efficient in defluoridation with the final fluoride concentration reaching an average of 0.439 ppm. This is below the 0.5 ppm level recommended by WHO for the tropical countries and the closest to our desired fluoride level of 0.4 ppm. This value was obtained for a mass of 0.5 g, prior to dosage optimization. Therefore FMFA5 was selected as the most efficient material for defluoridation. Hereafter FMFA5 will be referred to as $(FMFA)_{opt}$.

4.3.2. Single-solute studies for removal of calcium

The calcium removal of the different materials was studied to identify a material for the exclusive removal of fluoride when Ca and Na is present in the potable water. Ca has the highest affinity towards MFA rather than Na, therefore the concentration of Ca was recorded after adsorption to determine whether the Na/Ca ratio is affected by the adsorption. Table 4.11 gives the calcium removal by the materials.

Table 4.11: The final calcium concentrations with respective removal efficiencies for the different adsorbents

Material	Initial Ca^{2+} concentration (ppm)	Final Ca^{2+} Concentration (ppm)	% Adsorbance
FMFA5	200	198	1.01
FMFA4	200	196	2.04
FMFA3	200	198	1.01
FMFA2	200	195	2.56
FMFA1	200	188	6.38
MFA	200	165	21.21

It was conceptualized that when metal oxide nanoparticles are dispersed in a cation or anion exchanger, the anions or cations will be rejected by the respective ion exchanger according to the Donnan coion exclusion rule effect. According to this principle an amphoteric metal oxide nano particle can be tailored to behave either as a strictly metal selective sorbent or as a ligand selective exchanger (Sen Gupta, 2017).

In the MFA modification the nano calcium oxide particles will be dispersed on the MFA, rejecting calcium ions because of the resulting hybrid anion exchanger (FMFA) as illustrated in Figure 4.12. This phenomena also can be observed when nano MgO and nano Al_2O_3 dispersed in MFA.

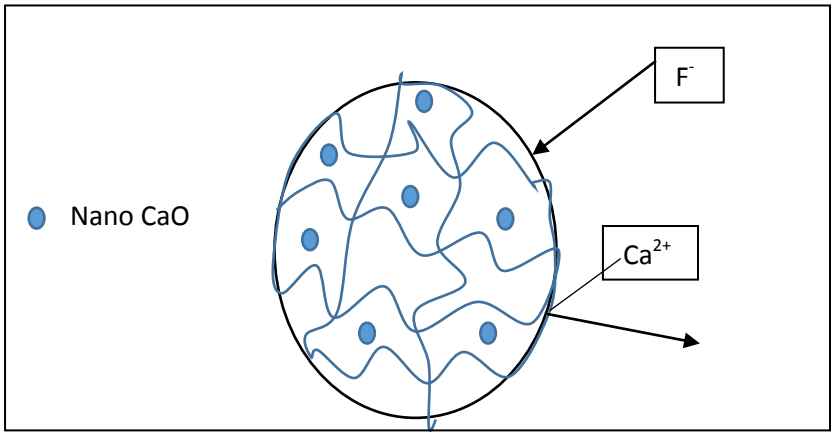

Figure 4.12: The structure of hybrid anion exchanger (FMFA)

The results given in Table 4.11 implied that the calcium removal of the FMFAs was very low. MFA in the other hand removed calcium to levels higher than that of the FMFAs. All the FMFAs show low calcium removals making the materials ideal for eliminating all synergistic effects that can occur when both fluoride and calcium ions were simultaneously present in potable water. Therefore, $(FMFA)_{opt}$ exhibiting the lowest calcium removal, with highest fluoride removal was selected as the ideal material for multi solute studies.

4.4 Characterization of $(FMFA)_{opt}$ using SEM, EDX, XRD and FTIR

4.4.1. ESEM-EDX analysis

4.4.1.1. ESEM-EDX analysis of $FMFA_{opt}$

The ESEM image of MFA and synthesized $(FMFA)_{opt}$ (Figure 4.13) shows a remarkable difference between the material surfaces.

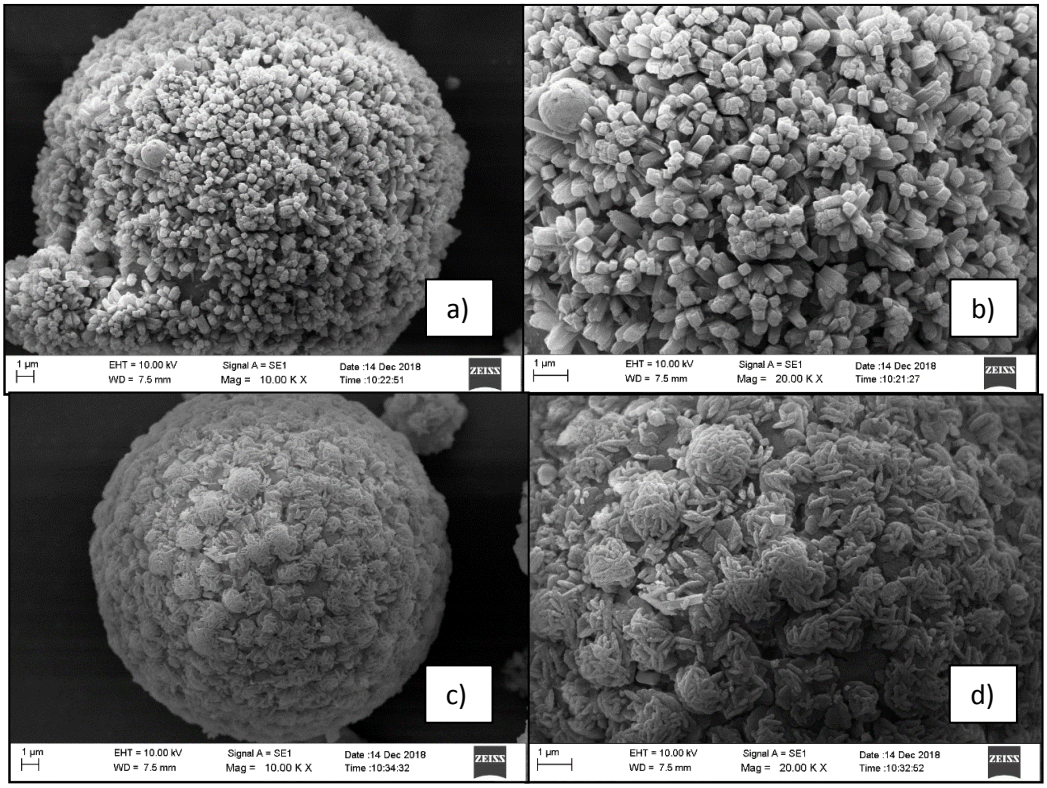

Figure 4.13: a) The SEM Image of MFA (10000x), b) The SEM Image of MFA (50000x), c) The SEM Image of $(FMFA)_{opt}$ (10000x), d) The SEM Image of $(FMFA_{)opt}$ (50000x)

MFA surface comprises of elongated, sharp edged, solid prisms. The surface is fully covered with these prisms perpendicular to the surface. In contrast the $(FMFA)_{opt}$ SEM image clearly shows small aggregates of elongated **worm-like structures**. These aggregates are covering the $(FMFA)_{opt}$ surface. There are small nodules like structures beneath the aggregates. The solid prism crystals that were present in MFA is covered by the nodular shaped layers and the aggregates in $(FMFA)_{opt}$.

EDX analysis confirms the incorporation of calcium and magnesium on the surface of the $(FMFA)_{opt}$. The Figure 4.14 portrays the elemental distribution of MFA and $(FMFA)_{opt}$.

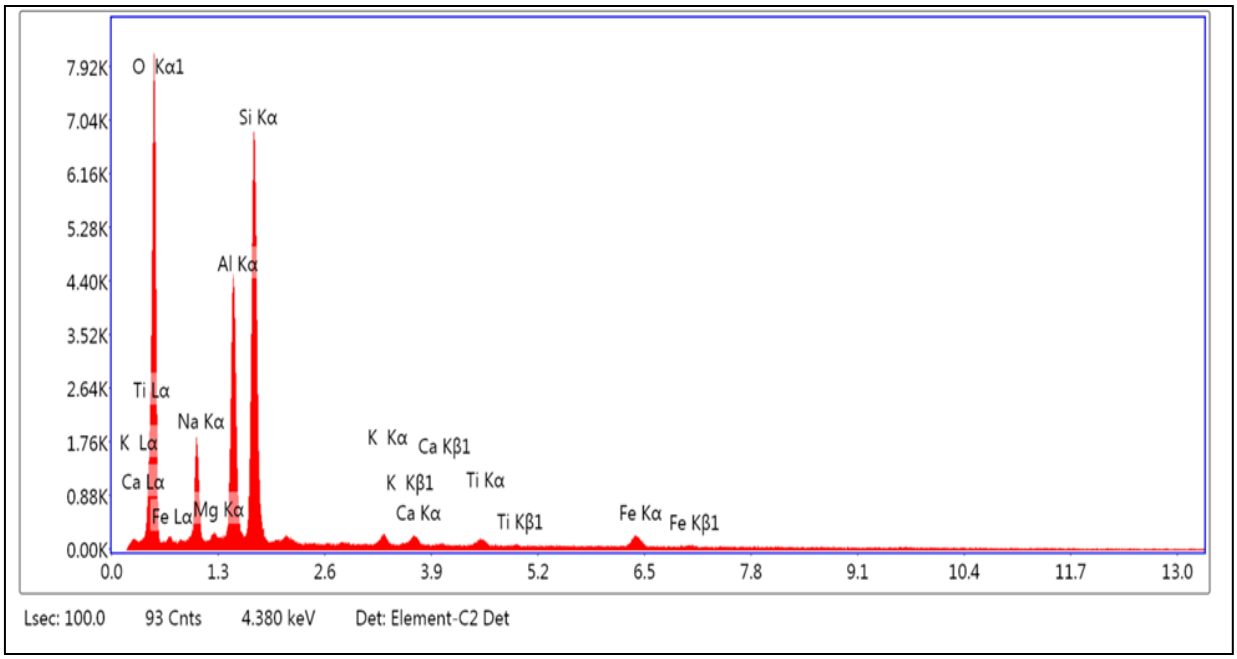

Figure 4.14: Energy-Dispersive X-ray Spectroscopy of $(FMFA)_{opt}$

The EDX data of MFA and $(FMFA)_{opt}$ are summarized in Table 4.12. The EDX data were analyzed to determine the weight and atomic changes that have occurred in $(FMFA)_{opt}$ after MFA modification.

Table 4.12: The EDX data of MFA and $(FMFA)_{opt}$

	MFA		$(FMFA)_{opt}$	
Element	Weight %	Atomic %	Weight %	Atomic %
O	45.53	59.39	48.91	63.72
Na	9.14	8.3	3.24	2.94
Mg	0.35	0.3	0.44	0.38
Al	14.54	11.25	13.42	10.37
Ca	1.06	0.55	2.59	1.35
Si	24.44	18.16	25.3	18.78
K	0.91	0.49	0.92	0.49
Ti	0.97	0.42	0.82	0.36
Fe	3.05	1.14	4.36	1.63

$(FMFA)_{opt}$ is a functionalized MFA. The Na weight percentage was reduced from 9.14 in MFA to 3.24 in $(FMFA)_{opt}$, indicating the replacement of the Na atoms by Ca or Mg ion oxides. Aluminium that was present in MFA, have been replaced by Ca or Mg atoms, since the weight percentage dropped from 14.54 in MFA to 13.42 in $(FMFA)_{opt}$. The weight drop indicates that during the synthesis of $(FMFA)_{opt}$, incorporation of Mg and Ca has been prioritized over the incorporation of aluminium. The weight percentage of oxygen had increased, indicating the oxide formation after calcination of $(FMFA)_{opt}$. The EDX data confirms that the MFA functionalization had been successful.

4.4.2. XRD analysis $(FMFA)_{opt}$

As illustrated in Figure 4.15, X-ray diffraction (XRD) pattern of synthesised $(FMFA)_{opt}$ exhibit peaks at 16.42°, 20.86°, 26.19°, 26.64°, 30.90°, 33.22°, 35.23°, 40.83°, 42.45°, 57.49°, 60.63°. Zeolite characteristic peak is available in $(FMFA)_{opt}$ XRD analysis, therefore it can be concluded that $(FMFA)_{opt}$ possess the same crystalline structure as P zeolite.

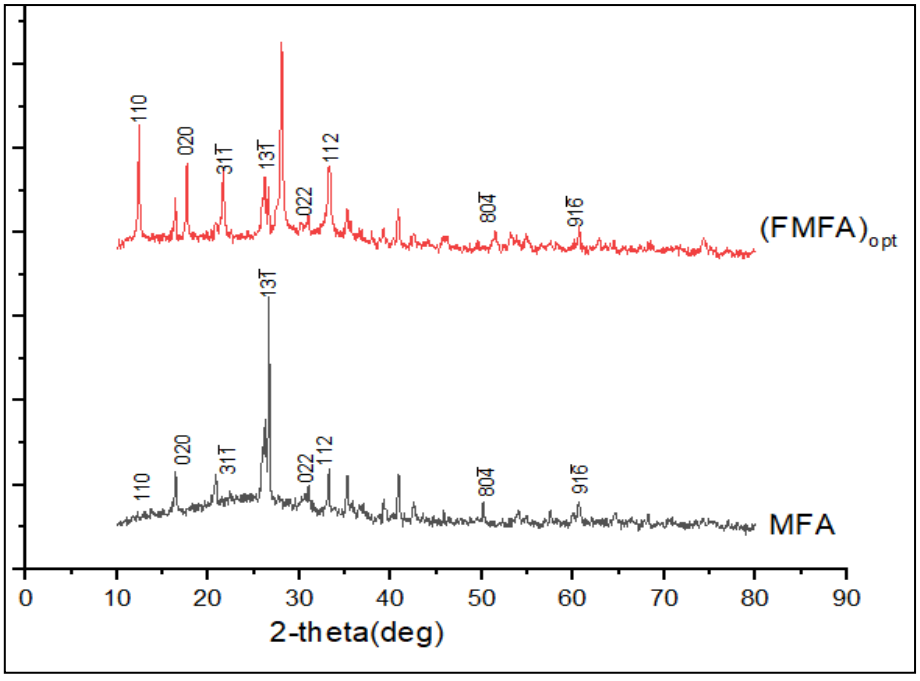

Figure 4.15: X-ray Powder Diffraction image for MFA and $(FMFA)_{opt}$

All samples showed similar diffraction peaks as the parent MFA. Peaks attributed to the oxides of the alkaline earth metals were absent. The only notable difference is the intensities of diffraction peaks. It was observed that the addition of Mg, Ca and Al led to an increase in some diffraction peaks of $(FMFA)_{opt}$. The degree of crystallinity remained unchanged.

4.4.3. FTIR analysis of $(FMFA)_{opt}$

The FTIR spectrum of $(FMFA)_{opt}$ was obtained in order to verify the bond pattern and the functional groups. The FTIR image is illustrated in Figure 4.16. The specific bands recorded in FTIR spectrum for $(FMFA)_{opt}$ and the corresponding bonds are indicated in Table 4.13.

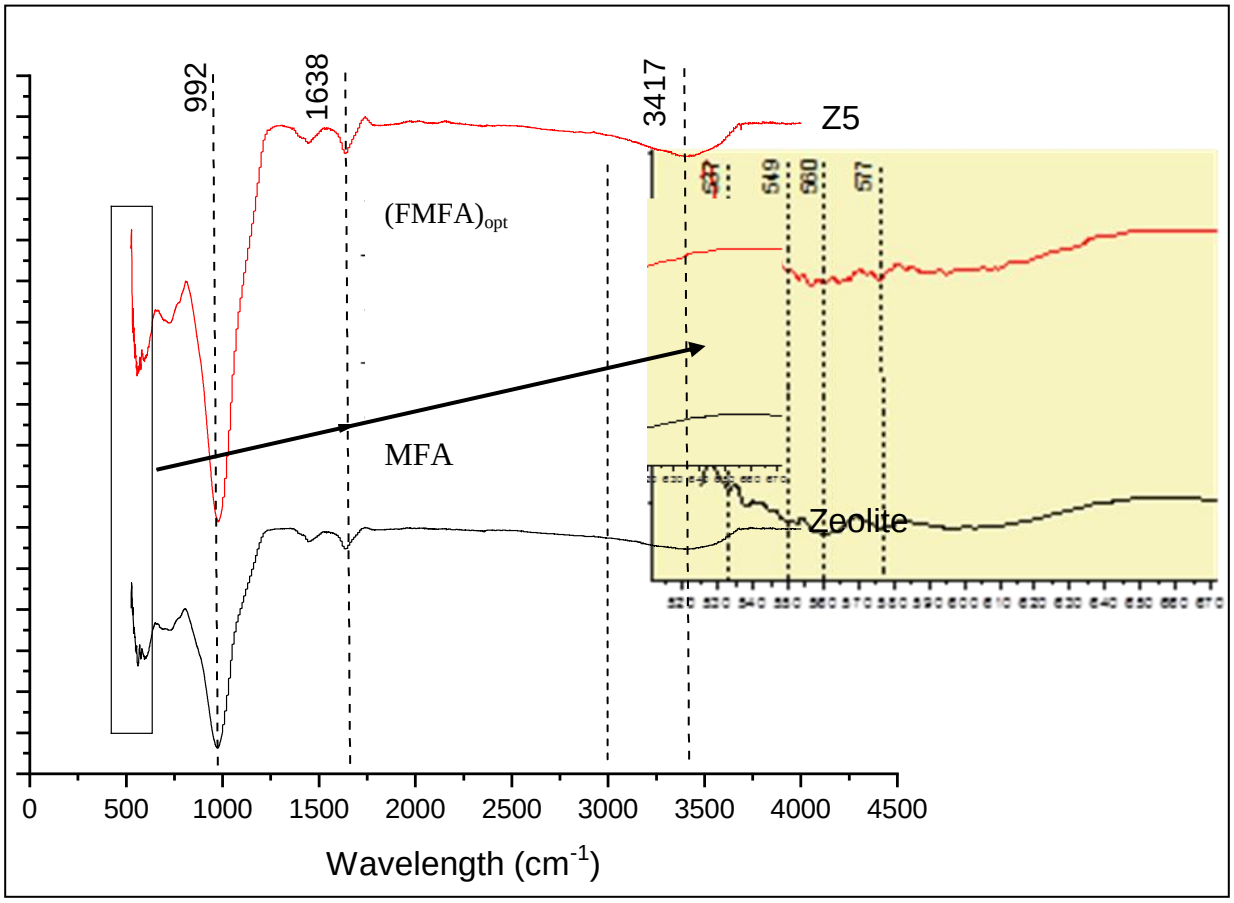

Figure 4.16: FTIR spectrum of $(FMFA)_{opt}$

Table 4.13: The specific bands recorded in (FMFA)opt FTIR spectrum with the corresponding bonds

Band	Corresponding bond
992.26	Si-O sym.stretching
722.79	Si–O–Si stretching
583.63	Ca=O
565.1	Al-O stretching
560.36	Al-O stretching
549.12	Mg-O
537.54	Ca-O
525.95	Ca-O

Source: Zholobenko et al., (1998); de Peña and Rondón, (2013); Choudhary et al., (2015); Djebaili, et al., (2015)

The FTIR spectrum of MFA and $(FMFA)_{opt,}$ gives the specicific peaks reflecting the surface functional groups. MFA shows broad bands around 992, 1632, and 3417 cm^{-1}, which were attributed to Si-O stretching, O–H bending, and O–H stretching vibrations, respectively (Zholobenko et al., 1998; Peña and Rondón, 2013; Choudhary et al., 2015; Djebaili, et al., 2015). The Functionalization give specific peaks in the range of 525-583 cm-1 corresponding to Mg-O, Ca-O and Al-O bonds as indicated in Table 4.13.

4.4.4. ESEM of fluoride adsorbed $(FMFA)_{opt}$

$(FMFA)_{opt}$ exhibited an impressive defluoridation. The SEM images of $(FMFA)_{opt}$, before and after adsorption are given in Figure 4.17. The elongated worm like structures are not seen in fluoride adsorbed $(FMFA)_{opt}$. The fluoride adsorbed $(FMFA)_{opt,}$ has a smooth surface with respect to virgin $(FMFA)_{opt.}$

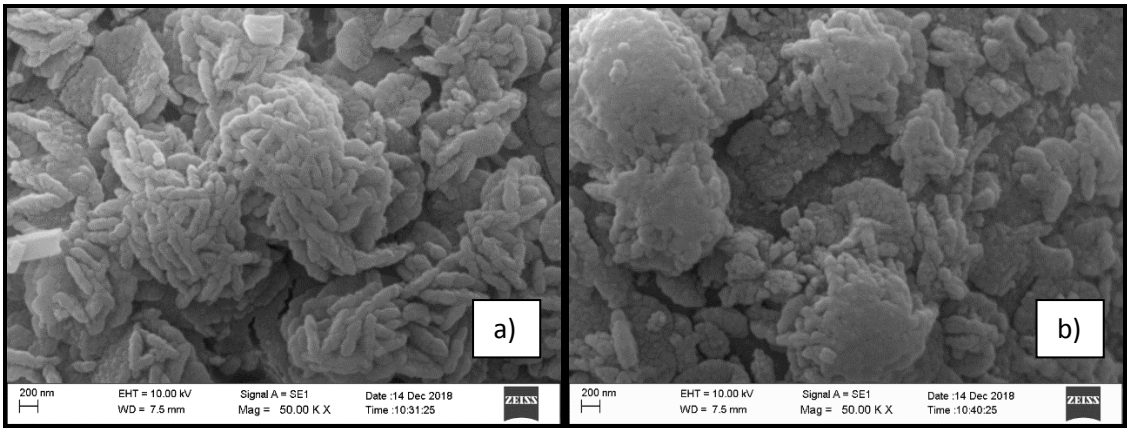

Figure 4.17: a) The SEM Image of (FMFA)opt (50000x) b) The SEM Image of (FMFA)opt after fluoride adsorption (50000x)

4.4.5. FTIR analysis of fluoride adsorbed $(FMFA)_{opt}$

The FTIR spectrum of $(FMFA)_{opt}$ after adsorption was obtained in order to verify the bond pattern and the functional groups. The FTIR image and the recorded bands with the corresponding bonds of $(FMFA)_{opt}$ are illustrated in Table 4.14 and Figure 4.17, respectively.

Table 4.14: The specific bands recorded in fluoride adsorbed $(FMFA)_{opt}$ spectrum and their corresponding bonds

Band	Corresponding bond
3417.69	O-H stretching vibration
1638.54	bending vibrations of water
988.57	Si-O sym. stretching
714.6	Si–O–Si stretching

Source: Zholobenko et al., (1998); Peña and Rondón, (2013); Choudhary et al., (2015); Djebaili, et al., (2015).

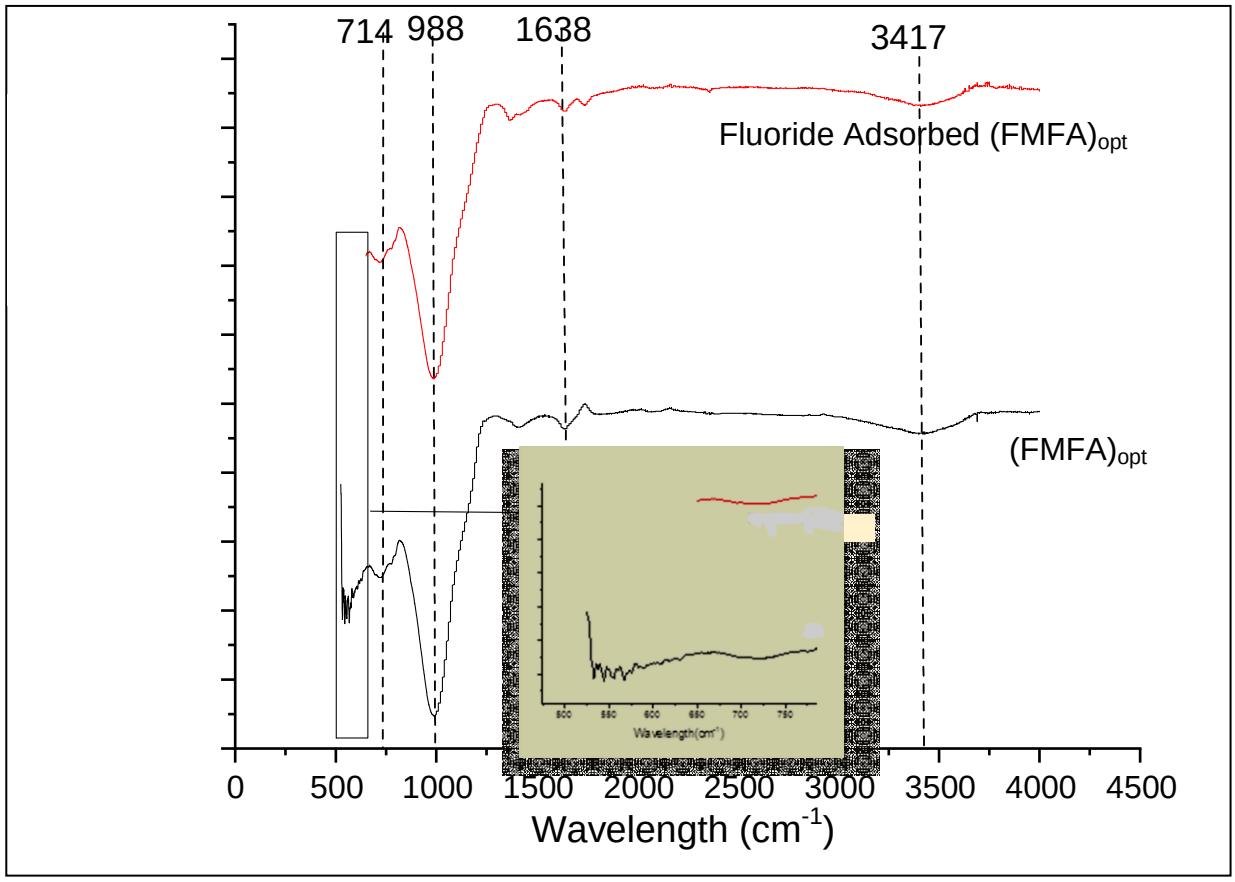

Figure 4.18: FTIR spectrum of $(FMFA)_{opt}$ and fluoride adsorbed $(FMFA)_{opt}$

The FTIR spectrums display the specific peaks reflecting the surface functional groups of $(FMFA)_{opt}$ prior to defluoridation. $(FMFA)_{opt}$ exhibited broad bands around 988, 1638, and 3417 cm^{-1}, which were attributed to Si-O stretching, O–H bending, and O–H stretching vibrations, respectively (Zholobenko et al., 1998; Peña and Rondón, 2013; Choudhary et al., 2015; Djebaili, et al., 2015). After defluoridation the intensities of the main peaks of (FMFA)opt have reduced, and the fingerprint region peaks were absent, indicating the reduction of available free bonds corresponding to functional groups in the fingerprint region.

4.5 Optimization of experiment condition for the (FMFA)opt for the removal of fluoride

4.5.1. Optimum dosage

The dosage studies were carried out with dosages from 0.5 g to 2.8 g at 0.2 g intervals. The contact time was 24 hours to facilitate in achieving the equilibrium between adsorbent and the solution. The initial concentration of the solution was maintained at 2.140 ± 0.084 ppm. The results of the batch study are illustrated in Table 4.15.

Table 4.15: The optimum dosage selection for $(FMFA)_{opt}$

Dosage (g)	Final F^- concentration (ppm)	SD	Removal efficiency (%)
0.5	0.460	0.007	78.50
1	0.450	0.005	78.98
1.2	0.435	0.000	79.66
1.4	0.425	0.001	80.13
1.6	0.418	0.001	80.48
1.8	0.384	0.006	82.04
2	0.364	0.011	82.99
2.2	0.355	0.013	83.39
2.4	0.389	0.001	81.81
2.5	0.407	0.007	80.98
2.6	0.560	0.007	73.81
2.8	0.811	0.013	62.09

According to the dosage selection for batch studies, the optimum adsorption was observed at 2.2 g (Figure 4.18). The increase in the dosage, reduces the adsorption and this phenomena can be attributed to the agglomeration of particles.

Agglomeration is a process by which smaller particles combine to form larger structures with the aid of a binding mechanism. Agglomeration occur in the presence of a binder or in the absence of a binder. There are some adsorption processes which require agglomeration (eg: Fluidized bed) while some processes of adsorption would require less of agglomeration.

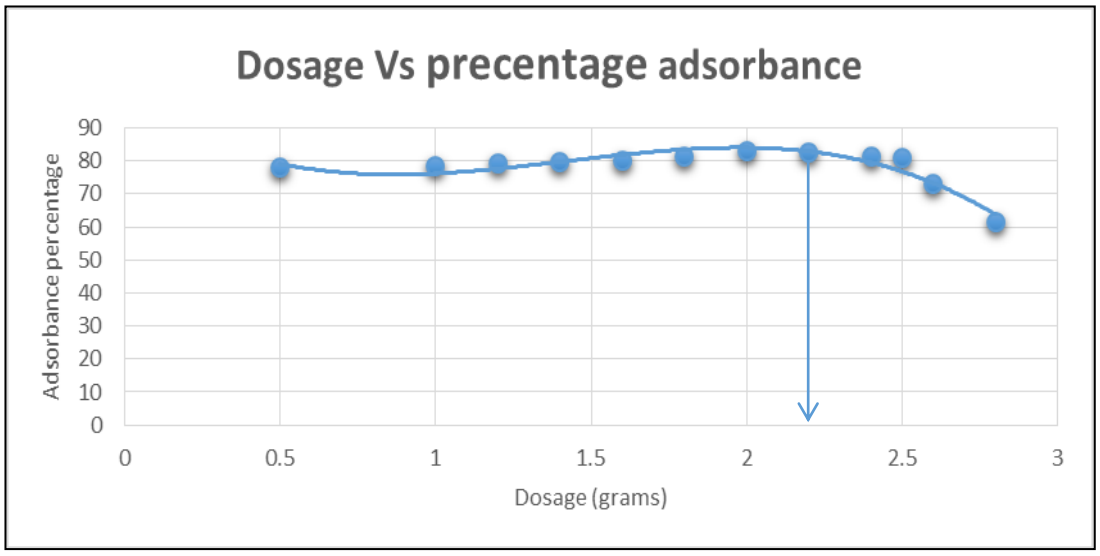

Figure 4.19: $(FMFA)_{opt}$ dosage VS percentage adsorbance

The basic binding mechanisms between two solid parts occur via liquid bridges, sintering bridges, chemical reactions, molecular electrostatic forces, and capillary forces. Figure 4.20 illustrates the mechanisms of agglomeration.

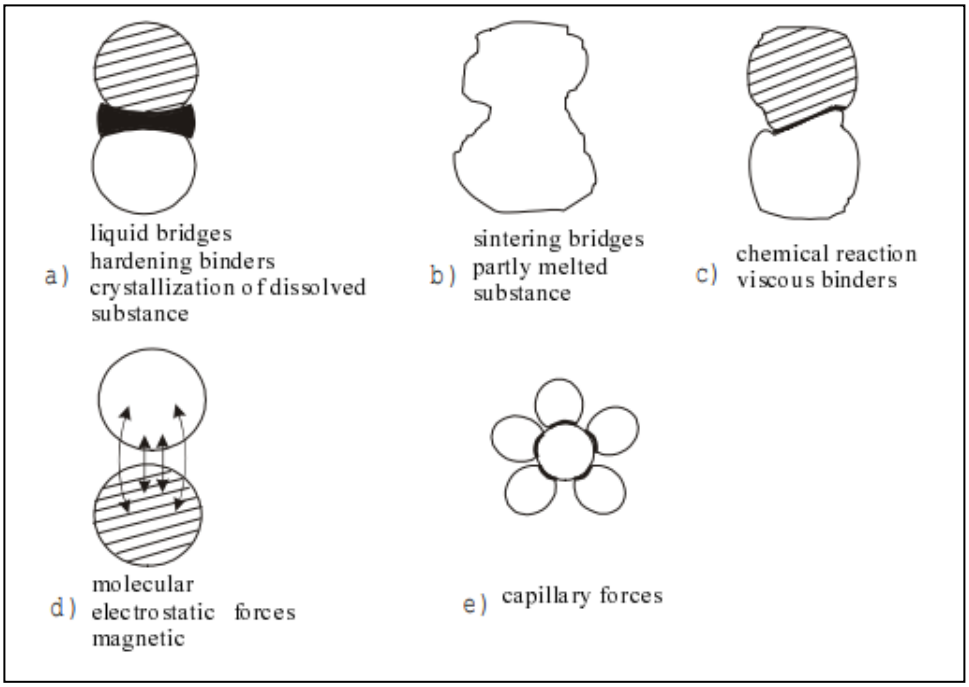

Figure 4.20: Basic binding mechanisms between two solid particles (Knez et al., 2001)

The smaller solid particles which are smaller than 10 µm will spontaneously form agglomerates when intensively mixed (Knez et al., 2001). In this batch reaction binders were absent, therefore does not contribute for the agglomeration process. $(FMFA)_{opt}$ was mechanically stirred during the batch study, promoting the agglomeration process The density of particles that came in contact with each other increased with the increase of the dosage, thereby giving rise to agglomeration. In $(FMFA)_{opt}$ the agglomeration can occur due to all basic binding mechanisms. Agglomeration will reduce the active surface area for adsorption, thereby giving lower adsorbance with increasing dosage. The lower fluoride/adsorbent ratio results due to the reduction in availability of fluoride ions per unit mass of adsorbent (Wang et al, 2009). The optimum dosage of 2.2 g was used for all the subsequent batch studies, for $(FMFA)_{opt}$ adsorbent.

4.5.2. Optimum contact time

The optimum contact time trials were carried out between 2 minutes to 300 minutes (5 hrs.). The optimum dosage of 2.2 g was used for the batch studies. The adsorbance results are given in Table 4.16 and Figure 4.20.

Table 4.16: The optimum contact time for $(FMFA)_{opt}$ for defluoridation

Time	Final Concentration	SD	Removal efficiency
0	2.263	0.012	0.0
2	2.203	0.006	2.6
5	1.897	0.006	16.2
10	1.540	0.017	32.0
15	0.670	0.017	70.4
30	0.627	0.031	72.3
60	0.553	0.012	75.6
120	0.347	0.006	84.7
180	0.313	0.006	86.2
240	0.287	0.006	87.3
300	0.247	0.006	89.1

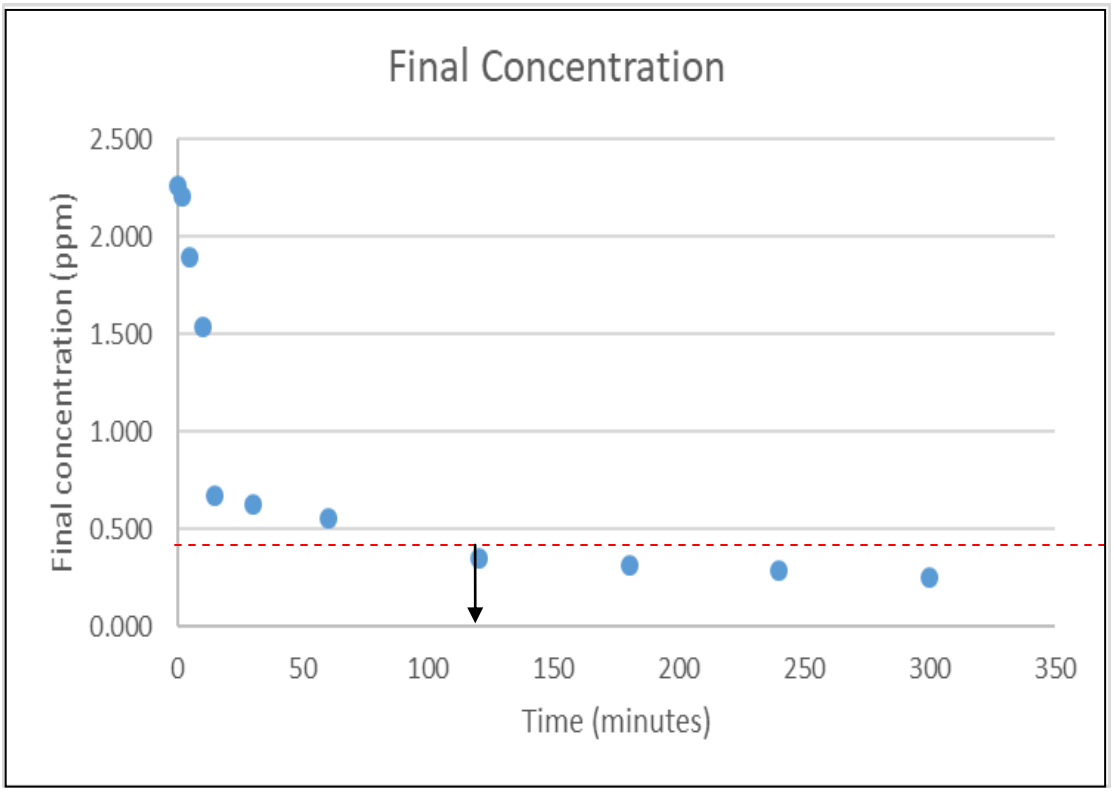

Figure 4.21 : Final concentration of fluoride vs. the contact time

In the course of the optimum contact time selection batch studies, (Figure 4.20), fluoride level reached the desirable fluoride level of 0.4 ppm after 2 hours. The final fluoride level reached 0.347 ppm and this fulfils our requirement of the final potable water concentration being less or equal to 4 ppm. When the contact time is increased further the adsorption will also increase. The optimum contact time was selected as 2 hours for the future batch studies. Further research could be done to determine the level of defluoridation for prolonged periods. In this study the main focus was the final desired fluoride level (4 ppm or less) for potable water with a minimum contact.

4.5.3. Optimum pH

The optimum pH was obtained using batch studies. A mass of 2.2 g of $(FMFA)_{opt}$ together with the contact time of two hours and a stirring speed of 100 rpm was used for the study. The initial fluoride concentration was 2.2785 ± 0.01 mg/L. The results of the batch studies are illustrated in Table 4.17.

Table 4.17: The optimum pH investigation for $(FMFA)_{opt}$

pH	Final F^- concentration (ppm)	SD	Defluoridation percentage
2	1.89	0.035	17.3
3	1.50	0.028	34.2
4	0.94	0.014	58.7
5	0.54	0.021	76.5
6	0.32	0.035	86.2
7	0.33	0.028	85.5
8	0.31	0.014	86.4
9	0.91	0.021	60.3
10	1.94	0.028	14.9
11	2.15	0.021	5.9
12	2.18	0.028	4.3

The results of the batch studies illustrated in Figure 4.22, depict that the optimum pH is 6.8. The pH 6.8 is similar to the pH of potable water that prevail in CKDu prevalent areas (Rango, 2014; Chandrajith et al., 2011; Wikramarathne et al., 2017; Jayasumana et al., 2015; Levine et al., 2016). Therefore $(FMFA)_{opt}$ can be used for defluoridation, without an acidification or basification of potable water. This is one of the advantages of the selected material.

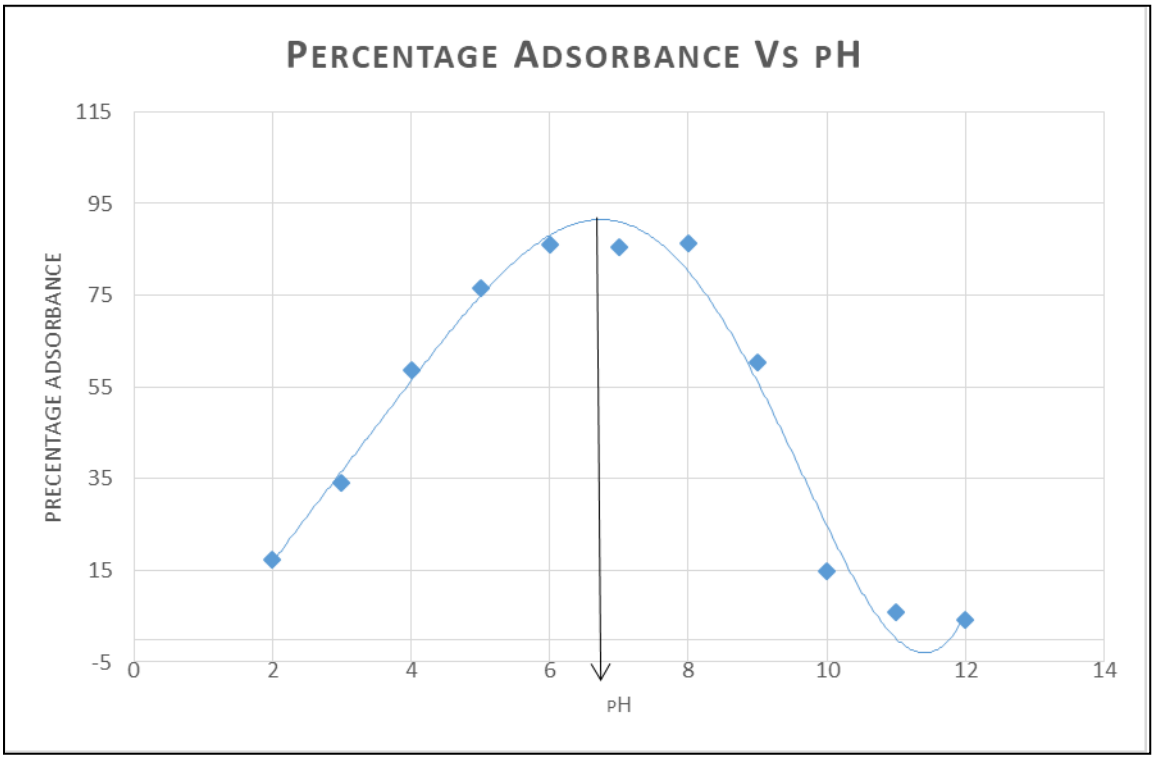

Figure 4.22: The percentage adsorbance of the (FMFA)opt with changing pH

As the adsorption mechanism is not always an electrostatic interaction between the adsorbate and the adsorbent. The pH of zero point charge (pH_{zpc}) is used to explain either the adsorption mechanism follows an electrostatic or another mechanism. The point of zero charge is the pH at which the surface of an adsorbent is globally neutral. In a pH below this value, the surface is positively charged; beyond this value, it is negatively charged. It is always easier to adsorb a cation on a negatively charged surface, and an anion on a positively charged surface (Kosmulski, 2009). The values of pH_{zpc} for zeolites are summarized in table 4.18.

Table 4.18: A summary of pH_{zpc} for zeolites

Material	Electrolyte	Temperature (^oC)	pH_{zpc}	Reference
ZSM-5 zeolite from Lanzho	0.001-0.1M $NaNO_3$	20	3.6	Shao et al., 2009
H-MFI-24 zeolite from Sud-Chemie	0.1 M $NaNO_3$	20	6.8	Chutia et al., 2009
H-MFI-90 zeolite from Sud-Chemie	0.1 M $NaNO_3$	20	3.6	Chutia et al., 2009
Zeolite from Vranjska Banja	0.1 M $NaNO_3$	20	6.5-7.5	Šljivić et al., 2009

The experiment results indicated that the optimum pH is pH 6.8, and at this point $(FMFA)_{opt}$ surface should be positively charged to adsorb fluoride ions. Therefore the pH_{zpc} for $(FMFA)_{opt}$ can be a higher value than pH 6.8. Therefore, the high efficiency in acidic medium can be attributed to the gradual increase in attractive forces, and low efficiency in alkaline medium can be explained by the repulsion between the negatively charged surface and fluoride (Mahramanlioglu et al., 2002).

The adsorption of fluoride at low pH ($pH<pH_{pzc}$) can be explained by a two-step protonation/ligand exchange reaction mechanism where Ca, Mg or Al is denoted as X.

$$XOH + H^+ \longrightarrow XOH^{2+}$$

$$XOH^{2+} + F^- \longrightarrow XF + H_2O$$

Which gives the net reaction:

$$XOH + H^+ + F \longrightarrow XF + H_2O$$

Similar reaction methodology was given in Wang et al., (2009) for defluoridation performance and mechanism of nano- scale aluminium oxide hydroxide, in an aqueous solution. The mechanism of the reaction is illustrated in Figure 4.23.

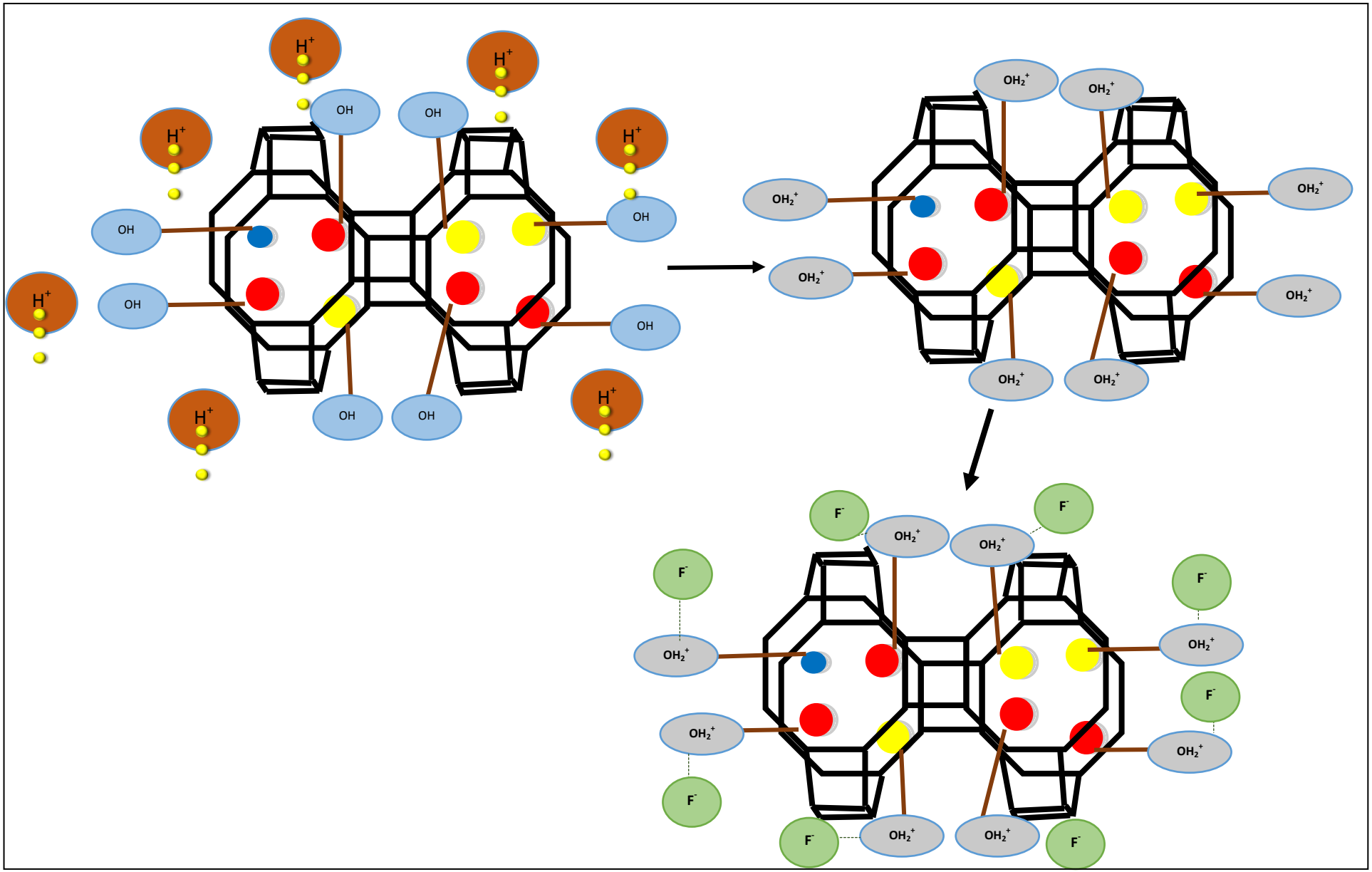

Figure 4.23: The fluoride adsorption mechanism for $(FMFA)_{opt}$

However, other interactions may be stronger than purely electrostatic forces, making the effect of surface charge not so important. Additionally, other mechanisms can also occur such as complexation, dissolution and precipitation. The zeta potential of $(FMFA)_{opt}$ at a well-defined pH value should be measured in order to point out that $(FMFA)_{opt}$ has a positively charged surface at pH 6.8.

Natural zeolite has a characteristic negatively charged surface, making it a good cation exchanger (Colella, 1996). The functionalization of MFA surface has given rise to a positively charged surface when in contact with the aqueous medium, so $(FMFA)_{opt}$ act as a good fluoride adsorbent.

4.6 Removal of different fluoride levels with different Na/Ca ratios using $(FMFA)_{opt}$

Identification of optimum levels for $(FMFA)_{opt}$ was carried out before commencing the main part of the research, which is the defluoridation in the presence of different Na/Ca ratios in potable water.

The experiment was conducted with the use of hard water. According to the literature review, potable water in CKDu prevalent areas is hard water. Therefore the calcium concentration was kept constant at 200 mg/L for all batch studies to demonstrate the high calcium concentration. The Na/Ca ratios of 01, 03 and 07 were selected for the study. The three ratios are within the Na/Ca ratios reported within CKDu prevalent areas.

The results of the batch study are given in Table 4.19 to Table 4.21.

Table 4.19: The defluoridation of (FMFA)opt with varying concentration with Na/Ca ratio of 01

Initial F^- concentration (ppm)	Final F^- concentration (ppm)	SD	Q_e (mg/g)	SD
4.00	0.956	0.006	0.138	0.098
3.50	0.762	0.003	0.124	0.088
3.00	0.646	0.006	0.107	0.076
2.50	0.441	0.013	0.094	0.066
2.00	0.366	0.023	0.074	0.052
1.50	0.297	0.004	0.055	0.039

Table 4.20: The defluoridation of (FMFA)opt with varying concentration with Na/Ca ratio of 03

Initial F^- concentration (ppm)	Final F^- concentration (ppm)	SD	Q_e (mg/g)	SD
4.00	0.853	0.004	0.143	0.101
3.50	0.762	0.003	0.124	0.088
3.00	0.561	0.001	0.111	0.078
2.50	0.464	0.006	0.093	0.065
2.00	0.348	0.003	0.075	0.053
1.50	0.294	0.006	0.055	0.039

Table 4.21: The defluoridation of (FMFA)opt with varying concentration with Na/Ca ratio of 07

Initial F^- concentration (ppm)	Final F^- concentration (ppm)	SD	Q_e (mg/g)	SD
4.00	0.758	0.003	0.147	0.104
3.50	0.447	0.259	0.139	0.104
3.00	0.527	0.004	0.112	0.080
2.50	0.411	0.001	0.095	0.067
2.00	0.306	0.008	0.077	0.054
1.50	0.251	0.001	0.057	0.040

The removal of fluoride indicated that with the increase of Na/Ca ratio, defluoridation also increased. The most probable mechanism operating for fluoride adsorption in the presence of sodium, by $(FMFA)_{opt}$ can be depicted as follows:

$$XOOH_yH_2O\ (solid) + Na^+\ (aq) + F^-\ (aq) \rightarrow XOOH_{(y-1)}H_2OOH{-}Na^+F^-\ (solid) + H^+(aq)$$

The mechanism of defluoridation in the presence of sodium is illustrated in Figure 4.24.

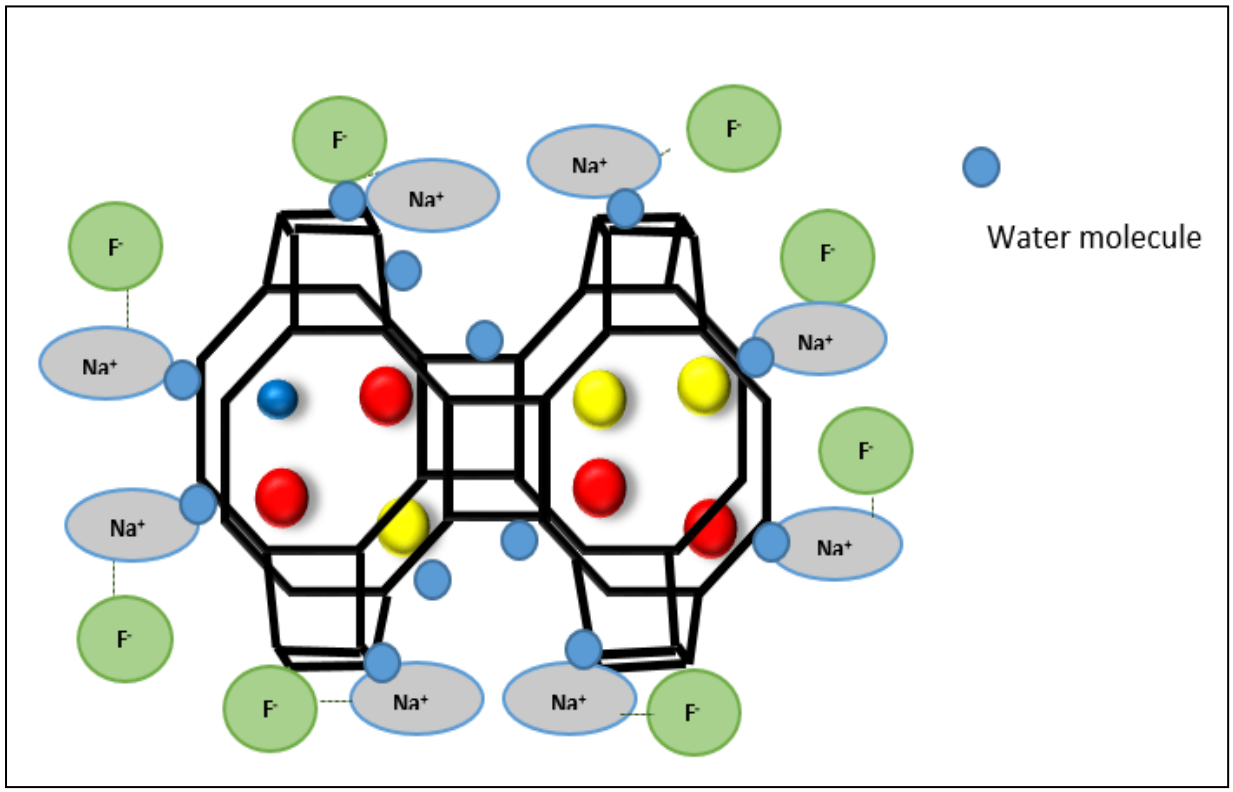

Figure 4.24: mechanism operating for defluoridation in the presence of sodium, by (FMFA)opt

The mechanism is a result of the surface layer hydration. The surface hydration will form an electrostatic bond with Na ions which will then attract the F ions to the surface. The increase in the sodium ion concentration will result in the increase of fluoride adsorption to the surface due to the above explained phenomena. A similar mechanism is also explained in Wang et al., (2009) for nano scale aluminium oxide. This is true if the Na/Ca ratio of the treated solution has changed significantly, which is contridictary with the proposed Donnan coion exclusion principle.

The calcium removal of $(FMFA)_{opt}$ at different Na/Ca levels are given in Table 4.22 to Table 4.24.

Table 4.22: The Calcium removal by (FMFA)opt with varying concentration when Na/Ca ratio is 01

Initial Concentration of fluoride (ppm)	Initial Concentration of calcium (ppm)	Final Concentration of calcium (ppm)	Calcium removal efficiency (%)
4.00	200.33	198.22	1.1
3.50	200.33	195.66	2.3
3.00	200.33	192.33	4.0
2.50	200.33	193.55	3.4
2.00	200.33	195.65	2.3
1.50	200.33	194.33	3.0

Table 4.23: The Calcium removal by (FMFA)opt with varying concentration when Na/Ca ratio is 03

Initial Concentration of fluoride (ppm)	Initial Concentration of calcium (ppm)	Final Concentration of calcium (ppm)	Calcium removal efficiency (%)
4.00	200.56	198.22	1.2
3.50	200.56	195.66	2.4
3.00	200.56	192.33	4.1
2.50	200.56	193.55	3.5
2.00	200.56	195.65	2.4
1.50	200.56	194.33	3.1

Table 4.24: The Calcium removal by (FMFA)opt with varying concentration when Na/Ca ratio is 07

Initial Concentration of fluoride (ppm)	Initial Concentration of calcium (ppm)	Final Concentration of calcium (ppm)	Calcium removal efficiency
4.00	200.75	198.35	1.2
3.50	200.75	194.55	3.1
3.00	200.75	192.33	4.2
2.50	200.75	196.55	2.1
2.00	200.75	195.65	2.5
1.50	200.75	196.55	2.1

In Figure 4.25 the calcium removal efficiency at different Na/Ca ratios are illustrated.

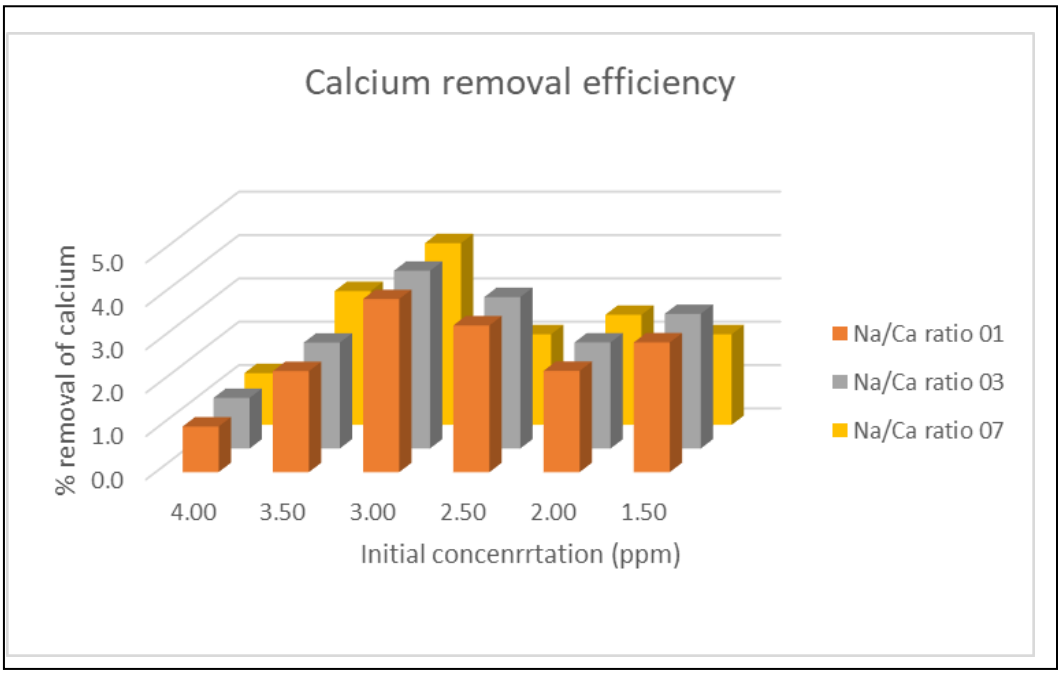

Figure 4.25: The calcium removal efficiency at different Na/Ca ratios

4.7 Adsorption Isotherms and kinetic studies for $(FMFA)_{opt}$

4.7.1. Adsorption Isotherms

A series of batch experiments were conducted to determine the adsorption isotherm behaviour of $(FMFA)_{opt}$. The results were fitted to both Langmuir and Fraundlich models.

The results of adsorption studies for different Na/Ca ratios, fitted to Langmuir model are given in Table 4.25 to Table 4.26. A volume of 100 mL of the Na/Ca ratio 01 solution with 2.2 g of $(FMFA)_{opt}$ was used for the experiment. The equations 01, 02 and 03 were used in the calculations to determine the favourability of the reaction.

$$Q_e = (C_o - C_e) \times \frac{V}{W} \quad (1)$$

$$\frac{1}{Q_e} = \frac{1}{Q_m} + \frac{1}{Q_m K_L C_e} \quad (2)$$

$$R_L = \frac{1}{[\,1 + (1 + K_L C_o)]} \quad (3)$$

Where C_e is the equilibrium concentration of adsorbate (mg/L), Q_e is the amount of adsorbate adsorbed per unit mass of the adsorbent at equilibrium (mg/g), Q_m is maximum monolayer coverage capacity (mg/g), and K_L is the Langmuir isotherm constant (L/mg).

The Langmuir isotherm and data for defluoridation with $(FMFA)_{opt}$ when Na/Ca ratio is 01 is given in Figure 4.26 and Table 4.25, respectively.

Table 4.25: The adsorption data of Na/Ca ratio 01, fitted to Langmuir model

Initial fluoride concentration (mg/L)	Final fluoride concentration (mg/L)	V/M (L/g)	Qe (mg/g)	1/Qe (g/mg)	Ce (mg/L)	1/Ce (L/mg)
4.000	0.960	0.045	0.138	7.23	0.96	1.04
3.500	0.760	0.045	0.125	8.04	0.76	1.32
3.000	0.650	0.045	0.107	9.35	0.65	1.54
2.500	0.450	0.045	0.093	10.68	0.45	2.22
2.000	0.350	0.045	0.075	13.46	0.35	2.86
1.500	0.300	0.045	0.055	18.29	0.30	3.33

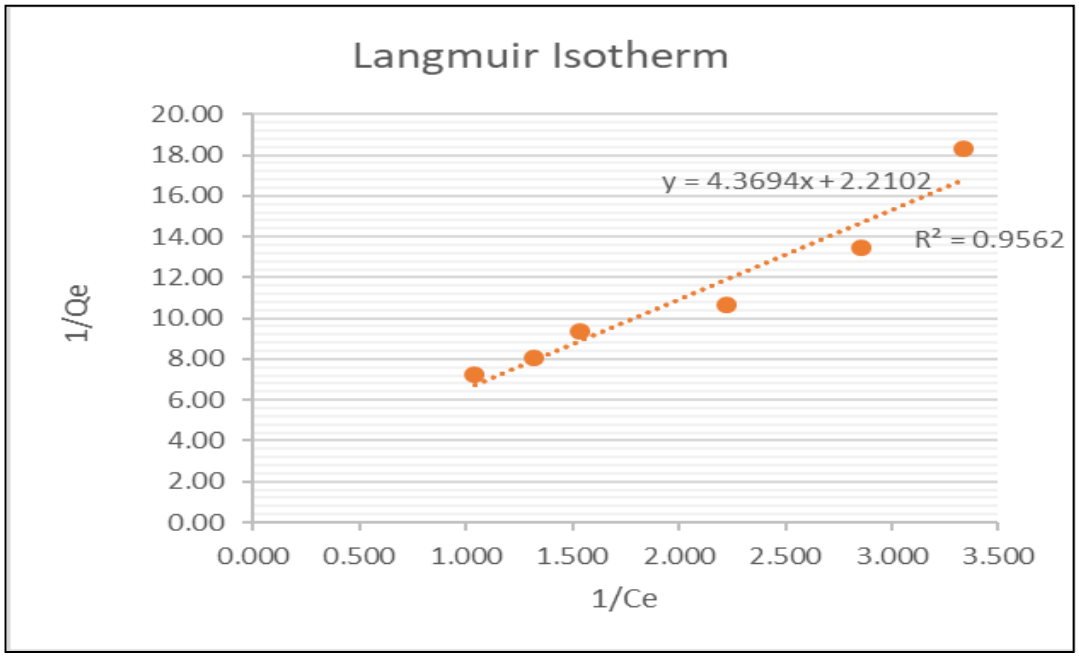

Figure 4.26: The Langmuir isotherm for defluoridation with (FMFA)opt when Na/Ca ratio is 01

Q_m 0.452 mg/g

K_L 0.506 L/mg

Q_m the maximum monolayer coverage capacity is 0.452 mg/g, and K_L the Langmuir isotherm constant was calculated to be 0.506 L/mg.

Separation factor or equilibrium parameter, R_L value describes the adsorption mechanisms, which is unfavorable ($R_L > 1$), linear ($R_L = 1$), favorable ($0 < R_L > 1$), or irreversible ($R_L = 0$) (Weber and Chakravorti, 1974).

The calculated R_L values given in Table 4.26 are between 0.25 and 0.36. When $0 < R_L > 1$, adsorption mechanism for Langmuir is favourable at all given concentrations.

Table 4.26: Separation factor calculated at different concentrations for Na/Ca ratio of 01

	4.0 ppm	3.5 ppm	3.0 ppm	2.5 ppm	2.0 ppm	1.5 ppm
R_L	0.25	0.27	0.28	0.31	0.33	0.36

The Langmuir isotherm and data for defluoridation with $(FMFA)_{opt}$ when Na/Ca ratio is 03 is given in Figure 4.27 and Table 4.27, respectively.

Table 4.27: The adsorption data of Na/Ca ratio 03, fitted to Langmuir model

Initial fluoride concentration (mg/L)	Final fluoride concentration (mg/L)	V/M (L/g)	Qe (mg/g)	1/Qe (g/mg)	Ce (mg/L)	1/Ce (L/mg)
4.000	0.850	0.045	0.143	6.99	1.18	1.18
3.500	0.760	0.045	0.125	8.04	0.76	1.32
3.000	0.560	0.045	0.111	9.02	0.56	1.79
2.500	0.460	0.045	0.093	10.81	0.46	2.17
2.000	0.350	0.045	0.075	13.32	0.35	2.86
1.500	0.290	0.045	0.055	18.24	0.29	3.45

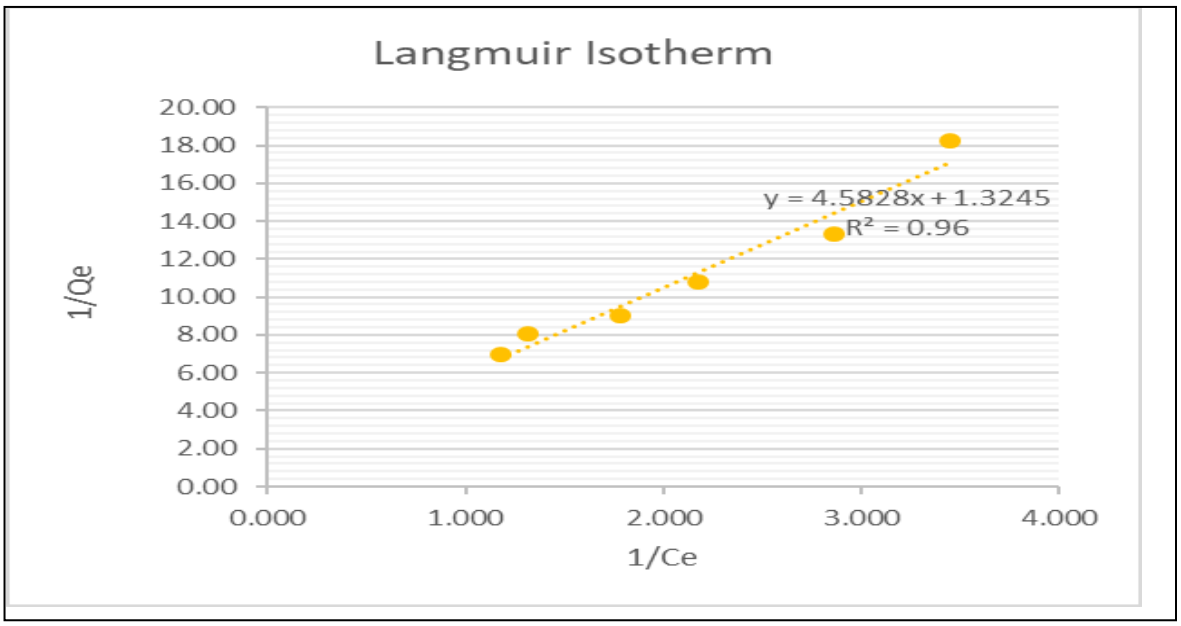

Figure 4.27: The Langmuir isotherm for defluoridation with (FMFA)opt when Na/Ca ratio is 03

Q_m 0.755 mg/g

K_L 0.289 L/mg

Q_m the maximum monolayer coverage capacity is 0.755 mg/g, and K_L the Langmuir isotherm constant was calculated to be 0.289 L/mg.

The calculated R_L values given in table 4.28 are between 0.32 and 0.41. When $0 < R_L > 1$, adsorption mechanism for Langmuir is favourable at all given concentrations.

Table 4.28: Separation factor calculated at different concentrations for Na/Ca ratio of 03

	4.0 ppm	3.5 ppm	3.0 ppm	2.5 ppm	2.0 ppm	1.5 ppm
R_L	0.32	0.33	0.35	0.37	0.39	0.41

The Langmuir isotherm and data for defluoridation with $(FMFA)_{opt}$ when Na/Ca ratio is 07 is given in Figure 4.27 and Table 4.27, respectively.

Table 4.29: The adsorption data of Na/Ca ratio 07, fitted to Langmuir model

Initial F^- concentration (mg/L)	Final F^- concentration (mg/L)	V/M (L/g)	Qe (mg/g)	1/Qe (g/mg)	Ce (mg/L)	1/Ce (L/mg)
4.000	0.760	0.045	0.147	6.79	0.76	1.32
3.500	0.630	0.045	0.130	7.21	0.63	1.59
3.000	0.530	0.045	0.112	8.90	0.53	1.89
2.500	0.410	0.045	0.095	10.53	0.41	2.44
2.000	0.300	0.045	0.077	12.98	0.30	3.33
1.500	0.250	0.045	0.057	17.61	0.25	4.00

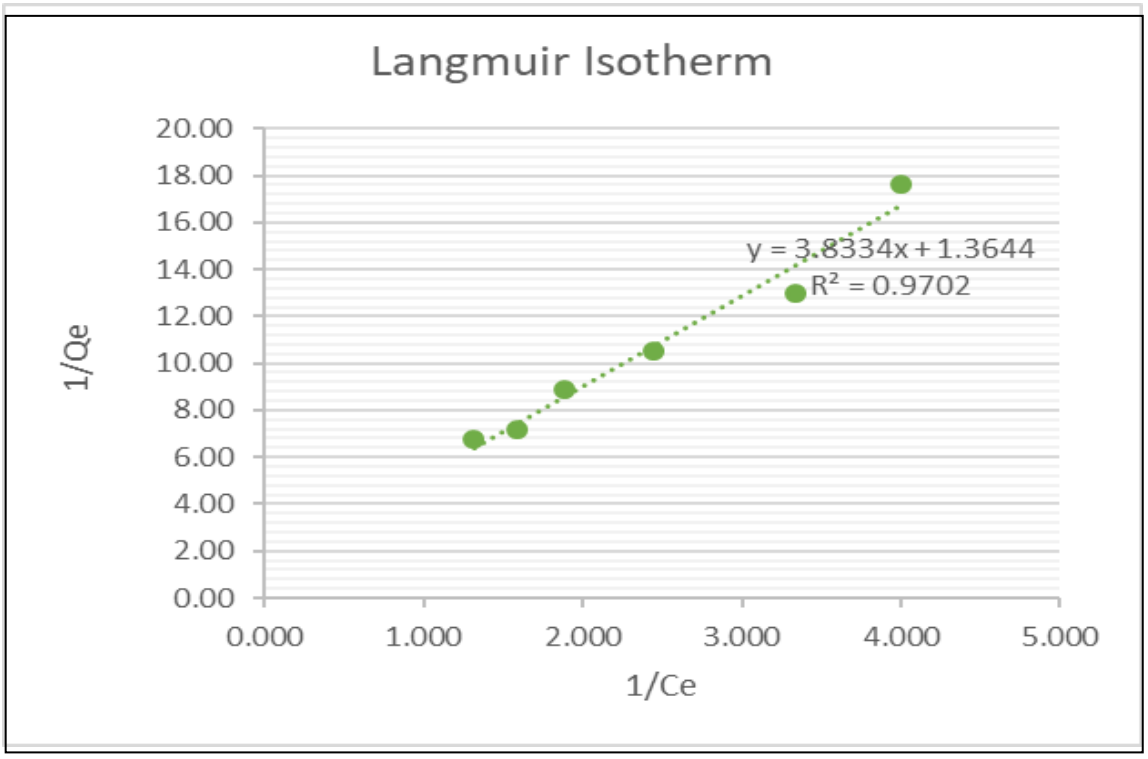

Figure 4.28: The Langmuir isotherm for defluoridation with (FMFA)opt when Na/Ca ratio is 07

Q_m 0.733 mg/g

K_L 0.356 L/mg

Q_m the maximum monolayer coverage capacity is 0.733 mg/g, and K_L the Langmuir isotherm constant was calculated to be 0.356 L/mg.

The calculated R_L values given in Table 4.30 are between 0.29 and 0.39. When $0 < R_L > 1$, adsorption mechanism for Langmuir is favourable at all given concentrations.

Table 4.30: Separation factor calculated at different concentrations for Na/Ca ratio of 07

	4.0 ppm	3.5 ppm	3.0 ppm	2.5 ppm	2.0 ppm	1.5 ppm
R_L	0.29	0.31	0.33	0.35	0.37	0.39

Freundlich model was applied for fluoride removal to ascertain the adsorption characteristics, assuming the heterogeneous surfaces where fluoride could bind by multi-layer formation, and there exists an interaction among adsorbed ions. Freundlich adsorption isotherm (Freundlich, 1906) is given by Eq. 4:

$$\log\left(Q_e\right)=\log\left(K_f\right)+\frac{1}{n}\log\left(C_e\right) \quad (4)$$

When the Freundlich Isotherm (Figure 4.29) is applied for all three Na/ Ca ratios, it was evident that the adsorption isotherm trendlines gives a lower R^2 values with respect to the value obtained when fitted to the Langmuir isotherm model.

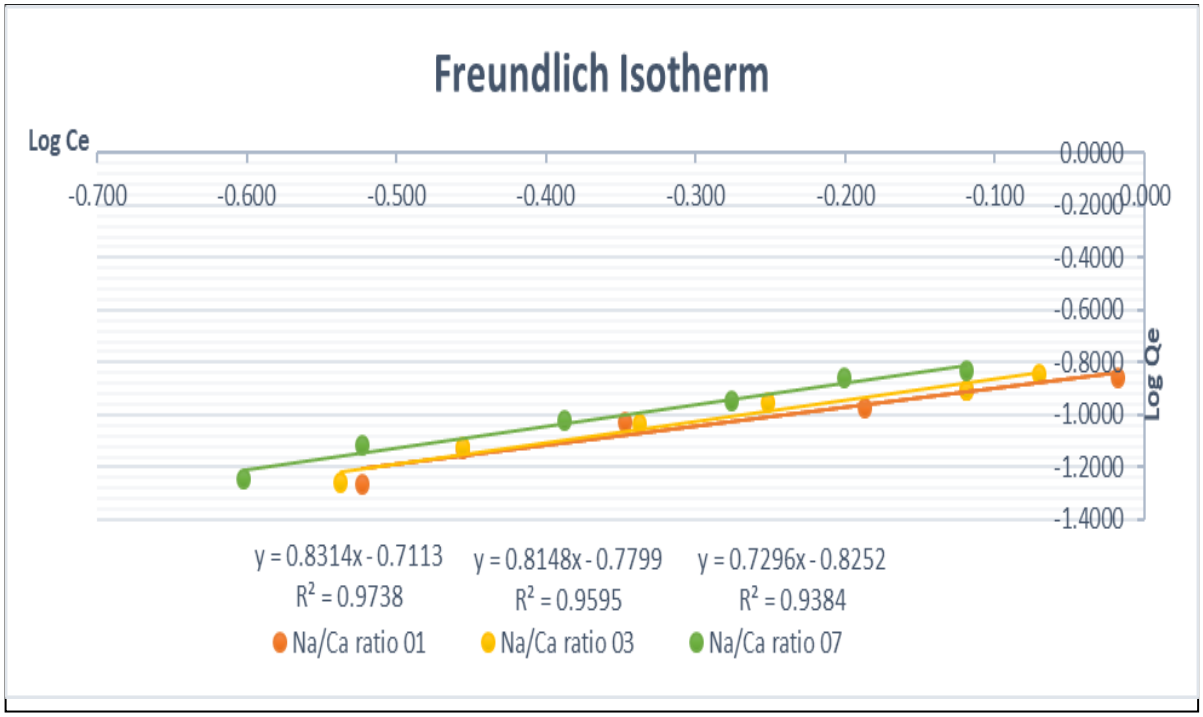

Figure 4.29: The Freundlich isotherm for defluoridation with $(FMFA)_{opt}$ when Na/Ca ratio is 01, 03 and 07

The incompatibility of the Freundlich isotherm with adsorption data can be further proved using the Freundlich exponent (n) calculate for each ratio.

Na/Ca ratio 01

n = 1/0.8314 = 1.203

Na/Ca ratio 03

n = 1/0.8148 = 1.227

Na/Ca ratio 07

n = 1/0.7296 = 1.371

The results obtained satisfies $1 < n < 2$, indicating moderately difficult adsorption. Therefore it can be concluded that the adsorption process favours the Langmuir model where adsorption is monolayer or unilayer.

4.7.2. Kinetic studies

The kinetic studies were conducted in order to determine the reaction order. The reaction order determination enables us to conclude the adsorption mechanism. Table 4.31 gives the pseudo first order reaction results for all three Na/Ca ratios

Table 4.31: The pseudo first order reaction results for all Na/Ca ratios

	Na/Ca ratio 01	Na/Ca ratio 03	Na/Ca ratio 07
Time (min)	Log (q_e-q_t)	Log (q_e-q_t)	Log (q_e-q_t)
0	0	0	0
2	Outlier	-0.657	-0.259
5	-0.431	-0.284	0.130
10	-0.131	0.049	0.227
15	0.201	0.191	0.255
30	0.219	0.214	0.269
60	0.232	0.245	0.281
120	0.283	0.296	0.324
180	0.290	0.304	0.335
240	0.296	0.309	0.340
300	0.305	0.315	0.342

The data cannot be fitted to pseudo first order (Figure 4.30), therefore the reaction does not follow the first order kinetics.

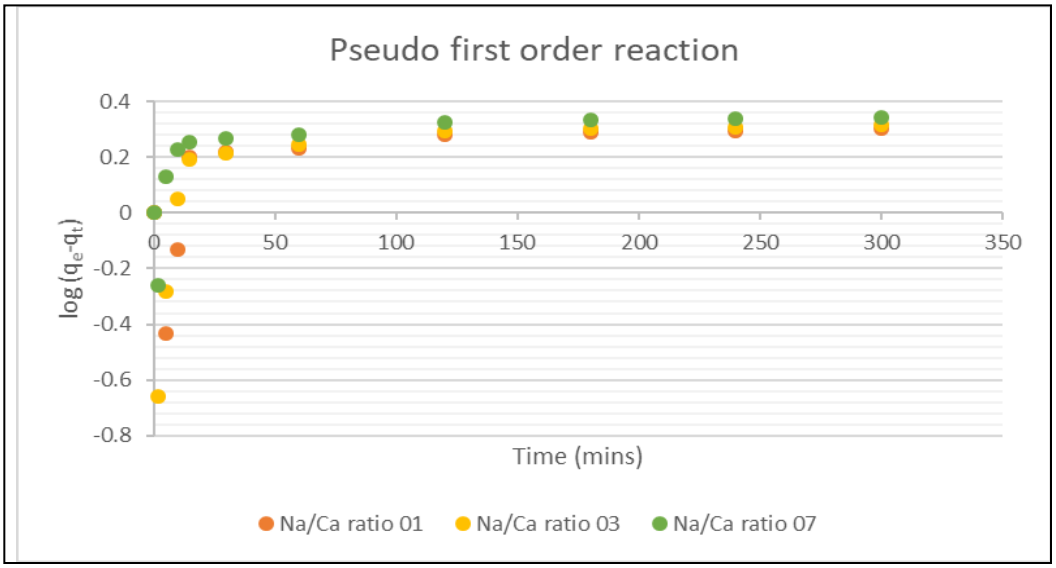

Figure 4.30: Pseudo first order graph for all Na/Ca ratios

The adsorption data were then fitted to pseudo second order to further study the behaviour of fluoride adsorption. The Tables 4.32 to 4.34 and the Figures 4.31 to 4.33 gives the results obtained for the tested Na/Ca ratios.

Table 4.32: The kinetic experiment results of $(FMFA)_{opt}$ for Na/Ca ratio of 01

Time (min)	Initial fluoride concentration (ppm)	Final fluoride concentration (ppm)	Removal efficiency (%)	v/m (L/g)	q_t (mg/g)	t/q_t (min.g/mg)
0	2.320	2.320	0.0	0.045	0.000	0.00
2	2.270	2.200	3.1	0.045	0.003	628.57
5	2.270	1.900	16.3	0.045	0.017	297.30
10	2.270	1.532	32.5	0.045	0.034	298.10
15	2.270	0.680	70.0	0.045	0.072	207.55
30	2.270	0.612	73.0	0.045	0.075	398.07
60	2.270	0.560	75.3	0.045	0.078	771.93
120	2.270	0.350	84.6	0.045	0.087	1375.00
180	2.270	0.316	86.1	0.045	0.089	2026.61
240	2.270	0.290	87.2	0.045	0.090	2666.67
300	2.270	0.250	89.0	0.045	0.092	3267.33

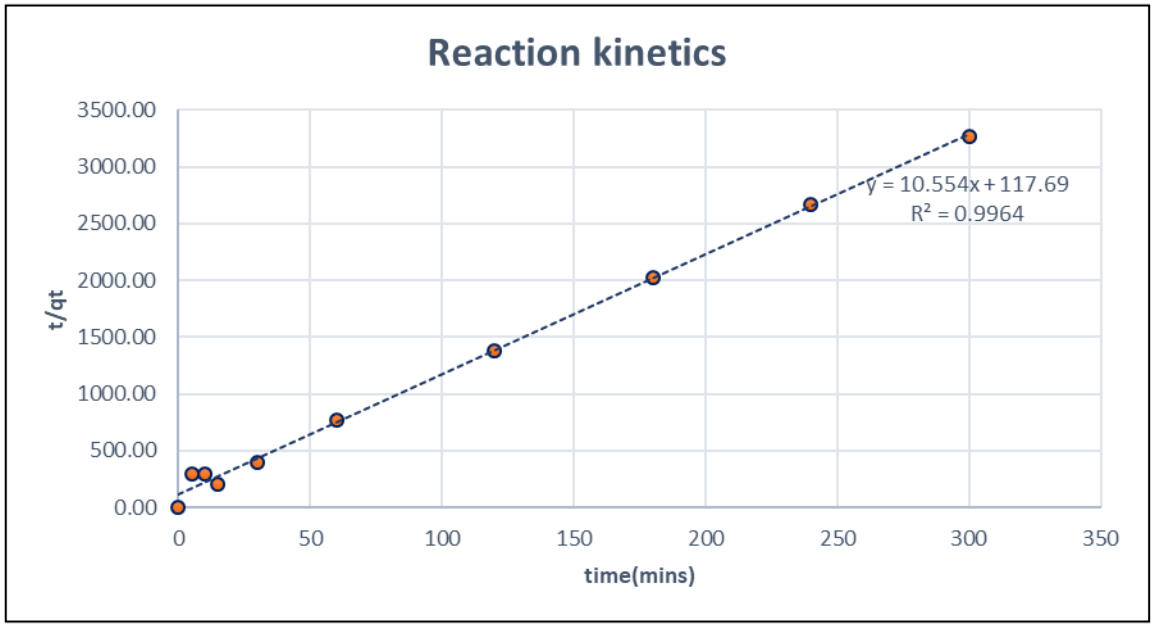

Figure 4.31: The reaction kinetic data for Na/Ca ratio 01 fitted to second order kinetic model

The amount of fluoride adsorbed on adsorbent at equilibrium (q_e) was 0.0975 mg/g for the Na/Ca ratio of 01. The rate constant K_2 was 1.522 $gmg^{-1}min^{-1}$ for this ratio.

Table 4.33: The kinetic experiment results of $(FMFA)_{opt}$ for Na/Ca ratio of 03

Time (min)	Initial fluoride concentration (ppm)	Final fluoride concentration (ppm)	Removal efficiency (%)	v/m (L/g)	q_t (mg/g)	t/q_t (min.g/mg)
0	2.320	2.320	0.0	0.045	0.000	0.00
2	2.320	2.100	9.5	0.045	0.010	200.00
5	2.320	1.800	22.4	0.045	0.024	211.54
10	2.320	1.200	48.3	0.045	0.051	196.43
15	2.320	0.765	67.0	0.045	0.071	212.15
30	2.320	0.680	70.7	0.045	0.075	402.44
60	2.320	0.560	75.9	0.045	0.080	750.00
120	2.320	0.340	85.3	0.045	0.090	1333.33
180	2.320	0.302	87.0	0.045	0.092	1962.34
240	2.320	0.280	87.9	0.045	0.093	2588.24
300	2.320	0.250	89.2	0.045	0.094	3188.41

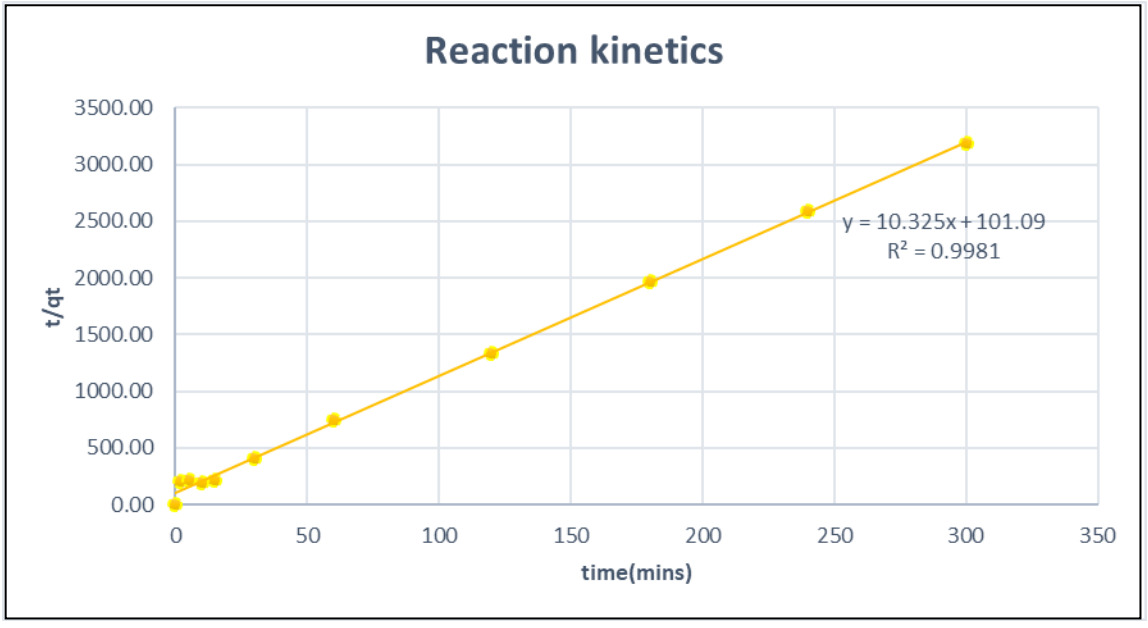

Figure 4.32: The reaction kinetic data for Na/Ca ratio 03 fitted to second order kinetic model

The amount of fluoride adsorbed on adsorbent at equilibrium (q_e) was 0.097 mg/g for the Na/Ca ratio of 03. The fluoride adsorbed per mass of adsorbent for Na/Ca ratio of 03 is higher when compared to Na/Ca ratio of 01. The rate constant K_2 was 1.454 $gmg^{-1}min^{-1}$ for this ratio.

Table 4.34: The kinetic experiment results of (FMFA)opt for Na/Ca ratio of 07

Time (min)	Initial fluoride concentration (ppm)	Final fluoride concentration (ppm)	Removal efficiency (%)	v/m (L/g)	q_t (mg/g)	t/q_t (min.g/mg)
0	2.450	2.450	12.2	0.045	0.014	0.00
2	2.450	1.900	22.4	0.045	0.025	80.00
5	2.450	1.100	55.1	0.045	0.061	81.48
10	2.450	0.760	69.0	0.045	0.077	130.18
15	2.450	0.651	73.4	0.045	0.082	183.44
30	2.450	0.590	75.9	0.045	0.085	354.84
60	2.450	0.540	78.0	0.045	0.087	691.10
120	2.450	0.340	86.1	0.045	0.096	1251.18
180	2.450	0.283	88.4	0.045	0.099	1827.41
240	2.450	0.260	89.4	0.045	0.100	2410.96
300	2.450	0.250	89.8	0.045	0.100	3000.00

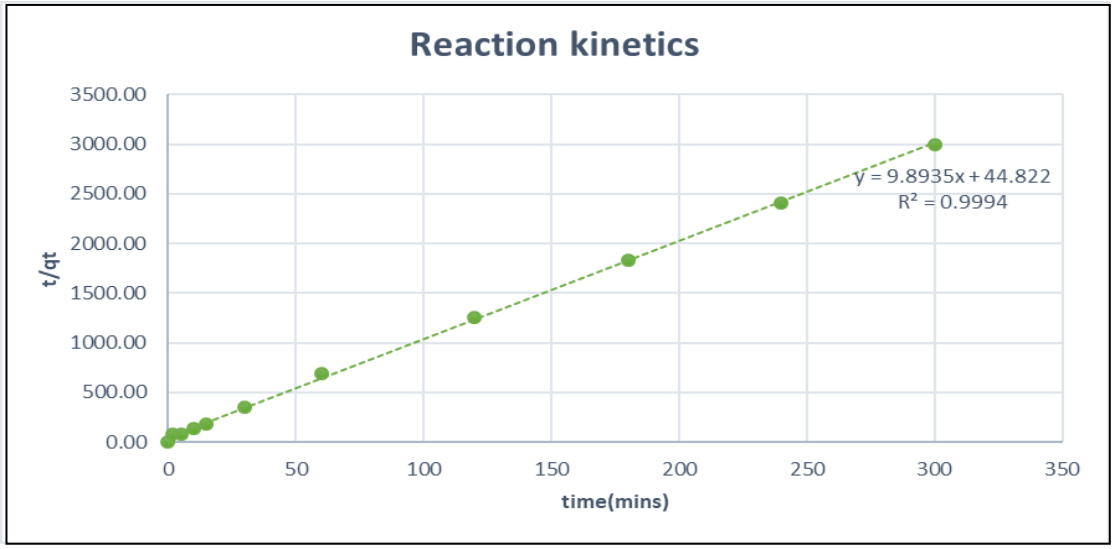

Figure 4.33: The reaction kinetic data for Na/Ca ratio 07 fitted to second order kinetic model

The amount of fluoride adsorbed on adsorbent at equilibrium (q_e) was 0.101 mg/g for the Na/Ca ratio of 7. This is the highest level of fluoride adsorbed per mass of adsorbent when compared with the other two Na/Ca ratios. The rate constant K_2 was 1.337 $gmg^{-1}min^{-1}$, which is the lowest rate constant of all three Na/Ca ratios. The results again confirm that the fluoride adsorbance capacity of $(FMFA)_{opt}$ increases with the increase in Na/Ca ratio while the reaction rate decreases.

Pseudo-second order chemical reaction kinetics provides the best correlation of the experimental data. In this kind of adsorption, the chemical reaction seems significant in the rate-controlling step. The adsorption mechanism is chemically rate controlling and because of this it is known as chemisorption. In this mechanism, the kinetics of sorption correspond to a reversible second order (Ho and McKay., 1999).

The feasibility of the reaction is one of the main attributes that needed to be calculated to determine whether a reaction would occur spontaneously or not. The delta G values of defluoridation in different Na/Ca ratios are given in Table 4.35.

Table 4.35: The feasibility of defluoridation in different Na/Ca ratios

	$1/K_2qe^2$	qe	K_2	log K_2	delta G
Na/Ca ratio 1	117.69	0.094751	1.521638	0.182311	-1054.73
Na/Ca ratio 3	101.09	0.096852	1.456321	0.163257	-944.493
Na/Ca ratio 7	44.822	0.101076	1.33714	0.126177	-729.973

According to the change in Gibbs free energy calculations, the adsorption reactions are spontaneous and exothermic.

When considering $FMFA_{opt}$ with **0.755–0.452** mg/g maximum monolayer adsorption capacity, together with the optimum contact time of 2 hours and optimum pH of 6.8 it can be concluded that it is superior to many other adsorbents available for defluoridation.

The adsorbents discussed in Table 4.36 exhibit similar or higher adsorbent capacity to $FMFA_{opt,}$ but the pH requirement and the contact time for the optimum adsorbance cannot be considered as efficient. Some adsorbents require a contact time of 10 to 24

hours when other adsorbents require an acidic pH to obtain the maximum adsorbance. Therefore $FMFA_{opt,}$ exhibit an optimum pH and a Contact time that is acceptable for to be used as a household filter medium.

Table 4.36: The defluoridation capacity of available adsorbents

Adsorbent	**Adsorption capacity**	**Concentration range**	**Contact time**	**pH**	**Reference**
Bio-char (pine wood) pine bark	2.11–4.08 mg/g	1–100 mg/L	48 h	2.0	Mohan et al., (2012)
Granular acid-treated bentonite	0.094 mg/g	2.85–20 mg/L	40 min	4.95	Ma et al., (2011)
Montmorillonite	0.263 mg/g	2–120 mg/L	180 min	6.0	Tor, (2006)
Metal ion loaded natural zeolite	2.04–4.13 mg/g	1–20 mg/L	24 h		Samatya et al., (2007)
MgCHT	1.185 mg/g	2–10 mg/L	10 h	7.5–10.5	Jimenez-Nu˜nez et al., (2007)
NiCHT	1.202 mg/g	2–10 mg/L	10 h	7.0–7.6	Jimenez-Nu˜nez et al., (2007)
CoCHT	0.842 mg/g	2–10 mg/L	10 h	6.9–7.6	Jimenez-Nu˜nez et al., (2007)
Algerian clay (with and without calcium)	1.013 mg/g and 1.324 mg/g	1-6 mg/L	30min	4.0	Ramdani et al., (2010)

The minimum fluoride levels reached after the adsorbance, for available adsorbents are summarized in Table 4.37. The minimum levels of fluoride reached after adsorbance, are higher than the WHO guideline value of 1.5 mg/L. $FMFA_{opt}$ exhibit a final fluoride level below 0.4 mg/L which cannot be obtained by most of the natural material and by-products used for defluoridation.

Table 4.37: The minimum fluoride levels reached after the adsorbance, for available adsorbents

Method	References	Disadvantages
Red mud	Mohapatra et al., (2009); Gandhi et al., (2012); Tor et al., (2009)	Minimum fluoride level to be 3.4 mg/L Red mud is too alkaline (pH 10-12) for use
Concrete	Huang et al., (1999); Gandhi et al., (2012)	Minimum fluoride level to be 5.6 mg/L
Ragi seed powder	Gandhi et al., (2012)	Minimum fluoride level to be 4.2 mg/L.
Horse gram seed powder	Gandhi et al., (2012)	Minimum fluoride level to be 3 mg/L
Orange peel Powder	Gandhi et al., (2012)	Minimum fluoride level to be 2.5 mg/L.
Chalk powder	Gandhi et al., (2012)	Minimum fluoride level to be 1.6 mg/L
Pineapple peel powder	Gandhi et al., (2012)	Minimum fluoride level to be. 1.6 mg/L.
Multhani mattered mud	Gandhi et al., (2012)	Minimum fluoride adsorption to be 5.26 mg/L

4.8 Regeneration studies for $(FMFA)_{opt}$

Water purification by desorption technology is economical when combined with the regeneration step. Moreover, reuse of adsorbent helps in reducing environmental impacts related with adsorbent disposal (Amin et al., 2015). Desorption can be done using different methods. The adsorbent can be contacted with a solution comprising no adsorbate, or by contacting with a solution which have high affinity for the target ion, or by changing the temperature.

The main drive to consider regeneration is the high cost involve in column refilling. The decision for regeneration can be justified using the cost calculation for refilling of the purification column. The calculation is given below.

Material cost for a single synthesis cycle

Fly ash (280g)	=	Rs.	0.00
NaOH (700 ml)	=	Rs.	1750.00
HNO_3 (10ml)	=	Rs.	15.00
Distilled water (4 L)	=	Rs.	40.00
Cost	=	Rs.	1805.00

Refluxing for the MFA synthesis

Watt value of the refluxer	=	500	w
Refluxing time	=	96	hrs.
Total Watt value	=	24000	wh
Kwh	=	24	Kwh
Cost	=	Rs. 240.00	

Total Cost	=	Rs.	2357.31
Cost per gram	=	Rs.	8.42

The volume of water required for a 5 member family, for 3 months = 900 L

Assuming the water fluoride concentration is 2 ppm and all the material is exhausted after 3 months

The mass of (FMFA)opt required for 3 months	=	19800	g
The mass of (FMFA)opt required for 2 months	=	13068	g
The mass of Z required for 1 month	=	6534	g

The total cost of material refill after 3 months	=	Rs.	166695.63
The total cost of material refill after 2 months	=	Rs.	110019.12
The total cost of material refill after 1 month	=	Rs.	55009.56

A material refill after one month will cost 55,010.00 rupees. This cost is not affordable for a local family. The purification unit provided purification, must at least be used for a period of three months. Therefore, regeneration option was tested on $(FMFA)_{opt}$.

Material regeneration can be done using an acid, a base, a solvent with high affinity towards the target ion and a salt solution (for the ion exchange). The regeneration is highly pH dependent. The regeneration reagents that are used are NaOH, NaCl, HCl, EDTA etc. In this experiment the regeneration reagents that were used are NaOH at pH 12, NaCl at pH 7 and HCl at pH 2.The regeneration results are given in Table 4.38.

Table 4.38: The regeneration of $(FMFA)_{opt}$ using NaOH, NaCl and HCl

	Initial F^- concentration (ppm)	Final F^- concentration (ppm)			
		regeneration cycle 1	regeneration cycle 2	regeneration cycle 3	regeneration cycle 4
NaOH	2.252	0.320	0.350	0.320	0.450
NaCl	2.252	0.320	0.320	0.400	1.181
HCl	2.252	0.320	0.380	0.989	1.093

The regeneration studies show that as the amount of cycles increase the final concentration of the solution will increase. This shows that with cycles of desorption, some previously active sites are no longer adsorbing fluoride. The Table 4.39 displays the percentage of defluoridation after every regeneration cycle of $(FMFA)_{opt}$

Table 4.39: The percentage of defluoridation after every regeneration cycle of $(FMFA)_{opt}$

	Percentages of defluoridation (%)			
	regeneration cycle 1	regeneration cycle 2	regeneration cycle 3	regeneration cycle 4
NaOH	84.46	85.79	80.02	50.27
NaCl	85.79	82.24	47.56	48.76
HCl	83.13	56.08	51.47	44.23

Once the desorption results were analyzed, NaOH was identified as the best desorption solvent. NaOH treated adsorbent exhibit higher defluoridation capacity even after the fourth desorption cycle.

The SEM images (Figure 4.34) clarify the reason for the reduction of desorption. It is evident that the surface morphology has significantly altered in $(FMFA)_{opt}$ due to desorption. The most significant change is seen in the material treated with HCl. The worm-like surface aggregates of $(FMFA)_{opt}$ have disappeared during regeneration, while the arrangement pattern of the remaining aggregates has been altered. The reduction in defluoridation can be attributed to the loss of worm-like aggregates, which must have played the major role in adsorbance of fluoride. The surface morphology of $(FMFA)_{opt}$ treated with NaOH and NaCl does exhibit significant reduction in the density of surface aggregates, without a major change in the arrangement of the aggregates.

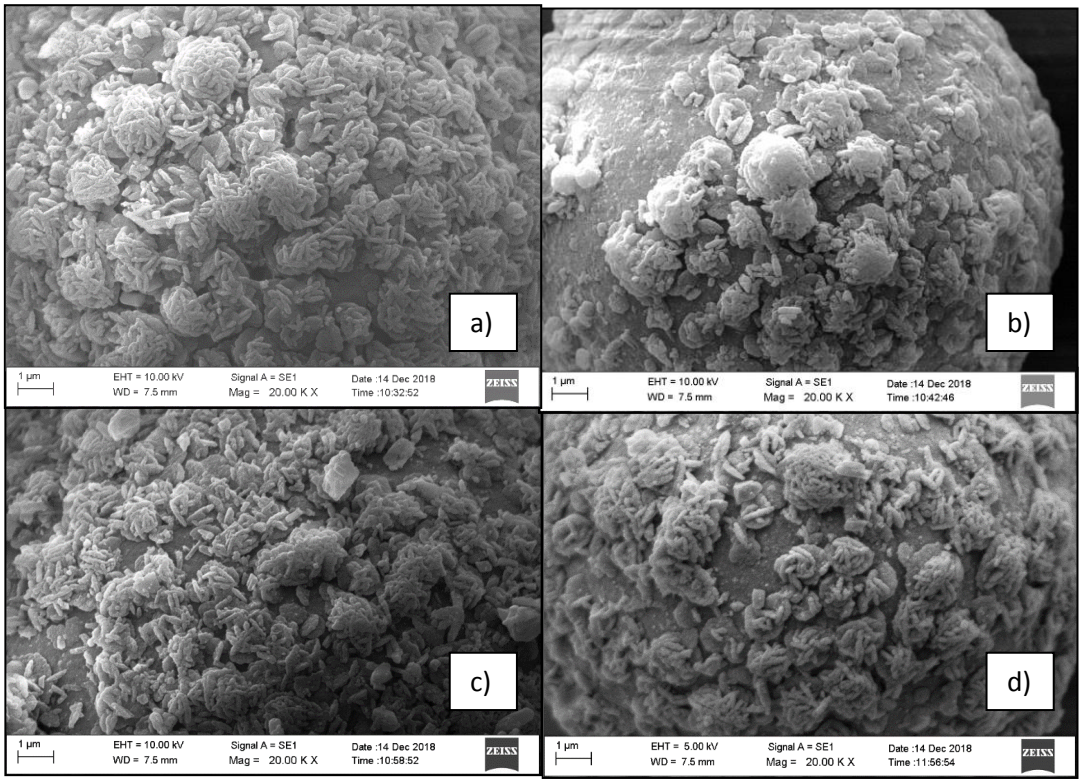

Figure 4.34: a)The SEM Image of (FMFA)opt (50000x) b)The SEM Image of (FMFA)opt after four cycles of HCl regeneration(50000x) c)The SEM Image of (FMFA)opt after four cycles of NaCl regeneration(50000x) b)The SEM Image of (FMFA)opt after four cycles of NaoH regeneration(50000x)

As illustrated in Figure 4.35, all peak intensities have increased in the order of virgin $(FMFA)_{opt}$, (FMFA)opt desorbed with HCl, (FMFA)opt desorbed with NaCl, and (FMFA)opt desorbed with NaOH. The FTIR bands obtained for (FMFA)opt after regeneration are given in Table 4.40. The increase in O-H bonding and the exposure of the Si-O bonds is evident when the peak intensities are observed. $(FMFA)_{opt}$ treated with NaOH four times, had undergone drastic changes according to the FTIR results.

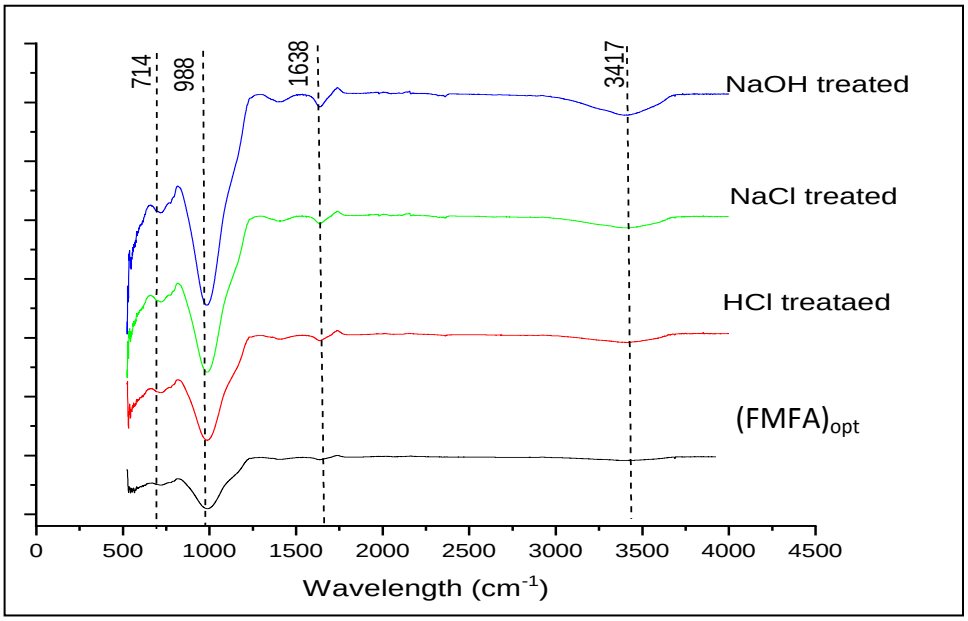

Figure 4.35: FTIR spectrum of $(FMFA)_{opt}$ and regenerated $(FMFA)_{opt}$

Table 4.40: The FTIR bands obtained for $(FMFA)_{opt}$ after regeneration

HCl regenerated $(FMFA)_{opt}$		NaOH regenerated $(FMFA)_{opt}$		NaCl regenerated $(FMFA)_{opt}$	
Band	Corresponding bond	Band	Corresponding bond	Band	Corresponding bond
3409.2	O-H stretching vibration	3397.4	O-H stretching vibration	3397.4	O-H stretching vibration
1636.66	bending vibration of water	1636.05	bending vibration of water	1636.05	bending vibration of water
985.02	Si-O sym.stretching	980.85	Si-O sym.stretching	980.85	Si-O sym.stretching
718.18	Si–O–Si stretching	548.5	Mg-O	525.53	Ca-O
572.02	Al-O stretching	541.32	Mg-O	540.51	Mg-O
560.18	Al-O stretching	529.23	Ca-O	548.98	Mg-O
544.74	Mg-O	525.53	Ca-O	984.6	Si-O sym.stretching
532.93	Ca-O				

In considering the regeneration data, NaOH is selected as the best desorbent for $(FMFA)_{opt}$.

4.8.1. Regeneration or adsorbent refill

The regeneration was performed on $(FMFA)_{opt}$, but there is a dilemma whether it is more effective and efficient than an adsorbent refill, after 3 months.

Adsorbent refill

The total cost of material refill after 3 months	=	Rs.	166695.63
The total cost of material refill after 2 months	=	Rs.	110019.12
The total cost of material refill after 1 month	=	Rs.	55009.56

Regeneration

The volume required for desorption of $(FMFA)_{opt}$ for 3 months	=	450000	mL
The volume required for desorption of $(FMFA)_{opt}$ for 2 months	=	297000	mL
The volume required for desorption of $(FMFA)_{opt}$ for 1 month	=	148500	mL

The price of 50 mL 0.01 M NaOH solution	=	Rs.	0.63
The cost for desorption of $(FMFA)_{opt}$ after 3 months	=	Rs.	5625.00
The cost for desorption of $(FMFA)_{opt}$ after 2 months	=	Rs.	3712.50
The cost for desorption of $(FMFA)_{opt}$ after 1 month	=	Rs.	1856.25

According to this calculations, it is evident that the regeneration is economical when compared to material refill. The material refill cost would always be lower than the above given value, because the exhausting point of the material was not considered. A unit mass of $(FMFA)_{opt}$ will adsorb more fluoride with the increase in contact time, therefore, to fully understand the mass of $(FMFA)_{opt}$ required for a family, it is required to run column studies. The breakthrough curve will be the key point in understanding the mass required for the defluoridation.

In regeneration studies the same NaOH volume will be used multiple times by just adding makeup water. Therefore the regeneration cost will also be much lower than predicted. The recirculation of the regeneration reagent is not practical when conducting

batch studies, therefore the recirculation was not considered in our studies. Recirculation of low concentrated NaOH, will result in inefficient regeneration, reduction in the adsorbance capacity and reduction of column lifetime due to irreversible accumulation of impurities. Base contact time is also important to regeneration efficiency. Regeneration efficiency is also dependent on the purity of the base and dilution water.

5. Conclusions and recommendations

5.1 Contribution from this study

According to the data it is evident that the Na/Ca ratio is distributed in lower ratios across the CKDu prevalent areas. The data closely match with Paranagama, (2014) range of 0.17-2.63 for CKDu prevalent areas. The toxicity of potable water from CKDu prevalent areas could be minimized, if the fluoride level of the CKDu prevalent areas can be brought below 0.4 mg/L, to overcome the synergistic effect between Na/Ca ratio and fluoride.

The functionalization of MFA is a cost effective method. The **optimum dosage of 2.2 g** is required for 100 mL of the sample, while the optimum pH for the material is pH 6.8. Since the potable water in CKDu affected area is of similar pH, **alteration in water pH is not required.**

The Adsorption studies confirm that the Ca^{2+} ions are rejected by $(FMFA)_{opt}$ while giving preference to F^- ion adsorption.

The defluoridation reaction fits the **Langmuir Model**. The Langmuir adsorption isotherm model assumes that the adsorbent surface is homogeneous with equal sorption sites, only monolayer adsorption occurs with no interaction between adjacent adsorbed ions, and adsorbate ions tend to either adsorb or desorb. The adsorption is chemisorption

The reaction fits **Pseudo second order.** The fluoride adsorption capacity of $(FMFA)_{opt}$ when present with different Na/Ca ratios, increased in the following order, **Na/Ca ratio 1 < Na/Ca ratio 3 < Na/Ca ratio 7. The maximum monolayer adsorption (Q_m) for** $(FMFA)_{opt}$ **ranges between 0.755 – 0.452 mg/g with the changing Na/Ca ratios**

The main outcome of the research, is the reduction of the initial concentration of the potable water fluoride content from 2 ppm, up to 0.4 ppm or a value below. Figure 5.1 illustrates the difference in the initial water quality and the final water quality with

respect to fluoride level and Na/Ca ratio. The Na/Ca ratio was assumed to be remained unchanged due to the Donnan coion exclusion. The results confirm that irrespective of the Na/Ca ratio, $(FMFA)_{opt}$ can remove fluoride, up to the desired level.

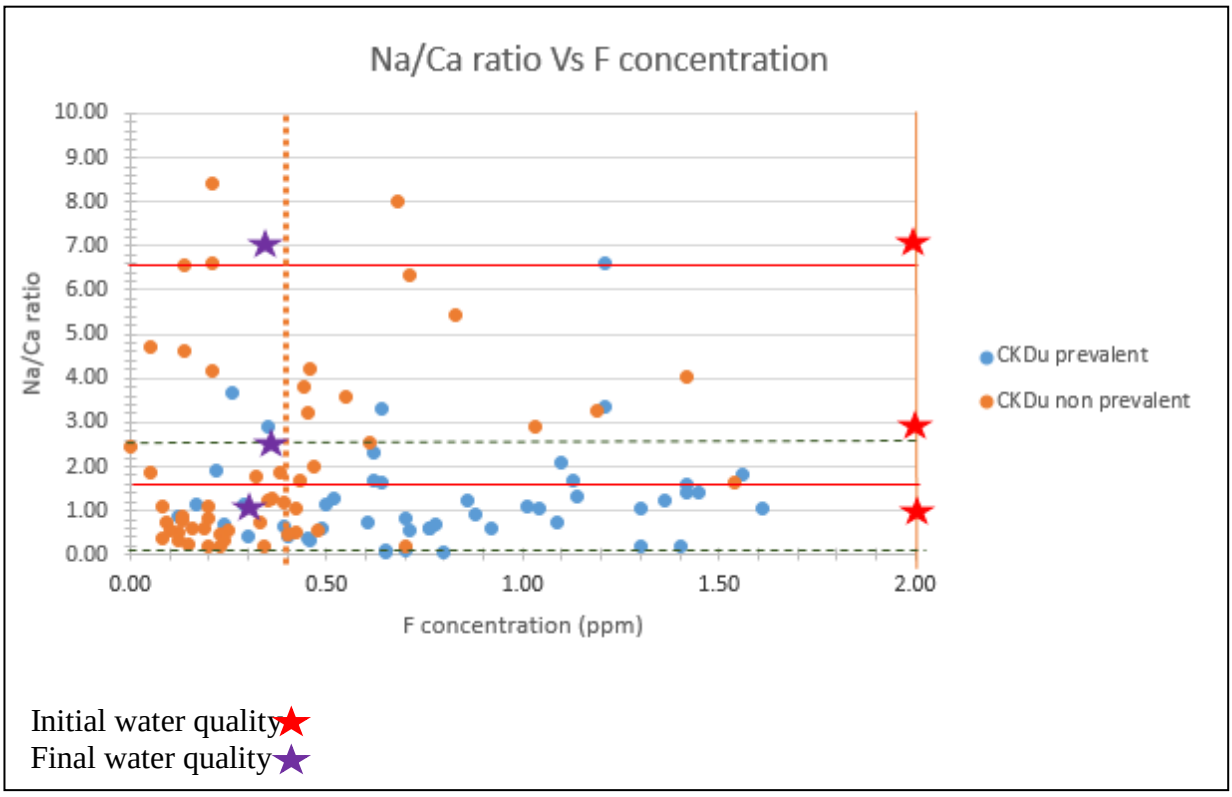

Figure 5.1: The final water quality achieved after potable water trated with $(FMFA)_{opt}$

The surface structure of the $(FMFA)_{opt}$ is changed when HCl and NaCl was used in regeneration. The surface changes of $(FMFA)_{opt}$ after NaOH regeneration are minimum. The defluoridation was maintained at an efficiency of 80%, even after 3 regeneration cycles using NaOH. NaOH was identified as the best desorbent for $(FMFA)_{opt.}$

$(FMFA)_{opt}$ is a low cost, an effective and efficient adsorbent to remove fluoride irrespective of the Na/Ca ratios present in CKDu prevalent areas.

5.2 Recommendations

There have been many investigations on inflicting CKD by fluoride alone and in contrast, there have been some case studies reported with no or less effect on the CKD by fluoride administered even at a higher level than that of maximum WHO recommended level. Hence, globally conceivable study with more CKD subjects in CKDu pervasive areas is of utmost importance. This type of study must take into account the possible variations of fluoride levels in different climatic seasons, preferably the dry period, during which fluoride levels are supposed to be many-fold higher than those in other seasons. Establishment of nephrotoxic levels for fluoride in the potable water considering the external factors by the respective governments should be undoubtedly promoted.

When administered with multi-ions, including fluoride, the combined effects on CKDu seem debatable and sometimes controversial; hence, further studies on toxicological impacts and their biochemical interactions need to be focused.

It is evident that fluoride-mediated hypotheses may be responsible for CKDu, mainly in the tropics of the world and a need for a concerted effort on the R&D work of several research groups is a requirement to unravel the plausible scenarios for CKDu. In this regard, undertaking toxicological studies and exploring probable biochemical pathways are considered as vital.

In this study, the change in the temperature was not a main area of focus. Due to the exothermic property of the reaction kinetics, the increase in temperature can expedite the reaction rates. This will reduce the reaction time required for the adsorbent to attain the desired fluoride levels. Therefore, the adsorbance studies with varying temperature settings is identified as a future study area related to $(FMFA)_{opt.}$

The adsorption was measured for a high calcium concentration to portray the high hardness recorded in the CKDu areas. This study can be repeated for a constant sodium concentration with varying calcium levels, facilitating the determination of the most critical correlations between the water quality parameters (calcium and sodium ion

concentration in potable water) and the removal efficiency of $(FMFA)_{opt}$.

The column studies with the usage of $(FMFA)_{opt}$ should be conducted to determine the column parameters for a household. Then $(FMFA)_{opt}$ has the potential to be used for a portable defluoridation unit in CKDu prevalent areas.

$(FMFA)_{opt}$ has been identified as an effective defluoridation material, but the effectiveness and efficiency can be further enhanced if the functionalization degree is altered using different concentrations of the nitrate solutions.

Furthermore the material can also be used to determine the effect of varying magnesium ion concentration, varying hardness and other multi ion interactions on defluoridation.

References

Abid, S., Hassen, W., Achour, A., Skhiri, H., Maaroufi, K., Ellouz, F., Creppy, E. and Bacha, H., 2003. Ochratoxin A and human chronic nephropathy in Tunisia: is the situation endemic?. Human & experimental toxicology, 22(2), pp.77-84

AbuZeid, K. and Elhatow, L., 2007. Impact of fluoride content in drinking water. In Arab Water Healthy Conference Egypt: Cairo.

Aguilera, I., Daponte, A., Gil, F., Hernández, A.F., Godoy, P., Pla, A. and Ramos, J.L., 2008. Biomonitoring of urinary metals in a population living in the vicinity of industrial sources: a comparison with the general population of Andalusia, Spain. Science of the total environment, 407(1), pp.669-678.

Akpata, E.S., Danfillo, I.S., Otoh, E.C. and Mafeni, J.O., 2009. Geographical mapping of fluoride levels in drinking water sources in Nigeria. African health sciences, 9(4).

Amin, F., Talpur, F.N., Balouch, A., Surhio, M.A. and Bhutto, M.A., 2015. Biosorption of fluoride from aqueous solution by white—rot fungus Pleurotus eryngii ATCC 90888. Environmental Nanotechnology, Monitoring & Management, 3, pp.30-37.

Apak, R., Tütem, E., Hügül, M. and Hizal, J., 1998. Heavy metal cation retention by unconventional sorbents (red muds and fly ashes). Water Research, 32(2), pp.430-440.

Athuraliya, N.T., Abeysekera, T.D., Amerasinghe, P.H., Kumarasiri, R., Bandara, P., Karunaratne, U., Milton, A.H. and Jones, A.L., 2011. Uncertain etiologies of proteinuric-chronic kidney disease in rural Sri Lanka. Kidney international, 80(11), pp.1212-1221.

Athuraliya, T.N.C., Abeysekera, D.T.D.J., Amerasinghe, P.H., Kumarasiri, P.V.R. and Dissanayake, V., 2009. Prevalence of chronic kidney disease in two tertiary care hospitals: high proportion of cases with uncertain aetiology. Ceylon Medical Journal, 54(1).

Auerbach, S.M., Carrado, K.A. and Dutta, P.K., 2003. Handbook of zeolite science and technology. CRC press.

Bhatnagar, A., Kumar, E. and Sillanpää, M., 2011. Fluoride removal from water by adsorption—a review. Chemical Engineering Journal, 171(3), pp.811-840.

Biswas, K., Gupta, K. and Ghosh, U.C., 2009. Adsorption of fluoride by hydrous iron (III)–tin (IV) bimetal mixed oxide from the aqueous solutions. Chemical Engineering Journal, 149(1-3), pp.196-206.

Bober, J., Kwiatkowska, E., Kedzierska, K., Olszewska, M., Stachowska, E., Ciechanowski, K. and Chlubek, D., 2006. Fluoride aggravation of oxidative stress in patients with chronic renal failure. Fluoride, 39(4), p.302.

Borke, J.L. and Whitford, G.M., 1999. Chronic fluoride ingestion decreases 45Ca uptake by rat kidney membranes. The Journal of nutrition, 129(6), pp.1209-1213.

Calafat, A.M., 2012. The US National Health and Nutrition Examination Survey and human exposure to environmental chemicals. International journal of hygiene and environmental health, 215(2), pp.99-101.

Carlson, C.H., Armstrong, W.D. and Singer, L., 1960. Distribution and excretion of radiofluoride in the human. Proceedings of the Society for Experimental Biology and Medicine, 104(2), pp.235-239.

Carton, R.J., 2006. Review of the 2006 United States National Research Council report: fluoride in drinking water. Fluoride, 39(3), pp.163-172.

Celestian, A.J., Parise, J.B., Tripathi, A., Kvick, A. and Vaughan, G.M., 2003. (K4Li4) Al8Ge8O32· 8H2O: an Li^+-exchanged potassium aluminogermanate with the zeolite gismondine (GIS) topology. Acta Crystallographica Section C: Crystal Structure Communications, 59(8), pp.i74-i76.

Cerdas, M\., 2005. Chronic kidney disease in Costa Rica. Kidney International, 68, pp.S31-S33.

Chandrajith, R., Nanayakkara, S., Itai, K., Aturaliya, T.N.C., Dissanayake, C.B., Abeysekera, T., Harada, K., Watanabe, T. and Koizumi, A., 2011. Chronic kidney diseases of uncertain etiology (CKDue) in Sri Lanka: geographic distribution and environmental implications. Environmental geochemistry and health, 33(3), pp.267-278.

Chandrajith, R., Padmasiri, J.P., Dissanayake, C.B. and Prematilaka, K.M., 2012. Spatial distribution of fluoride in groundwater of Sri Lanka. Journal of the National Science Foundation of Sri Lanka, 40(4).

Chandrajith, R., Seneviratna, S., Wickramaarachchi, K., Attanayake, T., Aturaliya, T.N.C. and Dissanayake, C.B., 2010. Natural radionuclides and trace elements in rice field soils in relation to fertilizer application: study of a chronic kidney disease area in Sri Lanka. Environmental Earth Sciences, 60(1), pp.193-201.

Choudhary, R., Koppala, S. and Swamiappan, S., 2015. Bioactivity studies of calcium magnesium silicate prepared from eggshell waste by sol–gel combustion synthesis. Journal of Asian Ceramic Societies, 3(2), pp.173-177.

Chouhan, S. and Flora, S.J.S., 2008. Effects of fluoride on the tissue oxidative stress and apoptosis in rats: biochemical assays supported by IR spectroscopy data. Toxicology, 254(1-2), pp.61-67.

Chutia, P., Kato, S., Kojima, T. and Satokawa, S., 2009. Arsenic adsorption from aqueous solution on synthetic zeolites. Journal of Hazardous Materials, 162(1), pp.440-447.

Cittanova, M.L., Lelongt, B., Verpont, M.C., Geniteau-Legendre, M., Wahbe, F., Prie, D., Coriat, P. and Ronco, P.M., 1996. Fluoride ion toxicity in human kidney collecting duct cells. Anesthesiology: The Journal of the American Society of Anesthesiologists, 84(2), pp.428-435.

Colella, C., 1996. Ion exchange equilibria in zeolite minerals. Mineralium Deposita, 31(6), pp.554-562.

Collins, T.F.X., Sprando, R.L., Shackelford, M.E., Black, T.N., Ames, M.J., Welsh, J.J., Balmer, M.F., Olejnik, N. and Ruggles, D.I., 1995. Developmental toxicity of sodium fluoride in rats. Food and Chemical Toxicology, 33(11), pp.951-960.

Correa-Rotter, R., Wesseling, C. and Johnson, R.J., 2014. CKD of unknown origin in Central America: the case for a Mesoamerican nephropathy. American journal of kidney diseases, 63(3), pp.506-520.

Cutrín, J.C., Zingaro, B., Camandola, S., Boveris, A., Pompella, A. and Poli, G., 2000. Contribution of γ glutamyl transpeptidase to oxidative damage of ischemic rat kidney. Kidney international, 57(2), pp.526-533.

de Peña, Y.P. and Rondón, W., 2013. Linde type a zeolite and type Y faujasite as a solid-phase for lead, cadmium, nickel and cobalt preconcentration and determination using a flow injection system coupled to flame atomic absorption spectrometry. American Journal of Analytical Chemistry, 4(08), p.387.

Devi, R.R., Umlong, I.M., Raul, P.K., Das, B., Banerjee, S. and Singh, L., 2014. Defluoridation of water using nano-magnesium oxide. Journal of Experimental Nanoscience, 9(5), pp.512-524.

Dharma-Wardana, M.W.C., 2018. Chronic kidney disease of unknown etiology and the effect of multiple-ion interactions. Environmental geochemistry and health, 40(2), pp.705-719.

Dharma-Wardana, M.W.C., Amarasiri, S.L., Dharmawardene, N. and Panabokke, C.R., 2015. Chronic kidney disease of unknown aetiology and ground-water ionicity: study based on Sri Lanka. Environmental geochemistry and health, 37(2), pp.221-231.

Dissanayake, C.B. and Chandrajith, R., 2017. Groundwater fluoride as a geochemical marker in the etiology of chronic kidney disease of unknown origin in Sri Lanka. Ceylon Journal of Science, 46(2).

Djebaili, K., Mekhalif, Z., Boumaza, A. and Djelloul, A.X.P.S., 2015. XPS, FTIR, EDX, and XRD analysis of Al2O3 scales grown on PM2000 alloy. Journal of Spectroscopy, 2015.

Dote, T., Kono, K., Usuda, K., Nishiura, H., Tagawa, T., Miyata, K., Shimahara, M., Hashiguchi, N., Senda, J. and Tanaka, Y., 2000. Toxicokinetics of intravenous fluoride in rats with renal damage caused by high-dose fluoride exposure. International archives of occupational and environmental health, 73(1), pp.S90-S92.

Drinking Water Quality for the Period of October 2013 - September 2014, (PDF). Water Supplies Department, The Government of Hong Kong Special Administrative Region. www.wsd.gov.hk -Archived from the original (PDF) on 15 January 2019.

El-Minshawy, O. and Kamel, E.G., 2011. Diabetics on hemodialysis in El-Minia Governorate, Upper Egypt: five-year study. International urology and nephrology, 43(2), pp.507-512.

Ergun, E., Tor, A., Cengeloglu, Y. and Kocak, I., 2008. Electrodialytic removal of fluoride from water: Effects of process parameters and accompanying anions. Separation and Purification Technology, 64(2), pp.147-153.

Ertan, A. and Çakicioğlu-ÖZKAN, F., 2005. CO 2 and N 2 adsorption on the acid (HCl, HNO 3, H 2 SO 4 and H 3 PO 4) treated zeolites. Adsorption, 11(1), pp.151-156.

Ferrarini, S.F., Cardoso, A.M., Paprocki, A. and Pires, M., 2016. Integrated synthesis of zeolites using coal fly ash: element distribution in the products, washing waters and effluent. Journal of the Brazilian Chemical Society, 27(11), pp.2034-2045.

Freundlich, H.M.F., 1906. Over the adsorption in solution. J. Phys. Chem, 57(385471), pp.1100-1107.

Gandhi, N., Sirisha, D., Shekar, K.C. and Asthana, S., 2012. Removal of fluoride from water and waste water by using low cost adsorbents. International Journal of ChemTech Research, 4(4), pp.1646-1653.

Ghorai, S. and Pant, K.K., 2005. Equilibrium, kinetics and breakthrough studies for adsorption of fluoride on activated alumina. Separation and purification technology, 42(3), pp.265-271.

Ghorai, S. and Pant, K.K., 2005. Equilibrium, kinetics and breakthrough studies for adsorption of fluoride on activated alumina. Separation and purification technology, 42(3), pp.265-271.

Gifford, F.J., Gifford, R.M., Eddleston, M. and Dhaun, N., 2017. Endemic nephropathy around the world. Kidney international reports, 2(2), pp.282-292.

Gogoi, S., Nath, S.K., Bordoloi, S. and Dutta, R.K., 2015. Fluoride removal from groundwater by limestone treatment in presence of phosphoric acid. Journal of environmental management, 152, pp.132-139.

Gunawardena, N. (2019, Jan 19). Science and politics of mass kidney failure in Sri Lanka. Retrieved from http://groundviews.org/2019/01/19/science-and-politics-of-mass-kidney-failurein-sri-lanka/

Ho, Y.S. and McKay, G., 1999. Pseudo-second order model for sorption processes. Process biochemistry, 34(5), pp.451-465.

Huang, C.J. and Liu, J.C., 1999. Precipitate flotation of fluoride-containing wastewater from a semiconductor manufacturer. Water Research, 33(16), pp.3403-3412.

Ileperuma, O.A., Dharmagunawardhane, H.A. and Herath, K.P.R.P., 2009. Dissolution of aluminium from sub-standard utensils under high fluoride stress: a possible risk factor for chronic renal failure in the North-Central Province. Journal of the National Science Foundation of Sri Lanka, 37(3).

Ingallinella, A.M., Pacini, V.A., Fernández, R.G., Vidoni, R.M. and Sanguinetti, G., 2011. Simultaneous removal of arsenic and fluoride from groundwater by coagulation-adsorption with polyaluminum chloride. Journal of Environmental Science and Health, Part A, 46(11), pp.1288-1296.

Inkovaara, J., Heikinheimo, R., Jarvinen, K., Kasurinen, U., Hanhijarvi, H. and Iisalo, E., 1975. Prophylactic fluoride treatment and aged bones. Br Med J, 3(5975), pp.73-74.

Jayasekara, J.M., Dissanayake, D.M., Adhikari, S.B. and Bandara, P., 2013. Geographical distribution of chronic kidney disease of unknown origin in North Central Region of Sri Lanka. Ceylon Med J, 58(1), pp.6-10.

Jayasekara, K.B., Dissanayake, D.M., Sivakanesan, R., Ranasinghe, A., Karunarathna, R.H. and Kumara, G.W.G.P., 2015. Epidemiology of chronic kidney disease, with special emphasis on chronic kidney disease of uncertain etiology, in the north central region of Sri Lanka. Journal of epidemiology, 25(4), pp.275-280.

Jayasekara, K.B., Dissanayake, D.M., Sivakanesan, R., Ranasinghe, A., Karunarathna, R.H. and Kumara, G.W.G.P., 2015. Epidemiology of chronic kidney disease, with special emphasis on chronic kidney disease of uncertain etiology, in the north central region of Sri Lanka. Journal of epidemiology, 25(4), pp.275-280.

Jayasumana, C., Fonseka, S., Fernando, A., Jayalath, K., Amarasinghe, M., Siribaddana, S., Gunatilake, S. and Paranagama, P., 2015. Phosphate fertilizer is a

main source of arsenic in areas affected with chronic kidney disease of unknown etiology in Sri Lanka. SpringerPlus, 4(1), p.90.

Jayasumana, C., Paranagama, P.A., Amarasinghe, M.D., Wijewardane, K.M.R.C., Dahanayake, K.S., Fonseka, S.I., Rajakaruna, K.D.L.M.P., Mahamithawa, A.M.P., Samarasinghe, U.D. and Senanayake, V.K., 2013. Possible link of chronic arsenic toxicity with chronic kidney disease of unknown etiology in Sri Lanka.

Jayatilake, N., Mendis, S., Maheepala, P. and Mehta, F.R., 2013. Chronic kidney disease of uncertain aetiology: prevalence and causative factors in a developing country. BMC nephrology, 14(1), p.180.

Jayawardana, D.T., Pitawala, H.M.T.G.A. and Ishiga, H., 2012. Geochemical assessment of soils in districts of fluoride-rich and fluoride-poor groundwater, north-central Sri Lanka. Journal of Geochemical Exploration, 114, pp.118-125.

Jayawardana, D.T., Udagedara, D.T., Silva, A.A.M.P., Pitawala, H.M.T.G.A., Jayathilaka, W.K.P. and Adikaram, A.M.N.M., 2016. Mixing geochemistry of cold water around non-volcanic thermal springs in high-grade metamorphic terrain, Sri Lanka. Chemie der Erde-Geochemistry, 76(4), pp.555-565.

Jha, V., Garcia-Garcia, G., Iseki, K., Li, Z., Naicker, S., Plattner, B., Saran, R., Wang, A.Y.M. and Yang, C.W., 2013. Chronic kidney disease: global dimension and perspectives. The Lancet, 382(9888), pp.260-272.

Jiménez- Núñez, M.L., Olguín, M.T. and Solache- Ríos, M., 2007. Fluoride Removal from Aqueous Solutions by Magnesium, Nickel, and Cobalt Calcined Hydrotalcite- like Compounds. Separation Science and Technology, 42(16), pp.3623-3639.

Jing, C., Cui, J., Huang, Y. and Li, A., 2012. Fabrication, characterization, and application of a composite adsorbent for simultaneous removal of arsenic and fluoride. ACS applied materials & interfaces, 4(2), pp.714-720.

Kakavandi, B., Jonidi, A., Rezaei, R., Nasseri, S., Ameri, A. and Esrafily, A., 2013. Synthesis and properties of Fe 3 O 4-activated carbon magnetic nanoparticles for removal of aniline from aqueous solution: equilibrium, kinetic and thermodynamic studies. Iranian journal of environmental health science & engineering, 10(1), p.19.

Karagas, M.R., Le, C.X., Morris, S.T.E.V.E.N., Blum, J.O.E.L., Lu, X.I.U.F.E.N., Spate, V.I.C.K.Y., Carey, M.A.R.K., Stannard, V.I.R.G.I.N.I.A., Klaue, B.J.O.E.R.N. and Tosteson, T.D., 2001. Markers of low level arsenic exposure for evaluating human cancer risks in a US population. International journal of occupational medicine and environmental health, 14(2), pp.171-175.

Knez, S., Strazisar, J., Golob, J. and Horvat, A., 2001. Agglomeration of zeolite in the fluidized bed. Acta chimica slovenica, 48(4), pp.487-504.

Kosmulski, M., 2009. pH-dependent surface charging and points of zero charge. IV. Update and new approach. Journal of Colloid and Interface Science, 337(2), pp.439-448.

Kovacheva, P., Arishtirova, K. and Vassilev, S., 2001. MgO/NaX zeolite as basic catalyst for oxidative methylation of toluene with methane. Applied Catalysis A: General, 210(1-2), pp.391-395.

Ku, Y. and Chiou, H.M., 2002. The adsorption of fluoride ion from aqueous solution by activated alumina. Water, air, and soil pollution, 133(1-4), pp.349-361.

Kumari, M.K.N., Pathmarajah, S., Dayawansa, N.D.K. and Nirmanee, K.G.S., 2016. Evaluation of groundwater quality for irrigation in Malwathu Oya cascade-I in Anuradhapura District of Sri Lanka. Tropical Agricultural Research, 27(4), pp.310-324.

Langmuir, I., 1938. Overturning and anchoring of monolayers. Science, 87(2266), pp.493-500.

Levine, K.E., Redmon, J.H., Elledge, M.F., Wanigasuriya, K.P., Smith, K., Munoz, B., Waduge, V.A., Periris-John, R.J., Sathiakumar, N., Harrington, J.M. and Womack, D.S., 2016. Quest to identify geochemical risk factors associated with chronic kidney disease of unknown etiology (CKDu) in an endemic region of Sri Lanka—a multimedia laboratory analysis of biological, food, and environmental samples. Environmental monitoring and assessment, 188(10), p.548.

Lough, J., Noonan, R., Gagnon, R. and Kaye, M., 1975. Effects of fluoride on bone in chronic renal failure. Archives of pathology, 99(9), pp.484-487.

Luan, I.O.B., 2010. Singapore water management policies and practices. International Journal of Water Resources Development, 26(1), pp.65-80.

Luke, J., 2001. Fluoride deposition in the aged human pineal gland. Caries Research, 35(2), pp.125-128.

Lydon, M.E., 2013. Properties of inorganically surface-modified zeolites and zeolite/polyimide nanocomposite membranes (Doctoral dissertation, Georgia Institute of Technology).

Ma, Y., Shi, F., Zheng, X., Ma, J. and Gao, C., 2011. Removal of fluoride from aqueous solution using granular acid-treated bentonite (GHB): Batch and column studies. Journal of hazardous materials, 185(2-3), pp.1073-1080.

Machiraju, R.S., Yaradi, K., Gowrishankar, S., Edwards, K.L., Attaluri, S., Miller, F., Grollman, A.P. and Dickman, K.G., 2009. Epidemiology of Udhanam endemic nephropathy. J Am Soc Nephrol, 20, p.643A.

Mahramanlioglu, M., Kizilcikli, I. and Bicer, I.O., 2002. Adsorption of fluoride from aqueous solution by acid treated spent bleaching earth. Journal of Fluorine Chemistry, 115(1), pp.41-47.

Manafia, S. and Joughehdoustb, S., Production of zeolite using different methods.

Marier, J.R., 1977. Some current aspects of environmental fluoride. Science of the Total Environment, 8(3), pp.253-265.

Martín-Cleary, C. and Ortiz, A., 2014. CKD hotspots around the world: where, why and what the lessons are. A CKJ review series. Clinical kidney journal, 7(6), pp.519-523.

Mohan, D., Sharma, R., Singh, V.K., Steele, P. and Pittman Jr, C.U., 2012. Fluoride removal from water using bio-char, a green waste, low-cost adsorbent: equilibrium uptake and sorption dynamics modeling. Industrial & Engineering Chemistry Research, 51(2), pp.900-914.

Mohapatra, M., Anand, S., Mishra, B.K., Giles, D.E. and Singh, P., 2009. Review of fluoride removal from drinking water. Journal of environmental management, 91(1), pp.67-77.

Mortier, W.J., 1982. Compilation of extra framework sites in zeolites. Butterworth Scientific Limited on behalf of the Structure Commission of the International Zeolite Association.

Mozgawa, W., Król, M. and Bajda, T., 2011. IR spectra in the studies of anion sorption on natural sorbents. Journal of Molecular Structure, 993(1-3), pp.109-114.

Nanayakkara, S., Stmld, S., Abeysekera, T., Chandrajith, R., Ratnatunga, N., Edl, G., Yan, J., Hitomi, T., Muso, E., Komiya, T. and Harada, K.H., 2014. An integrative study of the genetic, social and environmental determinants of chronic kidney disease characterized by tubulointerstitial damages in the North Central Region of Sri Lanka. Journal of occupational health, 56(1), pp.28-38.

Nanayakkara, Shanika, Toshiyuki Komiya, Neelakanthi Ratnatunga, S. T. M. L. D. Senevirathna, Kouji H. Harada, Toshiaki Hitomi, Glenda Gobe, Eri Muso, Tilak Abeysekera, and Akio Koizumi. "Tubulointerstitial damage as the major pathological lesion in endemic chronic kidney disease among farmers in North

Central Province of Sri Lanka." Environmental health and preventive medicine 17, no. 3 (2012): 213.

National Institute of Public Health and Environmental Protection, Netherlands ,1989. Advice on limiting the arsenal of antimicrobial drugs for veterinary use, RIVM, rapportnummer 358471003, Bilthoven.

Noble, A., Amerasinghe, P., Manthrithilake, H. and Arasalingam, S., 2014. Review of literature on chronic kidney disease of unknown etiology (CKDu) in Sri Lanka (Vol. 158). IWMI.

O'donnell, J.K., Tobey, M., Weiner, D.E., Stevens, L.A., Johnson, S., Stringham, P., Cohen, B. and Brooks, D.R., 2010. Prevalence of and risk factors for chronic kidney disease in rural Nicaragua. Nephrology Dialysis Transplantation, 26(9), pp.2798-2805.

Official web page of Presidential Task force on Prevention of Kidney Disease of uncertain etiology- http://www.presidentialtaskforce.gov.lk/en/kidney.html# - accessed on 25.02.2019-

Oshima, K.H., Evans-Strickfaden, T.T., Highsmith, A.K. and Ades, E.W., 1996. The use of a microporous polyvinylidene fluoride (PVDF) membrane filter to separate contaminating viral particles from biologically important proteins. Biologicals, 24(2), pp.137-145.

Padilla, A. P., & Saitua, H. (2010). Performance of simultaneous arsenic, fluoride and alkalinity (bicarbonate) rejection by pilot-scale nanofiltration. Desalination, 257(1-3), 16-21.

Paranagama, D., 2014. Chronic kidney disease of unknown origin in Sri Lanka and its relation to drinking water supplies: Doctoral dissertation.

Paranagama, D., Jayasuriya, N. and Bhuiyan, M., 2013. Water quality parameters in relation to chronic kidney disease in Sri Lanka. In Capacity Building for Sustainability (pp. 173-183). University of Peradeniya.

Peraza, S., Wesseling, C., Aragon, A., Leiva, R., García-Trabanino, R.A., Torres, C., Jakobsson, K., Elinder, C.G. and Hogstedt, C., 2012. Decreased kidney function among agricultural workers in El Salvador. American Journal of Kidney Diseases, 59(4), pp.531-540.

Perera, T., Ranasinghe, S., Alles, N. and Waduge, R., 2018. Effect of fluoride on major organs with the different time of exposure in rats. Environmental health and preventive medicine, 23(1), p.17.

Pietrelli, L., 2005. Fluoride wastewater treatment by adsorption onto metallurgical grade alumina. Annali di Chimica: Journal of Analytical, Environmental and Cultural Heritage Chemistry, 95(5), pp.303-312.

Pinon-Miramontes, M., Bautista-Margulis, R.G., Perez-Hernandez, A., 2003. Removalof arsenic and fluoride from drinking water with cake alum and a polymericanionic flocculent. Fluoride 36 (2), 122e128 (Research Report).

Podder, S., Chattopadhyay, A. and Bhattacharya, S., 2008. In vivo suppression by fluoride of chromosome aberrations induced by mitomycin-c in mouse bone marrow cells. Fluoride, 41(1), p.40.

Pontie, M., Buisson, H., Diawara, C.K. and Essis-Tome, H., 2003. Studies of halide ions mass transfer in nanofiltration—application to selective defluorination of brackish drinking water. Desalination, 157(1-3), pp.127-134.

Popat, K.M., Anand, P.S. and Dasare, B.D., 1994. Selective removal of fluoride ions from water by the aluminium form of the aminomethylphosphonic acid-type ion exchanger. Reactive polymers, 23(1), pp.23-32.

Puri, B.K. and Balani, S., 2000. Trace determination of fluoride using lanthanum hydroxide supported on alumina. Journal of Environmental Science & Health Part A, 35(1), pp.109-121.

Rajapurkar, M.M., John, G.T., Kirpalani, A.L., Abraham, G., Agarwal, S.K., Almeida, A.F., Gang, S., Gupta, A., Modi, G., Pahari, D. and Pisharody, R., 2012. What do we know about chronic kidney disease in India: first report of the Indian CKD registry. BMC nephrology, 13(1), p.10.

Ramdani, A., Taleb, S., Benghalem, A. and Ghaffour, N., 2010. Removal of excess fluoride ions from Saharan brackish water by adsorption on natural materials. Desalination, 250(1), pp.408-413.

Ramesh, K. and Reddy, D.D., 2011. Zeolites and their potential uses in agriculture. In Advances in agronomy (Vol. 113, pp. 219-241). Academic Press.

Ramírez, A.M., Melo, P.G., Robles, J.M.A., Castro, M.E.S., Khamkure, S. and de León, R.G., 2013. Kinetic and thermodynamic study of arsenic (V) adsorption on P and W aluminum functionalized zeolites and its regeneration. Journal of Water Resource and Protection, 5(08), p.58.

Roncal-Jimenez, C., García-Trabanino, R., Barregard, L., Lanaspa, M.A., Wesseling, C., Harra, T., Aragón, A., Grases, F., Jarquin, E.R., González, M.A. and Weiss, I., 2016. Heat stress nephropathy from exercise-induced uric acid crystalluria: a perspective on Mesoamerican nephropathy. American journal of kidney diseases, 67(1), pp.20-30.

Roncal-Jimenez, C., Lanaspa, M.A., Jensen, T., Sanchez-Lozada, L.G. and Johnson, R.J., 2015. Mechanisms by which dehydration may lead to chronic kidney disease. Annals of Nutrition and Metabolism, 66(Suppl. 3), pp.10-13.

Rubasinghe, R., Gunatilake, S.K. and Chandrajith, R., 2015. Geochemical characteristics of groundwater in different climatic zones of Sri Lanka. Environmental earth sciences, 74(4), pp.3067-3076.

Sabolić, I., 2006. Common mechanisms in nephropathy induced by toxic metals. Nephron Physiology, 104(3), pp.p107-p114.

Samatya, S., Yüksel, Ü., Yüksel, M. and Kabay, N., 2007. Removal of fluoride from water by metal ions (Al3+, La3+ and ZrO2+) loaded natural zeolite. Separation Science and Technology, 42(9), pp.2033-2047.

Sanoff, S.L., Callejas, L., Alonso, C.D., Hu, Y., Colindres, R.E., Chin, H., Morgan, D.R. and Hogan, S.L., 2010. Positive association of renal insufficiency with agriculture employment and unregulated alcohol consumption in Nicaragua. Renal failure, 32(7), pp.766-777.

Sehn, P., 2008. Fluoride removal with extra low energy reverse osmosis membranes: three years of large scale field experience in Finland. Desalination, 223(1-3), pp.73-84.

Senevirathna, L., Abeysekera, T., Nanayakkara, S., Chandrajith, R., Ratnatunga, N., Harada, K.H., Hitomi, T., Komiya, T., Muso, E. and Koizumi, A., 2012. Risk factors associated with disease progression and mortality in chronic kidney disease of uncertain etiology: a cohort study in Medawachchiya, Sri Lanka. Environmental health and preventive medicine, 17(3), p.191.

SenGupta, A.K., 2017. Ion Exchange in Environmental Processes: Fundamentals, Applications and Sustainable Technology. John Wiley & Sons.

Shao, D.D., Fan, Q.H., Li, J.X., Niu, Z.W., Wu, W.S., Chen, Y.X. and Wang, X.K., 2009. Removal of Eu (III) from aqueous solution using ZSM-5 zeolite. Microporous and Mesoporous Materials, 123(1-3), pp.1-9.

Shimelis, B., Zewge, F. and Chandravanshi, B.S., 2006. Removal of excess fluoride from water by aluminum hydroxide. Bulletin of the Chemical Society of Ethiopia, 20(1), pp.17-34.

Shuhua, X., Ziyou, L., Ling, Y., Fei, W. and Sun, G., 2012. A role of fluoride on free radical generation and oxidative stress in BV-2 microglia cells. Mediators of inflammation, 2012.

Simon, M.J.K., Beil, F.T., Rüther, W., Busse, B., Koehne, T., Steiner, M., Pogoda, P., Ignatius, A., Amling, M. and Oheim, R., 2014. High fluoride and low calcium levels in drinking water is associated with low bone mass, reduced bone quality and fragility fractures in sheep. Osteoporosis International, 25(7), pp.1891-1903.

Šljivić, M., Smičiklas, I., Pejanović, S. and Plećaš, I., 2009. Comparative study of Cu2+ adsorption on a zeolite, a clay and a diatomite from Serbia. Applied Clay Science, 43(1), pp.33-40.

Spencer H, Lewin I, Fowler J, Samachson J. Effect of sodium fluoride on calcium absorption and balances in man. Am J Clin Nutr 1969;22:381–90

Sri Lankan Standard Institute. (2013) SLS standard 614:2013. Colombo: Sri Lankan Standard Institute, Sri Lanka.

Sudasinghe, M. I, 2016. "Water quality data of CKDu prevalent areas", University of Moratuwa

Tor, A., 2006. Removal of fluoride from an aqueous solution by using montmorillonite. Desalination, 201(1-3), pp.267-276.

Tor, A., Danaoglu, N., Arslan, G. and Cengeloglu, Y., 2009. Removal of fluoride from water by using granular red mud: batch and column studies. Journal of hazardous materials, 164(1), pp.271-278.

Tripathi, A., Parise, J.B., Kim, S.J., Lee, Y., Johnson, G.M. and Uh, Y.S., 2000. Structural changes and cation site ordering in Na and K forms of aluminogermanates with the zeolite gismondine topology. Chemistry of materials, 12(12), pp.3760-3769.

Vithanage, M. and Bhattacharya, P., 2015. Fluoride in drinking water: health effects and remediation. In CO2 Sequestration, Biofuels and Depollution (pp. 105-151). Springer, Cham.

Vos, T., Barber, R.M., Bell, B., Bertozzi-Villa, A., Biryukov, S., Bolliger, I., rlson, F., Davis, A., Degenhardt, L., Dicker, D. and Duan, L., 2015. Global Burden of Disease Study 2013 Collaborators. Global, regional, and national incidence, prevalence, and years lived with disability for 301 acute and chronic diseases and injuries in 188 countries, 1990–2013: A systematic analysis for the Global Burden of Disease Study 2013. Lancet, 386(9995), pp.743-800.

Wanasinghe, W.C.S., Gunarathna, M.H.J.P., Herath, H.M.P.I.K. and Jayasinghe, G.Y., 2018. Drinking Water Quality on Chronic Kidney Disease of Unknown Aetiology (CKDu) in Ulagalla Cascade, Sri Lanka. Sabaragamuwa University, 16(1), pp.17-27.

Wang, S.G., Ma, Y., Shi, Y.J. and Gong, W.X., 2009. Defluoridation performance and mechanism of nano- scale aluminum oxide hydroxide in aqueous solution. Journal of Chemical Technology & Biotechnology: International Research in Process, Environmental & Clean Technology, 84(7), pp.1043-1050.

Wang, Y., Zhu, J.H., Cao, J.M., Chun, Y. and Xu, Q.H., 1998. Basic catalytic behavior of MgO directly dispersed on zeolites by microwave irradiation. Microporous and mesoporous materials, 26(1-3), pp.175-184.

Wanigasuriya, K., 2012. Aetiological factors of Chronic Kidney Disease in the North Central Province of Sri Lanka: A review of evidence to-date.

Wanigasuriya, K., 2014. Update on uncertain etiology of chronic kidney disease in Sri Lanka's north-central dry zone. MEDICC review, 16, pp.61-65.

Wanigasuriya, K.P., Peiris-John, R.J. and Wickremasinghe, R., 2011. Chronic kidney disease of unknown aetiology in Sri Lanka: is cadmium a likely cause?. BMC nephrology, 12(1), p.32.

Wasana, H.M., Perera, G.D., De Gunawardena, P.S. and Bandara, J., 2015. The impact of aluminum, fluoride, and aluminum–fluoride complexes in drinking water on chronic kidney disease. Environmental Science and Pollution Research, 22(14), pp.11001-11009.

Wasana, H. M., Perera, G. D., Gunawardena, P. D. S., Fernando, P. S., &Bandara, J. (2017). WHO water quality standards Vs Synergic effect (s) of fluoride, heavy metals and hardness in drinking water on kidney tissues. Scientific Reports, 7, 42516.

Weber, T.W. and Chakravorti, R.K., 1974. Pore and solid diffusion models for fixed- bed adsorbers. AIChE Journal, 20(2), pp.228-238.

Wickramarathna, S., Balasooriya, S., Diyabalanage, S. and Chandrajith, R., 2017. Tracing environmental aetiological factors of chronic kidney diseases in the dry zone of Sri Lanka—A hydrogeochemical and isotope approach. Journal of Trace Elements in Medicine and Biology, 44, pp.298-306.

Wilhelm, M., Ewers, U. and Schulz, C., 2004. Revised and new reference values for some trace elements in blood and urine for human biomonitoring in environmental medicine. International journal of hygiene and environmental health, 207(1), pp.69-73.

Wimalawansa, S.J. and Wimalawansa, S.A., 2014. Impact of changing agricultural practices on human health: chronic kidney disease of multi-factorial origin in Sri Lanka.

Wimalawansa, S.J., 2015. Escalating chronic kidney diseases of multi-factorial origin (CKD-mfo) in Sri Lanka: causes, solutions, and recommendations—update and responses. Environmental health and preventive medicine, 20(2), p.152.

Wu, H., Zhang, J., Wei, Q., Zheng, J. and Zhang, J., 2013. Transesterification of soybean oil to biodiesel using zeolite supported CaO as strong base catalysts. Fuel Processing Technology, 109, pp.13-18.

Xiong, X., Liu, J., He, W., Xia, T., He, P., Chen, X., Yang, K. and Wang, A., 2007. Dose–effect relationship between drinking water fluoride levels and damage to liver and kidney functions in children. Environmental Research, 103(1), pp.112-116.

XU, Q.L., LI, T.C. and YAN, Y.J., 2008. Effects of CaO-modified zeolite on one-step synthesis of dimethyl ether. Journal of Fuel Chemistry and Technology, 36(2), pp.176-180.

Yuh-Shan, H., 2004. Citation review of Lagergren kinetic rate equation on adsorption reactions. Scientometrics, 59(1), pp.171-177.

Zager, R.A. and Iwata, M., 1997. Inorganic fluoride. Divergent effects on human proximal tubular cell viability. The American journal of pathology, 150(2), p.735.

Zager, R.A. and Iwata, M., 1997. Inorganic fluoride. Divergent effects on human proximal tubular cell viability. The American journal of pathology, 150(2), p.735.

Zhao, B., Zhang, Y., Dou, X., Wu, X. and Yang, M., 2012. Granulation of Fe–Al–Ce trimetal hydroxide as a fluoride adsorbent using the extrusion method. Chemical Engineering Journal, 185, pp.211-218.

Zholobenko, V., Chapple, A., Rhodes, N. and Stuart, J., 1998. Structural transitions in zeolite P An in situ FTIR study. Journal of the Chemical Society, Faraday Transactions, 94(12), pp.1779-1781.

Annexures